NASA TECHNICAL MEMORANDUM

NASA TM X-73,134

NASA TM X-73,134

TEST-SECTION NOISE OF THE AMES 7- by 10-FOOT WIND TUNNEL NO. 1

Paul T. Soderman

Ames Research Center
and
Ames Directorate
U. S. Army Air Mobility R&D Laboratory
Moffett Field, CA 94035

May 1976

1. Report No.	2. Government Accession No.	3. Recipient's Catalog No.
TM X-73,134		

4. Title and Subtitle	5. Report Date
TEST-SECTION NOISE OF THE AMES 7- by 10-FOOT WIND TUNNEL NO. 1	6. Performing Organization Code

7. Author(s)	8. Performing Organization Report No.
Paul T. Soderman*	A-6601
	10. Work Unit No. 505-10-31-01
9. Performing Organization Name and Address NASA Ames Research Center and Ames Directorate, U.S. Army Air Mobility R&D Laboratory, Moffett Field, CA 94035	11. Contract or Grant No.
	13. Type of Report and Period Covered Technical Memorandum
12. Sponsoring Agency Name and Address National Aeronautics and Space Administration Washington, D.C. 20546; and U.S. Army Air Mobility R&D Laboratory, Moffett Field, CA 94035	14. Sponsoring Agency Code

15. Supplementary Notes

*Ames Directorate, U.S. Army Air Mobility R&D Laboratory

16. Abstract

An investigation was made of the test-section noise levels at various wind speeds in the Ames 7- by 10-Foot Wind Tunnel No. 1. No model was in the test section. Results showed that aerodynamic noise from various struts used to monitor flow conditions in the test section dominated the wind-tunnel background noise over much of the frequency spectrum. A tapered microphone stand with a thin trailing edge generated less noise than did a constant-chord strut with a blunt trailing edge. Noise from small holes in the test-section walls was insignificant.

17. Key Words (Suggested by Author(s))	18. Distribution Statement
Wind-tunnel acoustics Aerodynamic noise Wind noise Vortex noise	Unlimited STAR Category - 71

19. Security Classif. (of this report)	20. Security Classif. (of this page)	21. No. of Pages	22. Price*
Unclassified	Unclassified	69	$4.25

*For sale by the National Technical Information Service, Springfield, Virginia 22161

SYMBOLS

q	test-section dynamic pressure, N/m^2 (lb/ft^2)
V or U	air speed, m/s (ft/s)
S	Strouhal number
Re	Reynold's number
f	frequency, Hz
t	airfoil thickness, cm (in.)
c	airfoil chord, cm (in.)
d	characteristic dimension of airfoil
δ	boundary-layer thickness, cm (in.)

Subscripts

u	upper surface
l	lower surface

TEST-SECTION NOISE OF THE AMES 7- by 10-FOOT WIND TUNNEL NO. 1

Paul T. Soderman

Ames Research Center
and
Ames Directorate
U.S. Army Air Mobility R&D Laboratory

SUMMARY

An investigation was made of the test-section noise levels at various wind speeds in the Ames 7- by 10-Foot (2.1- by 3.0-m) Wind Tunnel No. 1. No model was in the test section, but the microphone was mounted on a strut in the flow. The purpose of the study was to identify as many noise sources in the test section as possible, remove those sources, and record the resulting noise floor.

Results showed that aerodynamic noise from various struts used to monitor flow conditions in the test section dominated the wind-tunnel background noise over much of the frequency spectrum. A tapered microphone stand with a thin trailing edge generated less noise than did a constant-chord strut with a blunt trailing edge. Noise from small holes in the test-section walls was insignificant.

INTRODUCTION

Wilby and Scharton (ref. 1) recently performed a study of the Ames 7- by 10-Foot (2.1- by 3.0-m) Wind Tunnel No. 1, shown in figure 1, to determine the acoustic characteristics which would have to be modified to convert the wind tunnel into an acoustic research facility. One of their conclusions was that a large part of the test-section noise was generated by various aerodynamic struts regularly used in the test section. They also suspected that holes and cavities in the walls generated noise. The purpose of the study reported here was to extend that work by identifying the contribution of each possible source in the test section. This was done by removing the sources one-by-one and recording the noise changes. It was hoped that the noise floor with all test-section noise sources removed could then be attributed to the drive fan. If that were so, then sound baffles upstream and downstream of the fan would be effective in reducing the test-section noise levels.

The reverberation characteristics of the test section, which are as important as background noise, are discussed in references 1 and 2. In

addition, reference 3 and an unpublished working paper by R. E. Arndt and D. A. Boxwell (A Preliminary Analysis of the Feasibility of Rotor Noise Measurements in the AMRDL-Ames 7 × 10 Foot Wind Tunnel, October, 1971) contain reverberation data acquired in an identical wind tunnel.

TEST SECTION APPARATUS

Airfoil Struts

Airfoil struts are used in the test section to a) support microphones, b) support a pitot-static pressure probe, c) support various wake survey probes, and d) stabilize the flow into the diffuser.

The two microphone struts used in this study are illustrated in figure 2(a). The tapered strut was used by Noiseux et al. in a previous study of microphone wind noise described in reference 4. The microphone body was faired to the strut. The constant-chord, airfoil-tubing strut was used by Wilby and Scharton (ref. 1). The constant-chord strut had a blunt trailing edge typical of commercial airfoil-shaped tubing.

Figure 2(b) illustrates the other airfoil struts evaluated in the study. The pitot-static probe is used to measure dynamic pressure, which is needed to compute wind speed. The wake-survey strut is shown raised to its highest position, the only position used in this study. The diffuser vanes, used to stabilize the flow in the diffuser, are located at the diffuser entrance.

Holes and Cavity

Over the years, hundreds of small holes 0.16 to 1.3 cm (1/16 to 1/2 in.) diameter have been drilled in the four walls of the test section. In the rear of the test section a screen-covered cavity, 30 cm by 1.4 m (1 ft by 4. 4.6 ft), in the ceiling is used for pressure equalization between the test section and shop area.

INSTRUMENTATION

Most of the noise data were recorded using a 0.6 cm (1/4 in.) condenser microphone adapted to a 1.3 cm (1/2 in.) preamplifier. Some data were obtained with a 1.3 cm (1/2 in.) microphone. The microphones were protected with nose cones. The data were recorded on a tape recorder for narrow-band frequency analyses.[1] On-line third-octave band analyses of the data were made.

[1]Nominal bandwidths are listed on the figures. Effective noise bandwidth, which is the bandwidth of an ideal rectangular filter required to pass the same power as the actual filter, is 1.875 × bandwidth.

TEST CONDITIONS

Acoustic measurements were made at wind speeds of 19.8, 30.0, 39.5, 55.9 and 79.1 m/s (64.8, 91.7, 129.7, 183.4, 259.4 ft/s) which correspond to test-section dynamic pressures, q, of 239, 479, 958, 1915 and 3830 N/m^2 (5, 10, 20, 40, 80 lb/ft^2). Unless noted otherwise, the data presented were recorded with a 0.6 cm (1/4 in.) microphone mounted on the tapered strut.

The temperatures, barometric pressures and relative humidities encountered during the test are listed in table 1.

RESULTS AND DISCUSSION

Noise Floor

Figures 3(a) and (b) show test-section noise levels at various dynamic pressures measured with the struts in figure 2(b) installed and all wall holes and the cavity uncovered. Plotted on the same figures are the noise levels measured with all struts, except the tapered microphone strut, removed and the holes and cavity covered. Removing the struts eliminated the tones and lowered the level of broadband noise by as much as 5 dB. The holes and cavity had little effect as will be shown. Aerodynamic noise from the struts dominated the wind-tunnel fan noise at frequencies above 400 Hz, except at the lowest dynamic pressure. The acoustic effect of each potential noise source is examined in the next section.

Data reported by Wilby and Scharton (ref. 1) for the same strut installations as above, except for the microphone stand geometry, are shown in figure 4. The data of figure 4 are around 5 dB greater than the data of figure 3 at frequencies above 1000 Hz. The reasons for the lack of agreement between the two figures are not clear. Stand vibration and/or microphone mounting procedure may have been responsible, as was suggested in an unpublished memorandum from John F. Wilby to Paul Soderman (Subject: Clarification of Figures 19 and 54 in BBN Report 2936, dated August 11, 1975). Stand geometry was not responsible. In any case, data repeatability during the study reported here was quite good even though data from the two studies do not match exactly.

Noise Sources

Microphone strut - Figures 5(a)-(e) show test-section noise levels measured with the two different microphone/strut configurations. The measurements were made at five wind speeds. For these series of measurements all other test-section struts were removed. Typically, the constant-chord strut/microphone configuration was somewhat noisier than the tapered-strut/microphone configuration in the mid-range frequencies around 1000 Hz and

above 3000 Hz. The mid-range noise can be attributed to vortex shedding by using the method described in reference 2.

Assume the Strouhal number is

$$S = \frac{fd}{V} = 0.28 \tag{1}$$

where the dimension d is given by

$$d = 0.6(\delta_u + \delta_l + t) \tag{2}$$

and $\delta_u = \delta_l = 0.48$ cm are the boundary-layer thicknesses at the separation point.[2] Thickness t is the airfoil thickness at the same point (0.75 cm). So, for a speed of $V = 40$ m/s, the vortex shedding frequency, f, is 1090 Hz which agrees with the peak in figure 5(c). The chord-based Reynold's number at 40 m/s was 1380.0; a Reynold's number which lies in a regime in which vortex tones from cylinders (ref. 5) and airfoils (ref. 6) have been recorded.

The high-frequency noise from the constant-chord strut was probably due to flow separation at the blunt trailing edge. The tapered strut had a sharp trailing edge and generated less noise than the other strut at high frequencies.

The tapered strut did not have a dominant vortex shedding tone as shown in figures 5(a)-(e). At first it was suspected that the variation in airfoil thickness, root to tip, spread out the vortex shedding frequencies as predicted by equation 1. However, Schlinker et al. (ref. 5) have shown that a tapered airfoil can generate multiple tones which are stronger than tones from constant-chord airfoils, depending on the Reynold's number. The explanation for the lack of tones from the tapered strut is simply that the chord-based Reynold's numbers were sufficiently high ($Re_{root} = 1 \times 10^6$ at V V = 40 m/s) and the airfoil was sufficiently thick ($t/c_{root} = 0.19$, $t/c_{tip} = 0.29$) that the resulting turbulent boundary layers destroyed any coherent vortex shedding. Paterson et al. (ref. 6) showed that an 18% thick airfoil had no tones for flow Reynold's numbers from 0.4×10^6 to 2.2×10^6 (zero angle of attack). Lower Reynold's number flow was not evaluated.

Pitot-static probe - Figures 6(a)-(f) show the test section noise levels with the pitot-probe support strut at its full 51 cm (20 in.) length and decreased to 18 cm (7 in.). This series of tests were made before the wake-survey strut or diffuser vanes were removed and before the cavity was covered. However, those sources did not mask the pitot-static tone which existed at wind speeds above 30 m/s. At full length the upper airfoil fairing of the pitot-static strut and the lower 0.6 cm (1/4 in.) bar were exposed to the flow. When raised to 18 cm, only the bar was exposed.

---

[2]As the flow approaches separation, the boundary layer grows extremely rapidly resulting in a very thick boundary layer at separation.

The strong tone in the range 1600-3150 Hz was reduced up to 8.5 dB by decreasing the strut length. The tone shifted frequency as the wind speed changed, a characteristic of vortex-shedding noise. Figure 6(f) shows that a tone still existed at 3150 Hz (q = 80 psf) with the probe raised to 18 cm. (Note that the broadband noise in fig. 6(f) had decreased because other struts were removed from the flow.) The tone disappeared only when the strut was removed from the flow. Hence, the airfoil fairing and the 0.6-cm bar generated vortex noise in the same frequency band. The airfoil fairing generated the stronger tone. A plausible reason for the similarity in shedding frequencies is that the vortices shed from the airfoil fairing near the trailing edge where the thickness was similar to that of the 0.6 cm bar. In fact, the airfoil fairing had a blunt trailing edge which, we calculate, allowed turbulent boundary-layer flow separation at 85% chord. Reference 7 contains flow-visualization photographs of the vortex street and resulting acoustic radiation patterns of an airfoil with a blunt trailing edge.

Wake-survey strute - Figures 7(a)-(e) show the test-section noise with and without the wake-survey strut in the flow. The strut was tested in its raised position only. The data show that the strut generated considerable noise in the mid- and high-frequencies. With more of the strut exposed to the flow the noise probably would have been greater. Like the pitot-support strut, the wake-survey strut was not well shaped. It had a 25% thickness-to-chord ratio and a blunt trailing edge (see fig. 2(b)). For acoustic studies, this type of strut should be removed from the test section.

To summarize the results of these sections, strut noise can be minimized by using properly streamlined airfoils, such as the NACA series of airfoils, of a size to operate at sufficiently high Reynold's number. A sufficient Reynold's number is one that results, for the particular airfoil, in a turbulent boundary layer on both airfoil surfaces (ref. 6). The turbulent boundary layers will eliminate coherent vortex shedding. At low Reynold's number the laminar boundary layer can be tripped to achieve the necessary turbulence (ref. 6). Blunt bodies, even airfoil tubing with blunt trailing edges, should be avoided because they can shed coherent vortices in the presence of turbulent boundary layers. It is estimated that the pitot-support strut boundary-layer became turbulent at 50% chord (computations by L. Olson of NASA Ames based on ref. 8) and still did not destroy the coherent vortex shedding. In addition, the pitot-support strut had high-frequency noise probably caused by flow separation near the trailing edge.

Diffuser-entry vanes - The struts which had the least effect on the test-section noise were the two large airfoils used to stabilize the flow into the diffuser (see figs. 8(a)-(e)). The diffuser vanes were also the farthest struts from the microphone. However, due to the reverberant field in the test section, the diffuser vane noise would have decayed only 2 dB more during propagation to the microphone than did the noise from the other struts. The low noise of the vanes was undoubtedly due to the vanes streamlined shape, sharp trailing edge, and high Reynold's number (Re = 1.6×10^6 at V = 40 m/s).

Holes and cavity - Figures 9(a)-(e) show the test-section noise measured with and without the numerous holes in the walls, and the ceiling cavity covered. The holes and cavity had very little effect on the noise. Perhaps that was because of the low speeds used or because the pressures inside and outside the test section were equal so that there was no flow through the holes. Also, the cavity had a screen cover and was open in the back so that a trapped vortex was unlikely. A trapped vortex is characteristic of cavity noise.

Microphone - A comparison of the noise measured by a 1.3 cm (1/2 in.) (B&K 4133) and a 0.6 cm (1/4 in.) (B&K 4135) microphone is shown on figures 10(a)-(e). The microphones and nose cones were mounted on the same preamp and support stand. The acoustic spectra are quite similar except at frequencies above 12 kHz. Note that the 0.6 cm (1/4 in.) microphone-data lower limit was 60 dB, so comparisons cannot be made below that level.

Fan noise - Figure 11 shows the noise of the empty test section (fig. 4) compared with predicted fan noise in the test section. The predicted fan noise was extrapolated from noise levels in the settling chamber measured during the experiment described in reference 1. The measurements and extrapolation are described in appendix A. Except for the lower dynamic pressures, the data and predictions agree up to 800 Hz. Above 1000 Hz, the predicted noise levels are much lower than the measured levels. Two possible explanations come to mind: 1) other noise sources, such as microphone strut noise or turning-vane noise, were responsible for the high frequency sound; or 2) the fan noise prediction is inaccurate. With respect to explanation 1, microphone wind noise is discounted as a major noise source based on the data of Noiseux et al. (ref. 4) shown in figure 12. Those results show quite low levels of microphone self-noise for low turbulence flow.

Narrow-band Frequency Analysis

Figures 13(a)-(c), from reference 1, show the test-section noise spectra filtered in constant bandwidths 5 Hz and 12.5 Hz wide. The pitot-strut tone is clearly shown. All struts were in the test section. The microphone was mounted to the constant-chord airfoil tubing.

Similar data measured in this study are shown in figures 14(a)-(f). The estimated sources of the tones are noted on the figures. The airfoil struts, especially the wake-survey strut, were responsible for the broadband noise above 250 Hz.

The clean-test-section noise spectra are shown in figures 15(a)-(f). As expected, the tones disappeared and the broadband noise decreased except at the low frequencies where fan noise dominated.

CONCLUDING REMARKS

Despite the entry of wind-tunnel fan noise into the test section, the background noise in the 7- by 10-Foot (2.1- by 3.0 m) Wind Tunnel No. 1 test section above 400 Hz was dominated by aerodynamic noise from various struts in the test section. The two major sources were a pitot-support strut and a wake-survey strut. Strong tones from the pitot-support strut were related to a vortex shedding rate. Broadband noise was generated by the wake-survey strut. Both airfoils had large thickness-to-chord ratios (20 to 25%) and blunt trailing edges which could cause flow separation and strong vortex shedding. Although these types of airfoils are acceptable for their particular aerodynamic functions, they are unnecessarily noisy. Streamline shapes like the NACA airfoils should be less noisy as long as the boundary layers are tripped when used at low Reynolds numbers.

The holes and screen-covered cavity in the test-section walls did not generate measurable noise at the test air speeds. It should be noted that the wind tunnel did not have a pressure difference across the test-section walls and, therefore, no significant air flow through the holes. Air flow might affect hole-generated noise.

With the struts removed, the wind-tunnel fan noise dominated the acoustic spectrum below 1000 Hz. Therefore, acoustic treatment upstream and downstream of the fans is necessary to reduce test-section noise below 1000 Hz. The noise above 1000 Hz, struts removed, did not match predicted fan noise levels. Either the prediction was erroneous or there was some other noise source in the wind tunnel, as yet unknown.

APPENDIX A

FAN NOISE PREDICTION

(From reference 1 and John F. Wilby/Paul Soderman memorandum)

The estimated fan noise spectra shown in figure 11 are based on measured fan sound pressure levels in the diffuser and estimated fan noise variation with fan speed. Starting with the noise variation method, it was assumed that the fan sound level is proportional to fan tip speed to the power five. That assumption was based on emperical fan laws (see ref. 1). Since tip speed is proportional to fan rotational speed, rpm, the data would scale as follows:

$$\Delta dB = 50 \log \frac{rpm_2}{rpm_1} + 10 \log \frac{f_2}{f_1} \qquad (A1)$$

where the last term is the bandwidth correction factor. Since the acoustic frequencies of blade-passage noise and vortex noise are also proportional to rpm, $f_2/f_1 = rpm_2/rpm_1$, and equation (A1) can be written:

$$\Delta dB = 60 \log \frac{rpm_2}{rpm_1} \qquad (A2)$$

Dynamic pressure, q, is proportional to tip speed squared. Therefore, equation (A2) can be written:

$$\Delta dB = 30 \log \frac{q_2}{q_1} \qquad (A3)$$

The above scaling equation was checked by measuring noise levels in the settling chamber at various test-section dynamic pressures. Because of the low wind speeds in the settling chamber, it was felt that the noise was predominantly fan noise. When normalized to q = 25 psf using equation (A3), the data collapsed fairly closely to the following values.

f, Hz	1/3 oct. band SPL -30 log (q/25)
125	84
250	84
500	81
1000	76
2000	70
4000	63
8000	55

By placing a calibrated noise source in the fan section, it was determined that the settling chamber noise levels are approximately 2 dB lower than the test-section levels. That correction added to the above spectrum levels resulted in the q = 25 spectrum of figure 11. The other spectra were estimated using equation (A3).

REFERENCES

1. Wilby, J. F.; and Scharton, T. D.: Evaluation of the NASA Ames #1 7 × 10 Foot Wind Tunnel As An Acoustic Test Facility. NASA CR-137712, 1975.

2. Soderman, P. T.: Instrumentation and Techniques for Acoustic Research in Wind Tunnels. ICIASF '75 RECORD, International Congress on Instrumentation in Aerospace Simulation Facilities, Sept. 22-24, 1975, Ottawa, Canada, pp. 270-276, IEEE Publication 75 CHO 993-6 AES.

3. Bender, J.; and Arndt, R. E. A.: Aeroacoustic Research in Wind Tunnels: A Status Report. NASA CR-114575, 1973.

4. Noiseux, D. U.; Noiseux, N. P.; and Kadman, Y.: Study of a Porous Microphone Sensor in an Aerofoil. NASA CR-137652, 1975.

5. Schlinker, R. H.; Fink, M. R.; and Amiet, R. K.: Vortex Noise from Nonrotating Cylinders and Airfoils. AIAA Paper No. 76-81, January 1976.

6. Paterson, R. W.; Vogt, P. G.; Fink, M. R.; and Munch, C. L.: Vortex Noise of Isolated Airfoils. AIAA Paper No. 72-656, June 1972.

7. Lawrence, L. F.; Schmidt, S. F.; and Looschen, F. W.: A Self-Synchronizing Stroboscopic Schlieren System for the Study of Unsteady Air Flows. NACA TN-2309, 1951.

8. Dvorak, F. A.; and Woodward, F. A.: A Viscous/Potential Flow Interaction Analysis Method for Multi-Element Infinite Swept Wings. Volume 1, NASA CR-2476, 1974.

TABLE 1.- ATMOSPHERIC CONDITIONS

Time	Date	Run	Temperature[a]	Relative humidity[b]	Barometer
----	6/6/75	1	72°F	.61	30.11 in. Hg
----	6/6/75	2	72	.57	30.10
1000	6/9/75	3	70	.68	30.05
1600	6/9/75	5	82	.48	30.00
0820	6/10/75	6	64	.75	30.00
1035	6/10/75	7	74	.57	29.90
1335	6/10/75	8	77	.63	30.02
1615	6/10/75	9	78	.43	30.02
0900	6/11/75	10	63	.69	30.08
1350	6/11/75	11	70	.68	30.01
1555	6/11/75	13	73	.53	30.10
0920	6/12/75	14	66	.62	30.08
1045	6/12/75	15	69	.59	30.09

[a]Measured in test section before or after run.

[b]Computed from wet and dry temperature and barometric pressure.

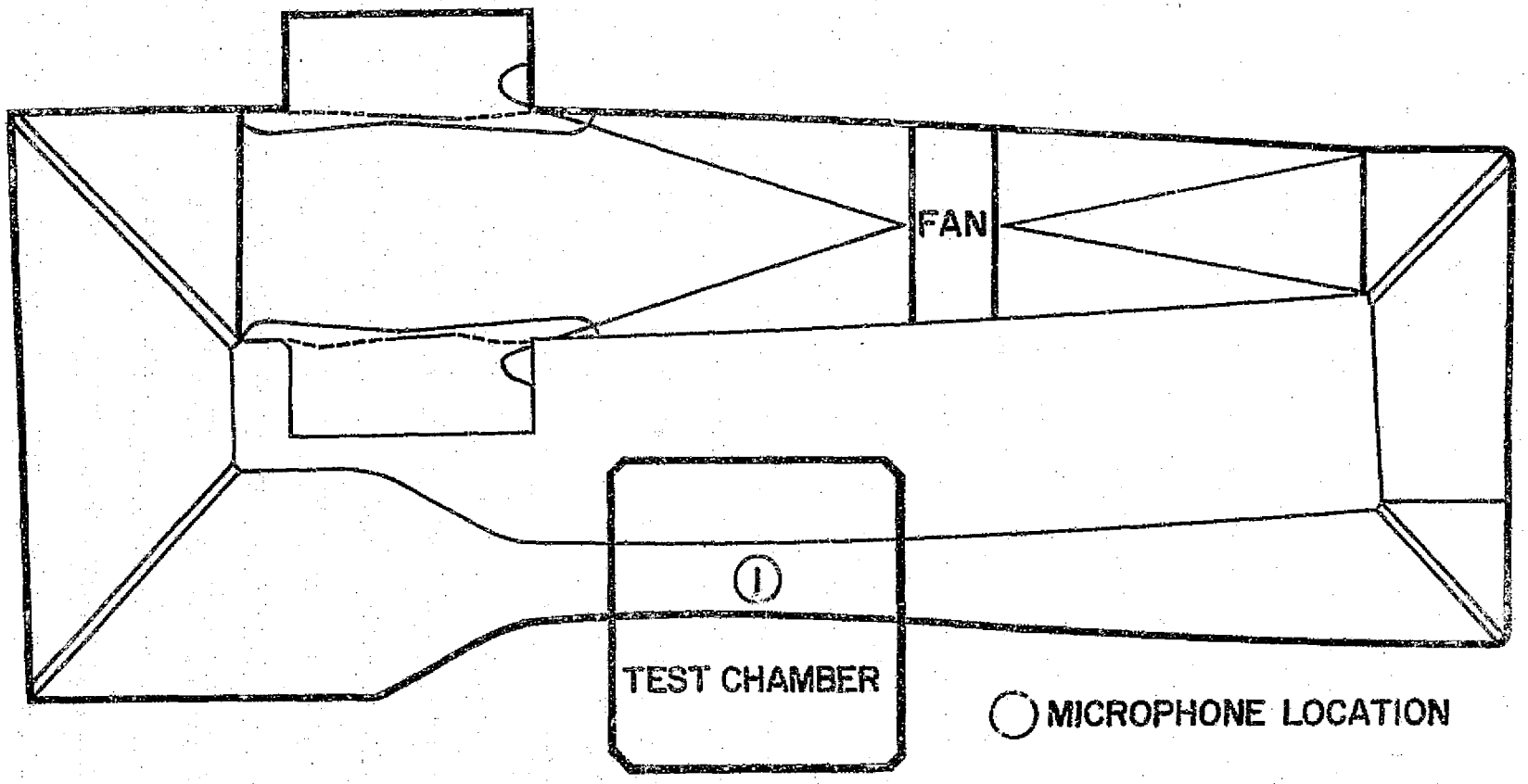

Figure 1a.- Schematic of 7 × 10 Ft Wind Tunnel.

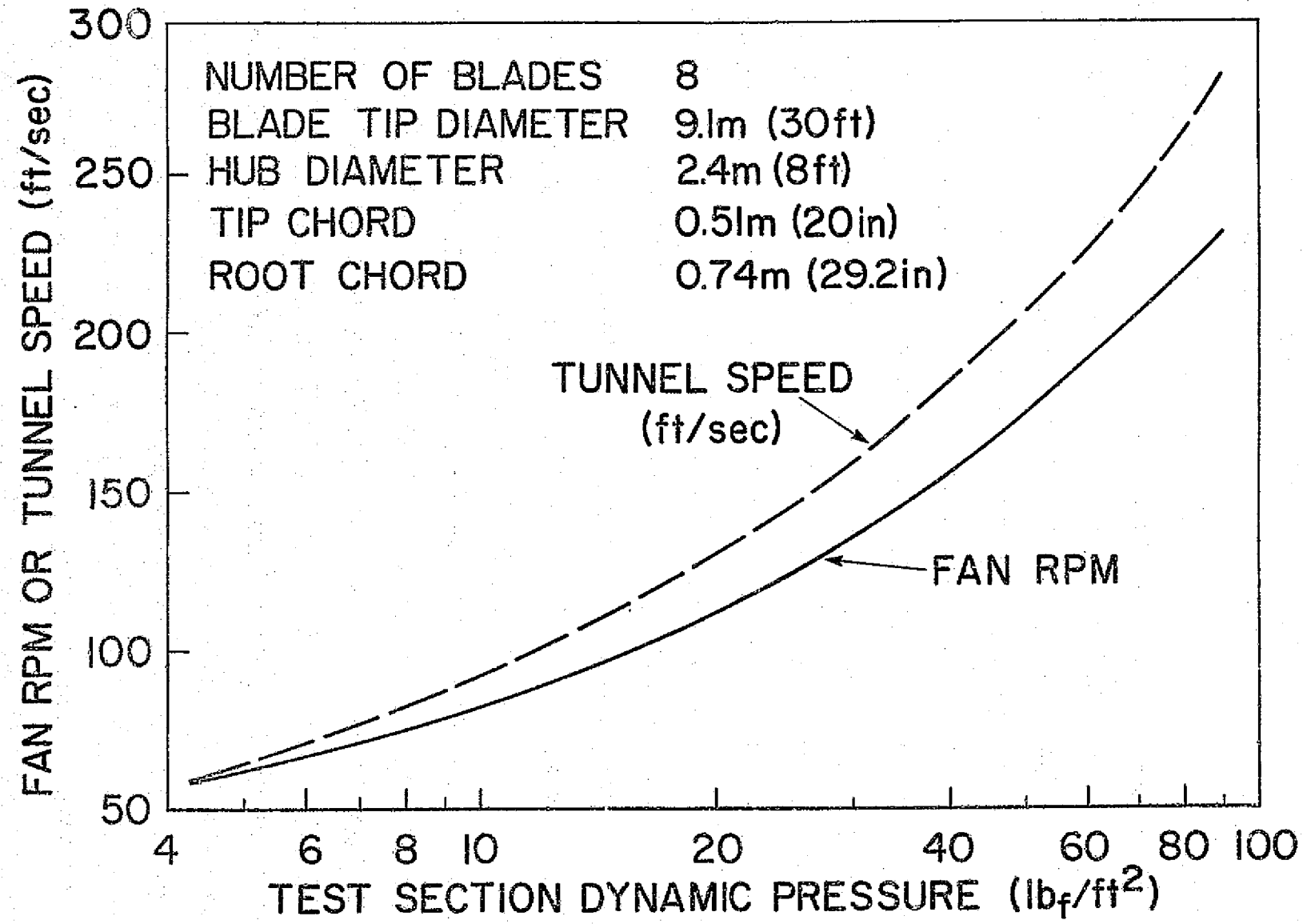

Figure 1b.- Tunnel operating conditions and fan geometry.

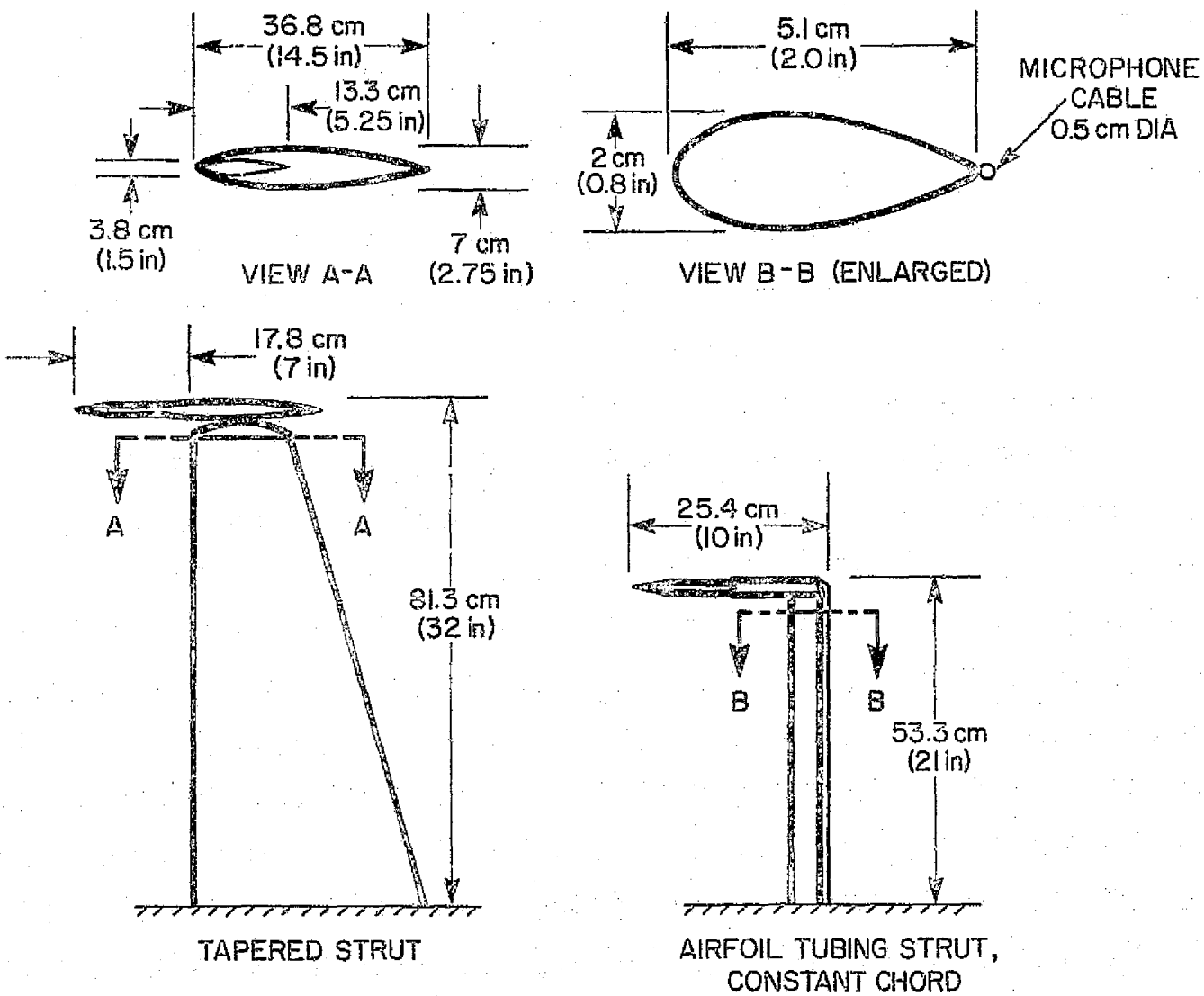

(a) Microphone support stands.

Figure 2.- Airfoil struts in the test section.

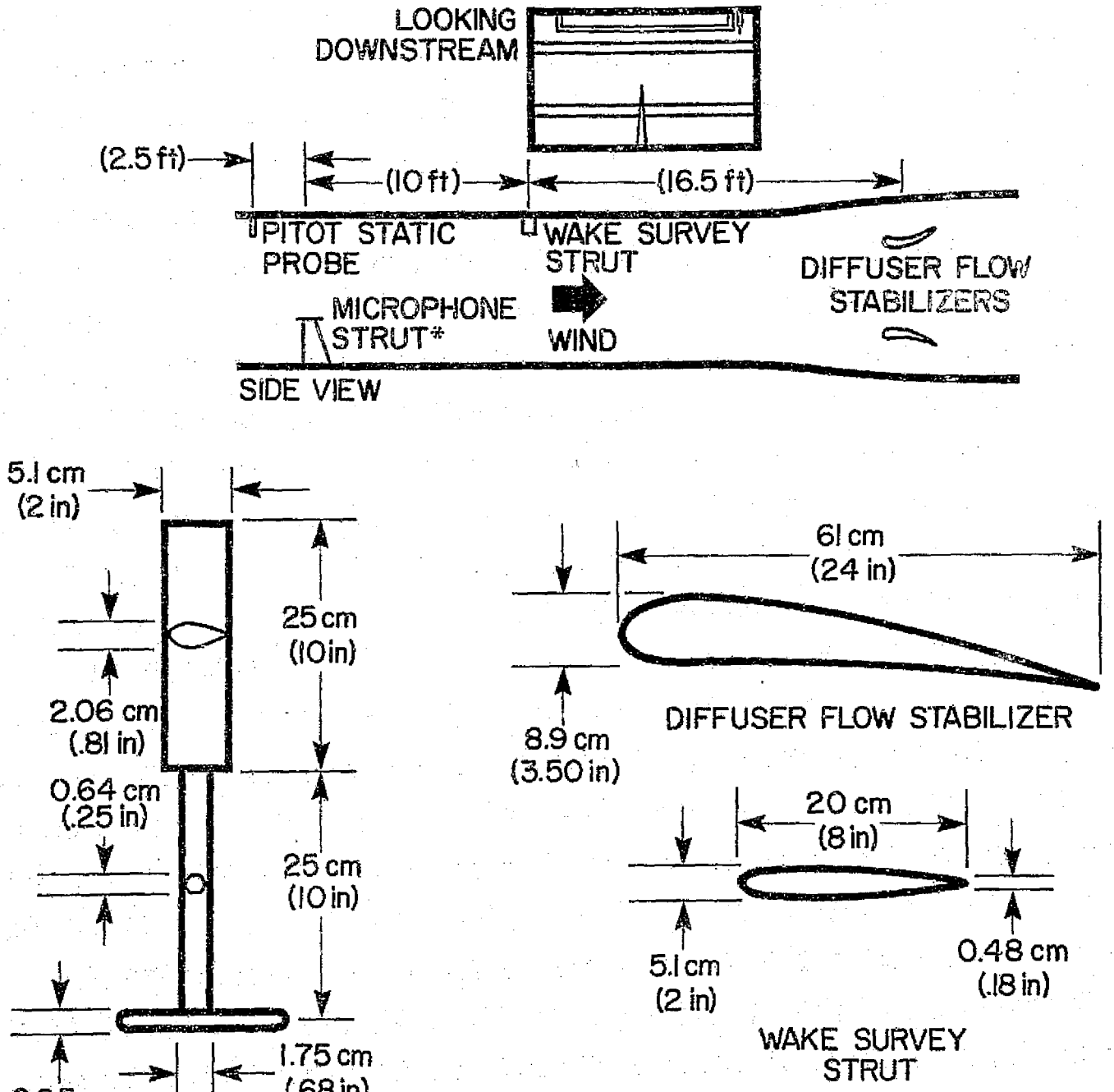

(b) Miscellaneous struts.

* SEE FIG. 2A

Figure 2.- Concluded.

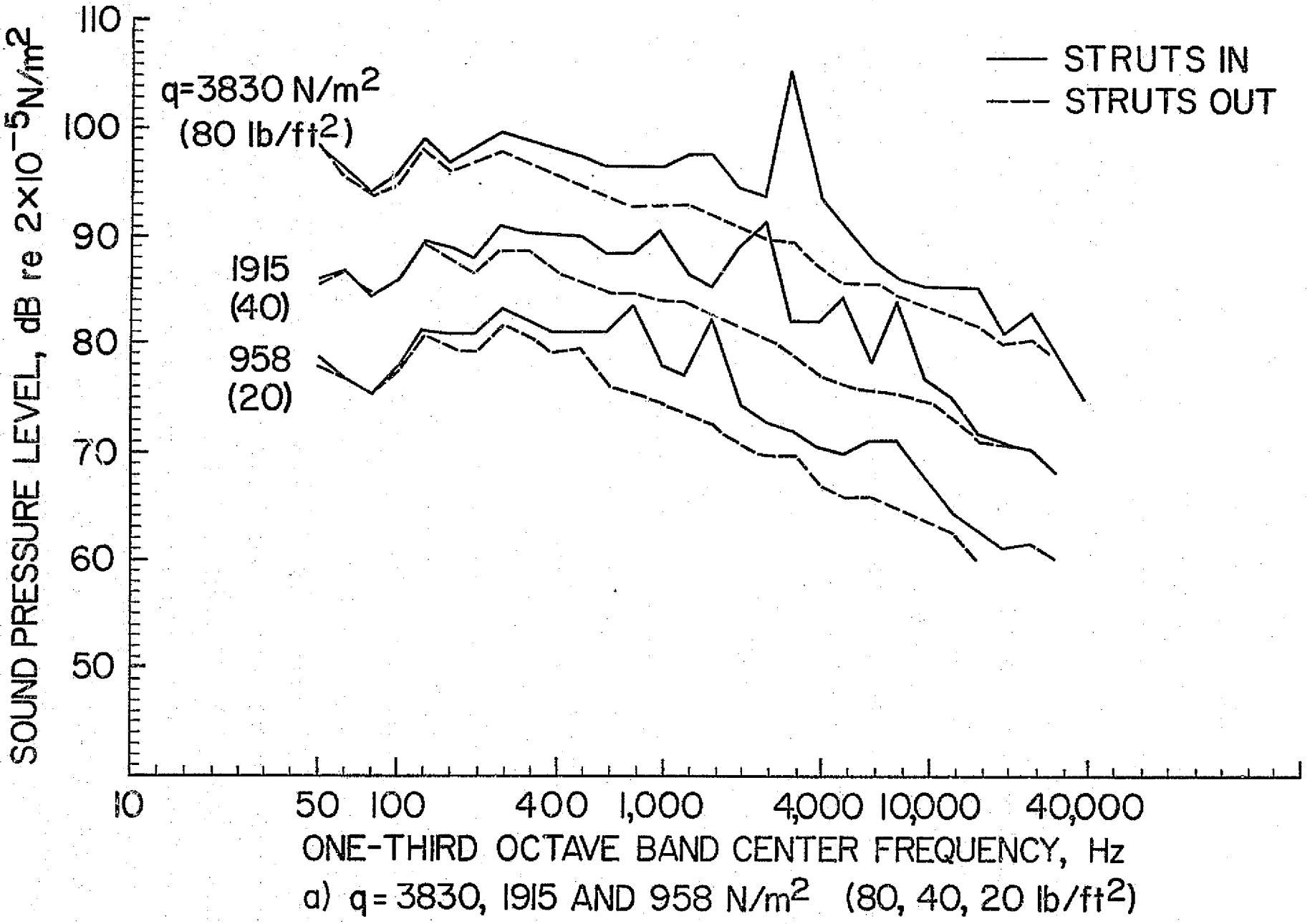

Figure 3.- Comparison of test-section noise levels with struts of fig. 2b in and out; microphone on tapered stand.

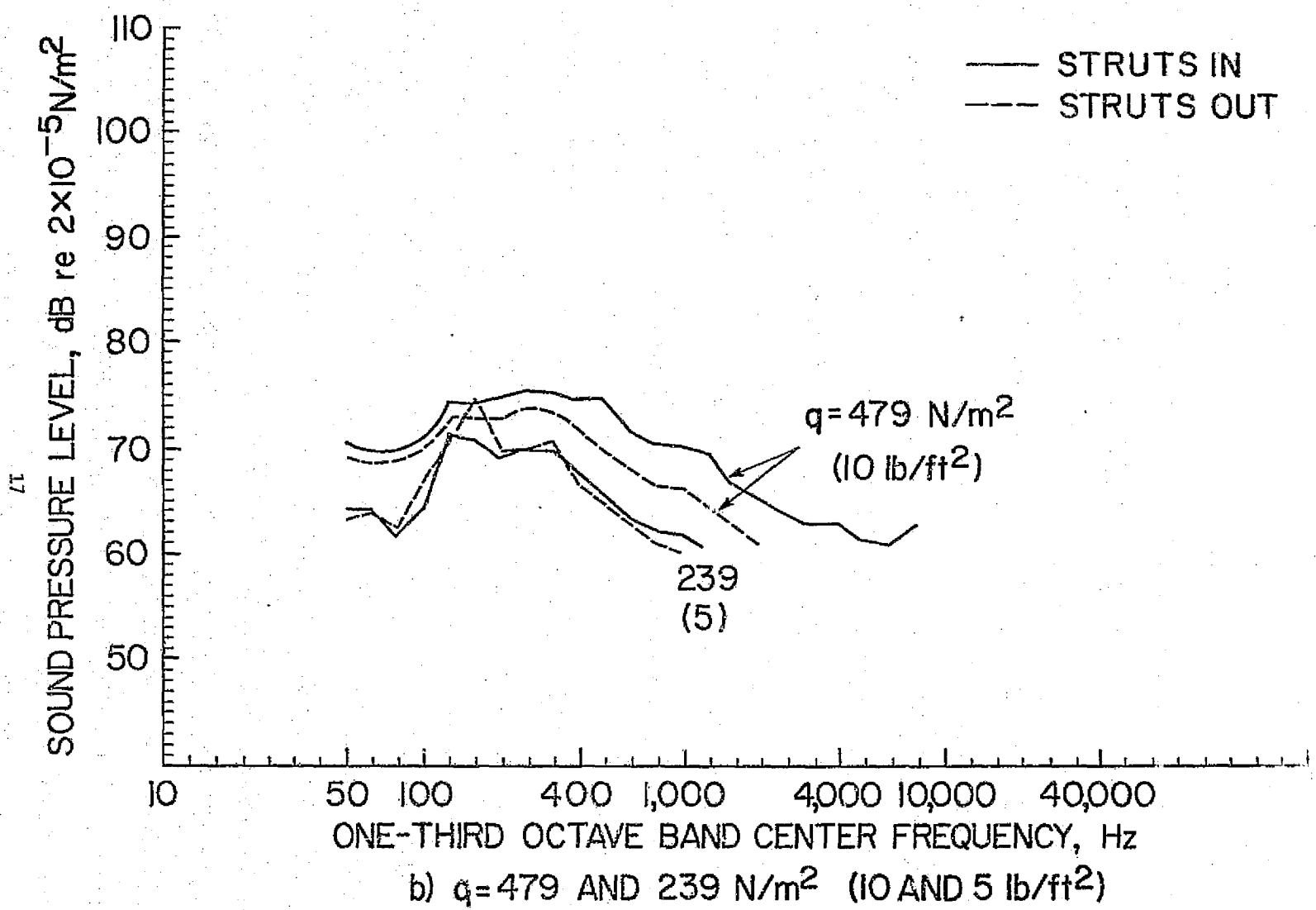

Figure 3.- Concluded.

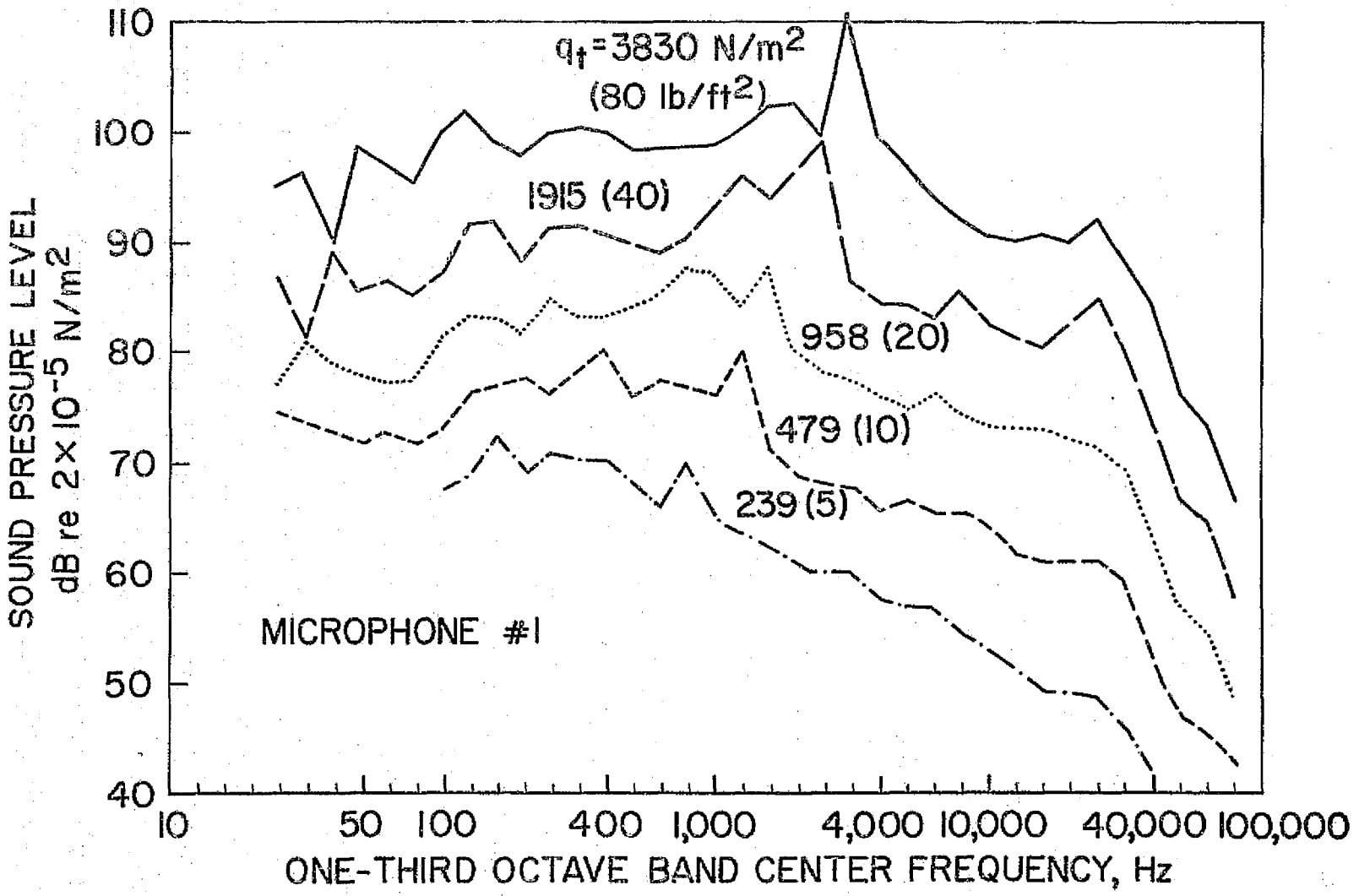

Figure 4.- Test-section noise levels with struts of fig. 2b installed; data from ref. 1; microphone on constant-chord stand.

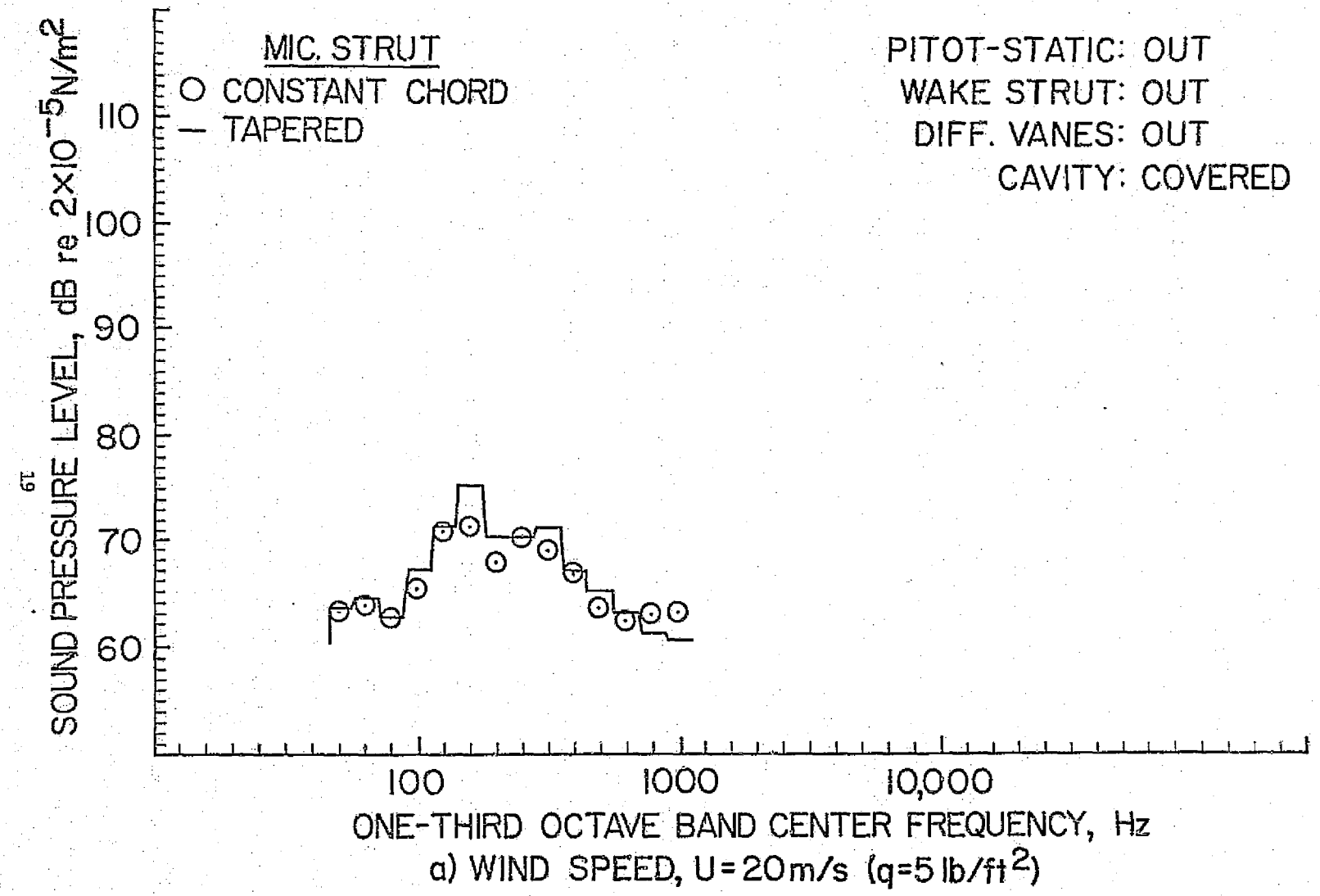

Figure 5.- Effect of microphone strut shape on test-section noise.

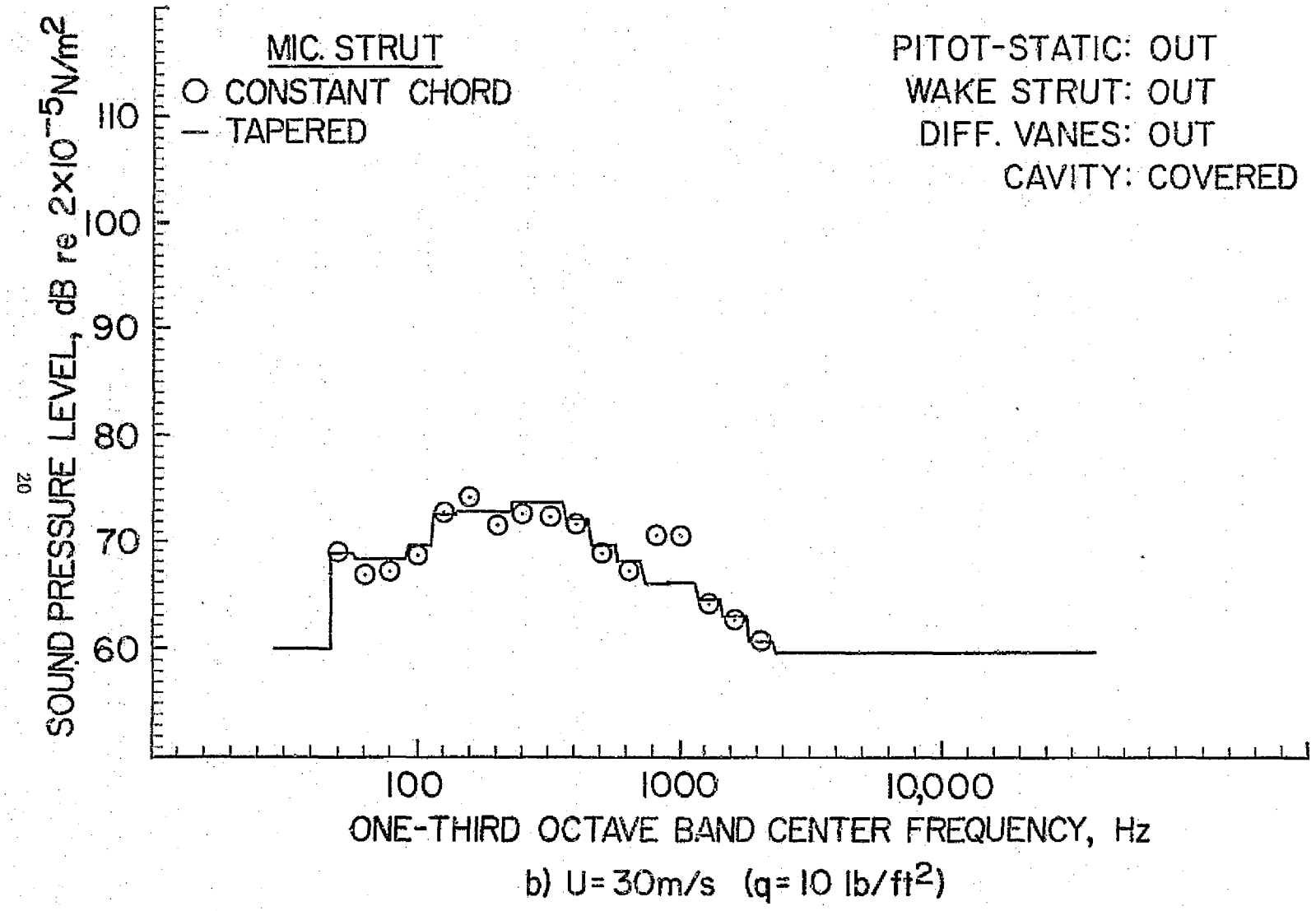

b) U = 30m/s (q = 10 lb/ft^2)

Figure 5.- Continued.

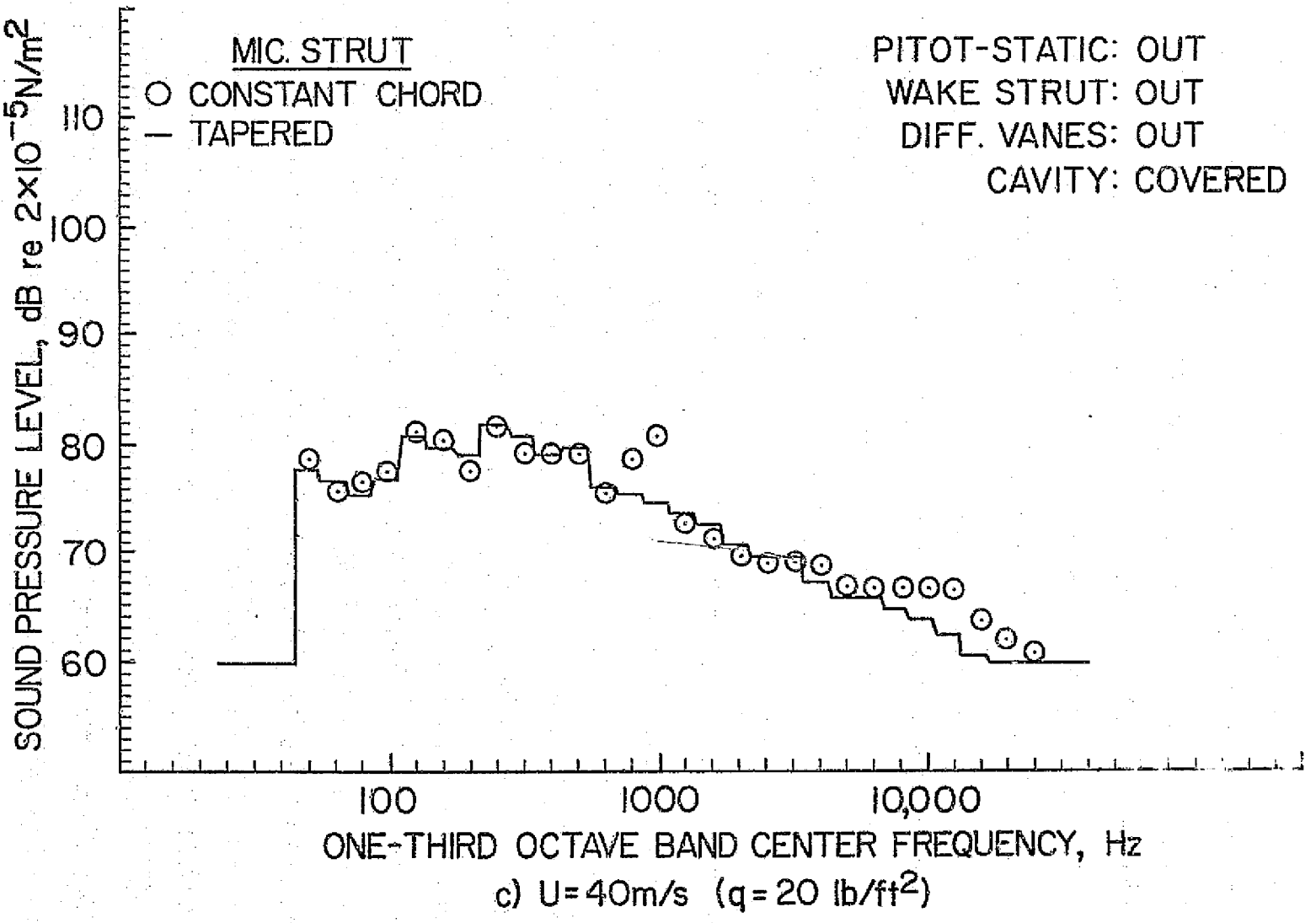

c) U = 40m/s (q = 20 lb/ft^2)

Figure 5.- Continued.

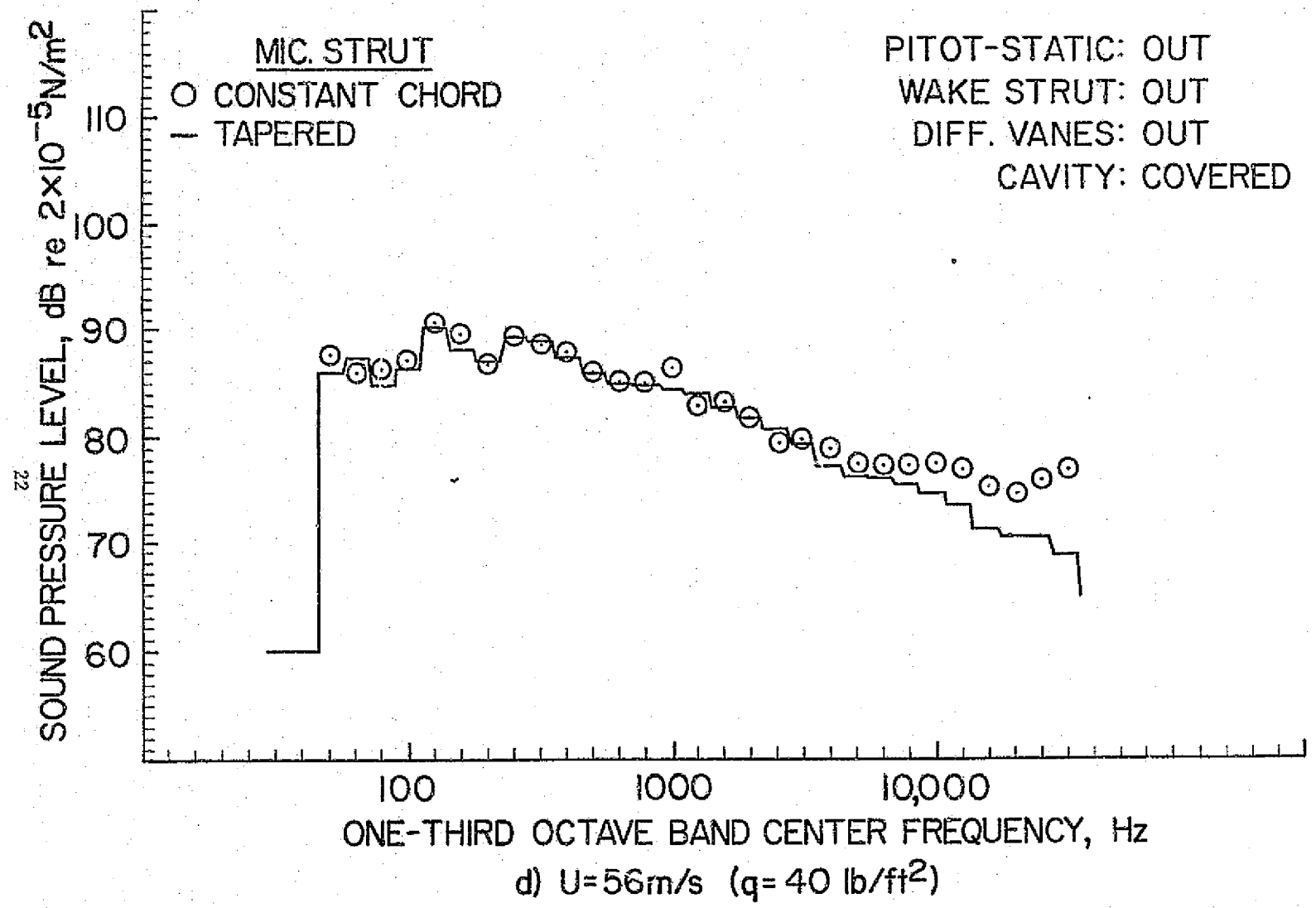

d) U=56m/s (q= 40 lb/ft^2)

Figure 5.- Continued.

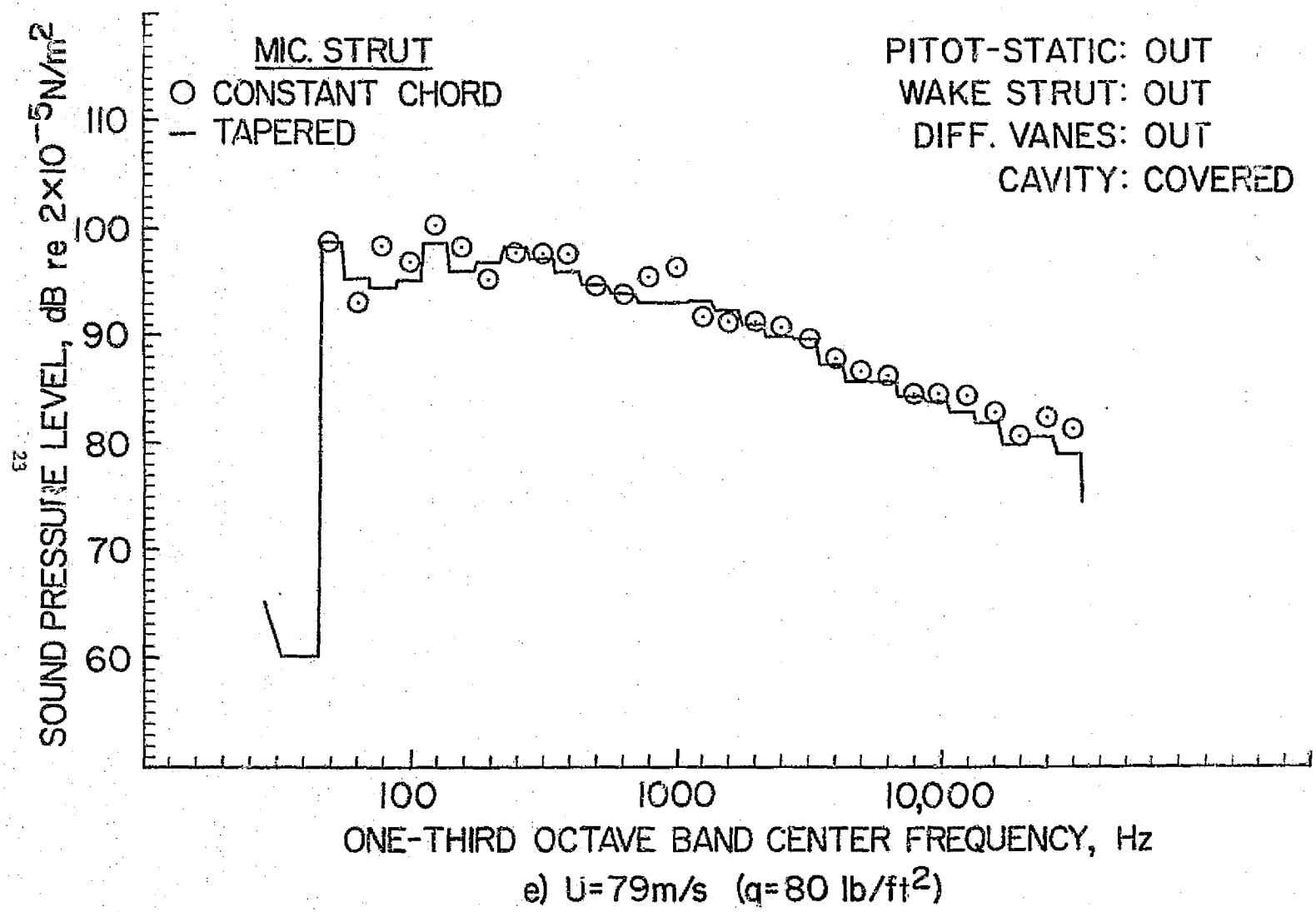

Figure 5.- Concluded.

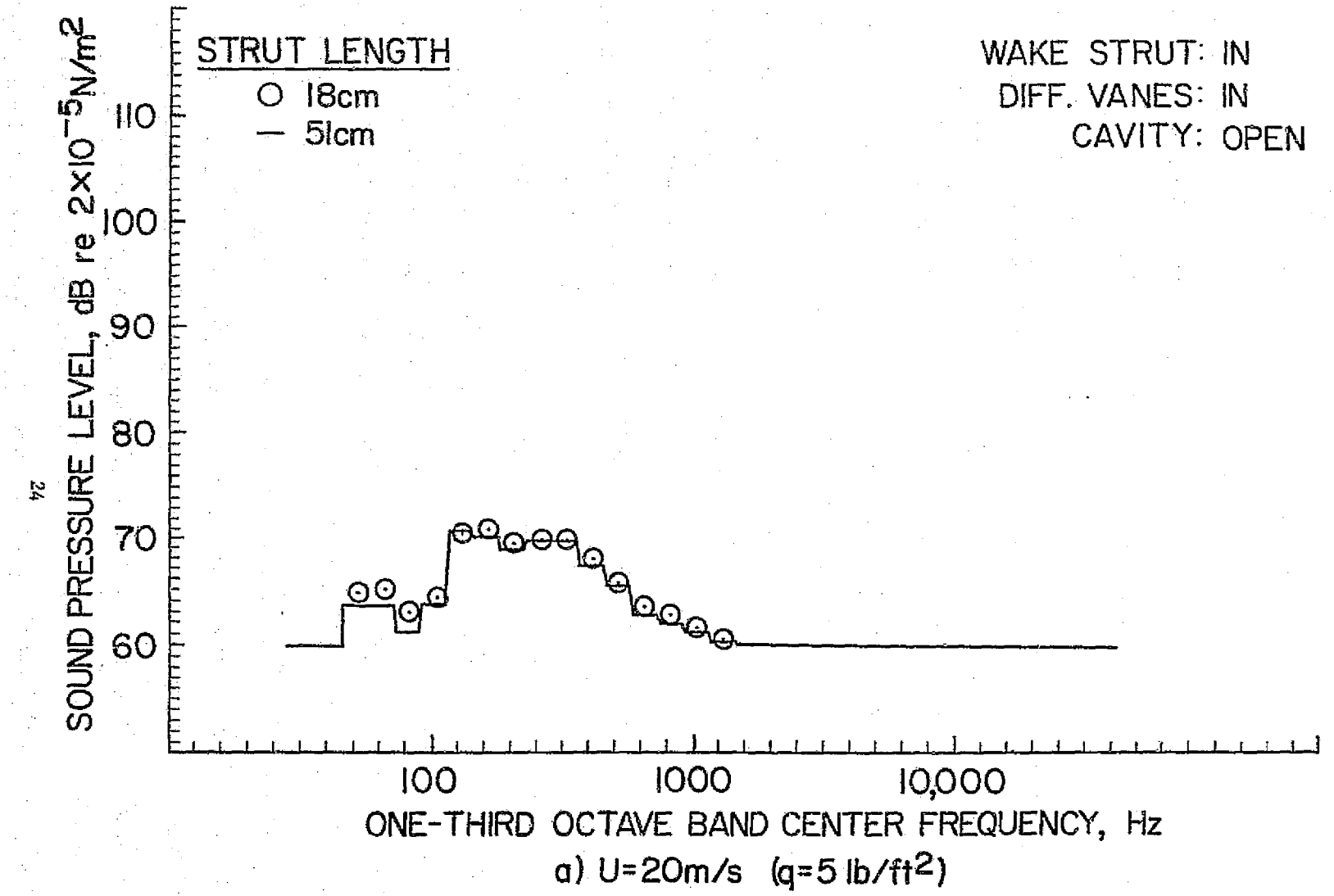

Figure 6.- Effect of pitot-static probe support strut on test-section noise.

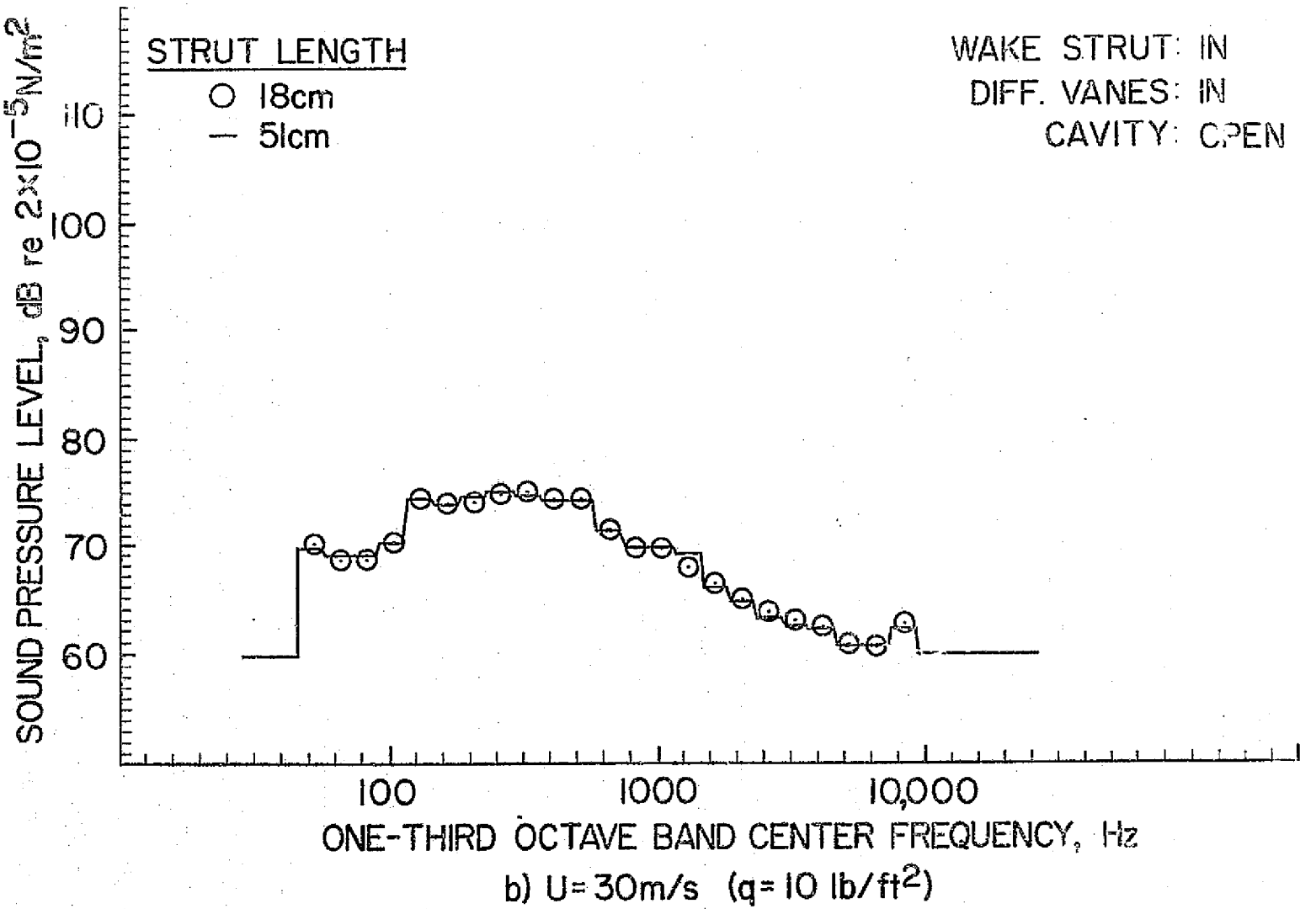

b) U = 30m/s (q = 10 lb/ft^2)

Figure 6.- Continued.

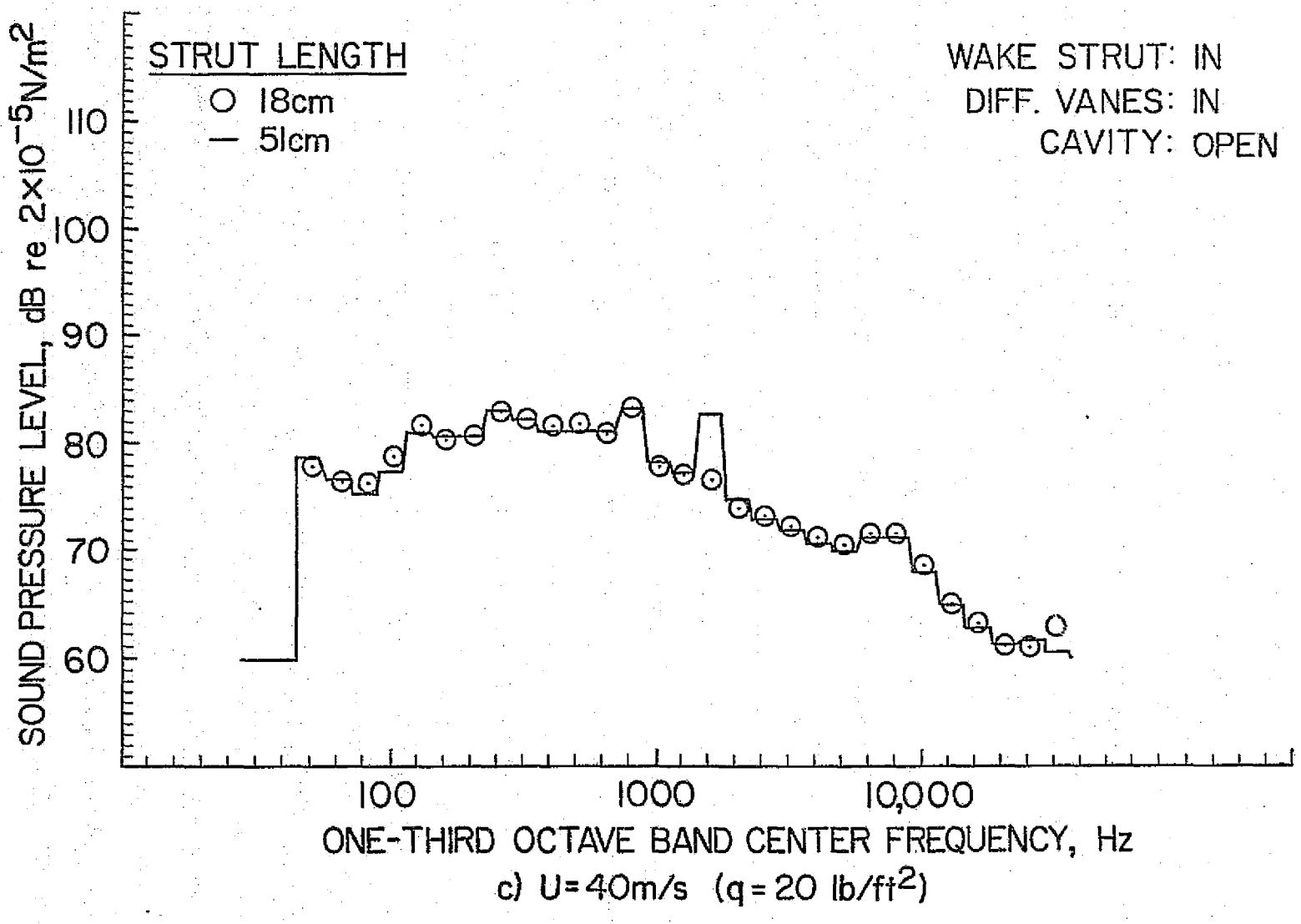

Figure 6.- Continued.

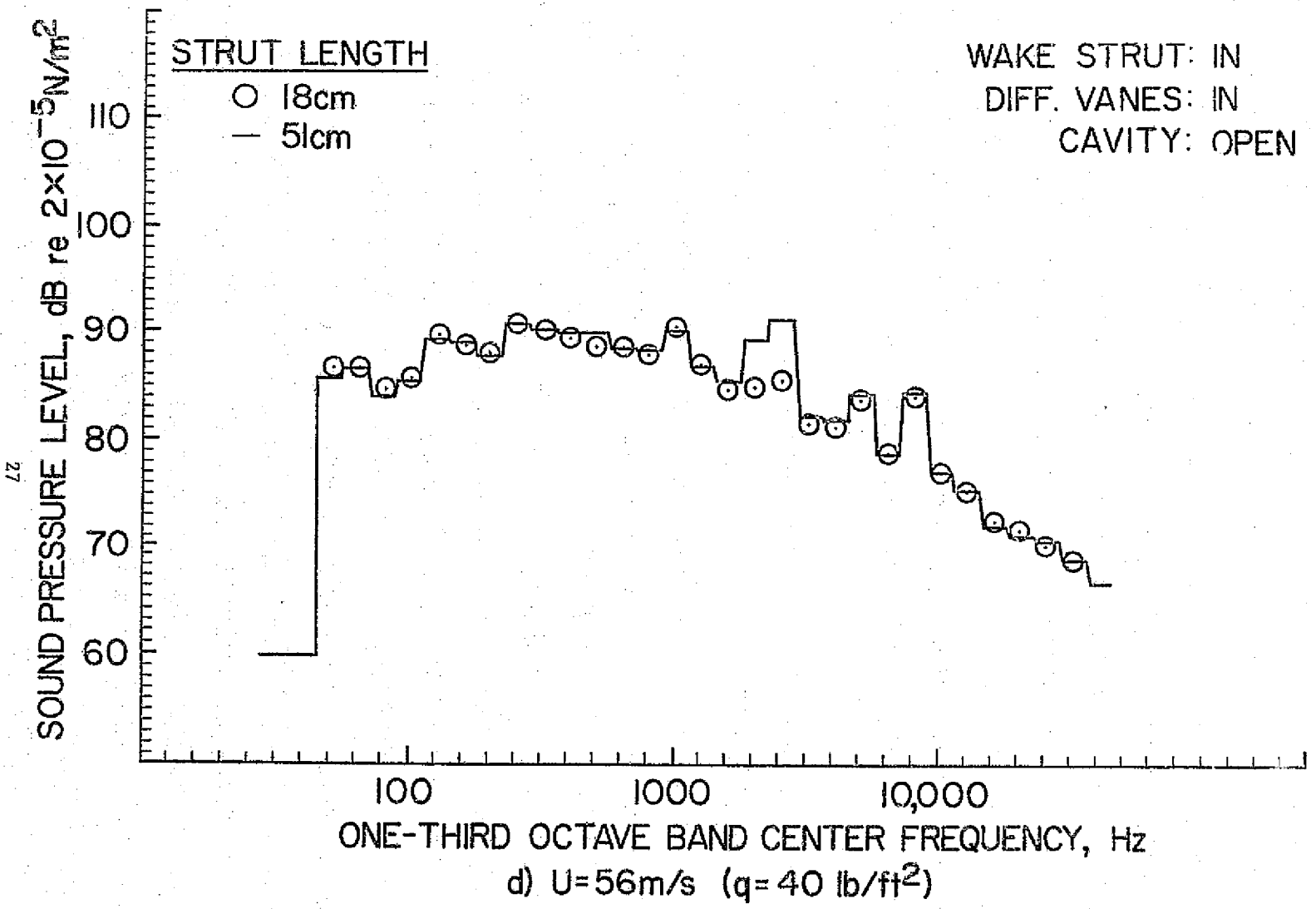

Figure 6.- Continued

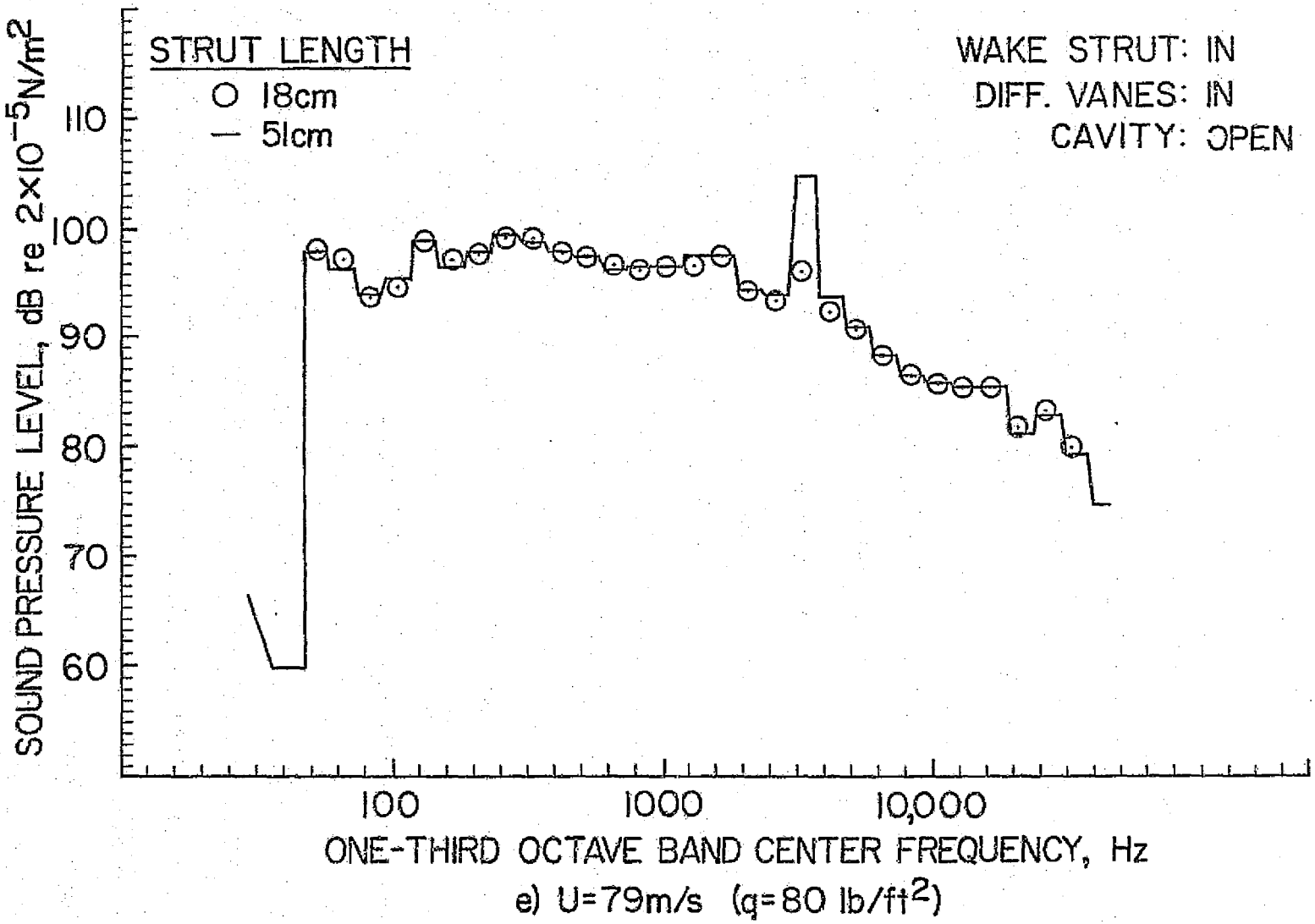

Figure 6.- Continued.

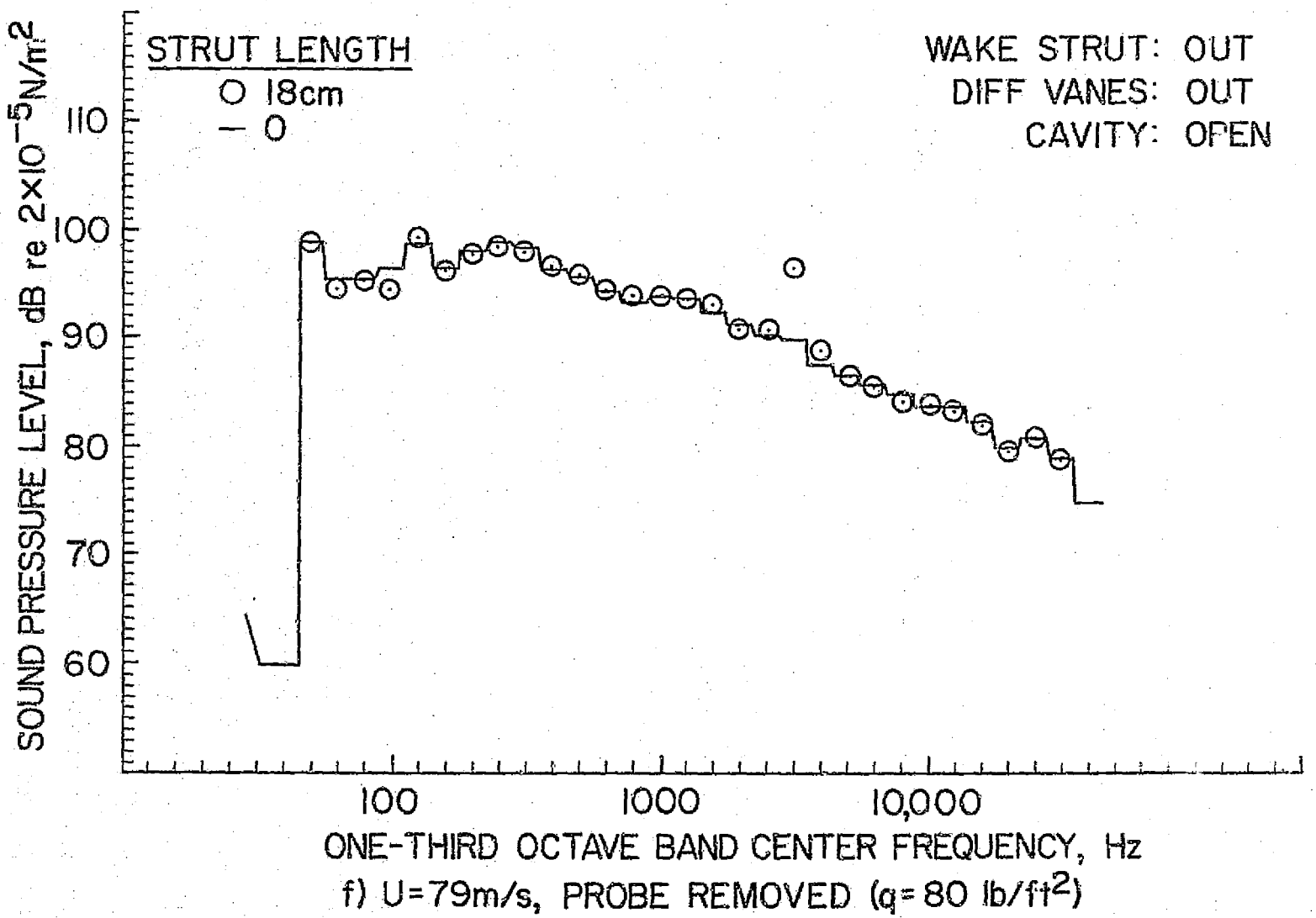

Figure 6.- Concluded.

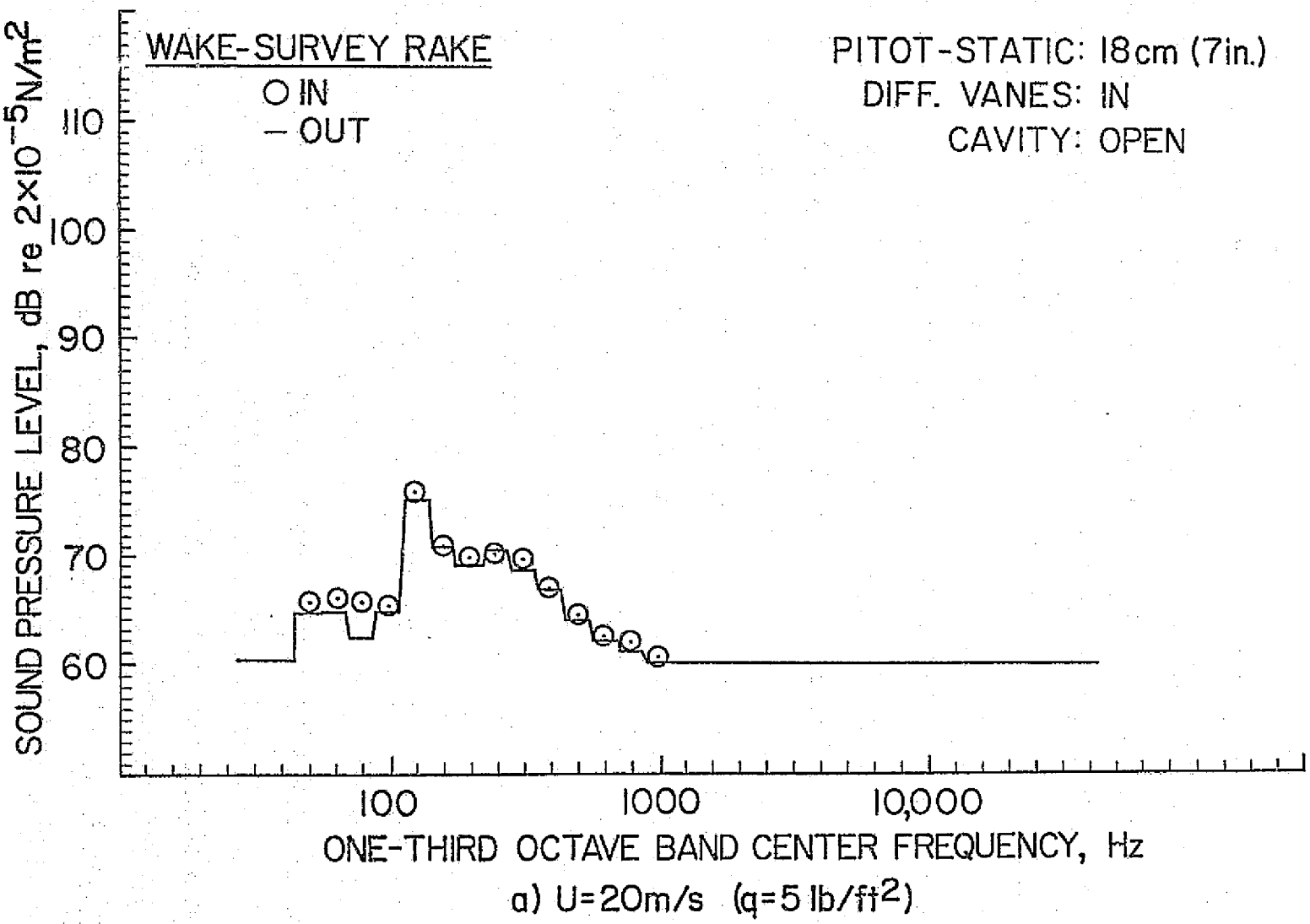

Figure 7.- Effect of wake survey strut on test-section noise.

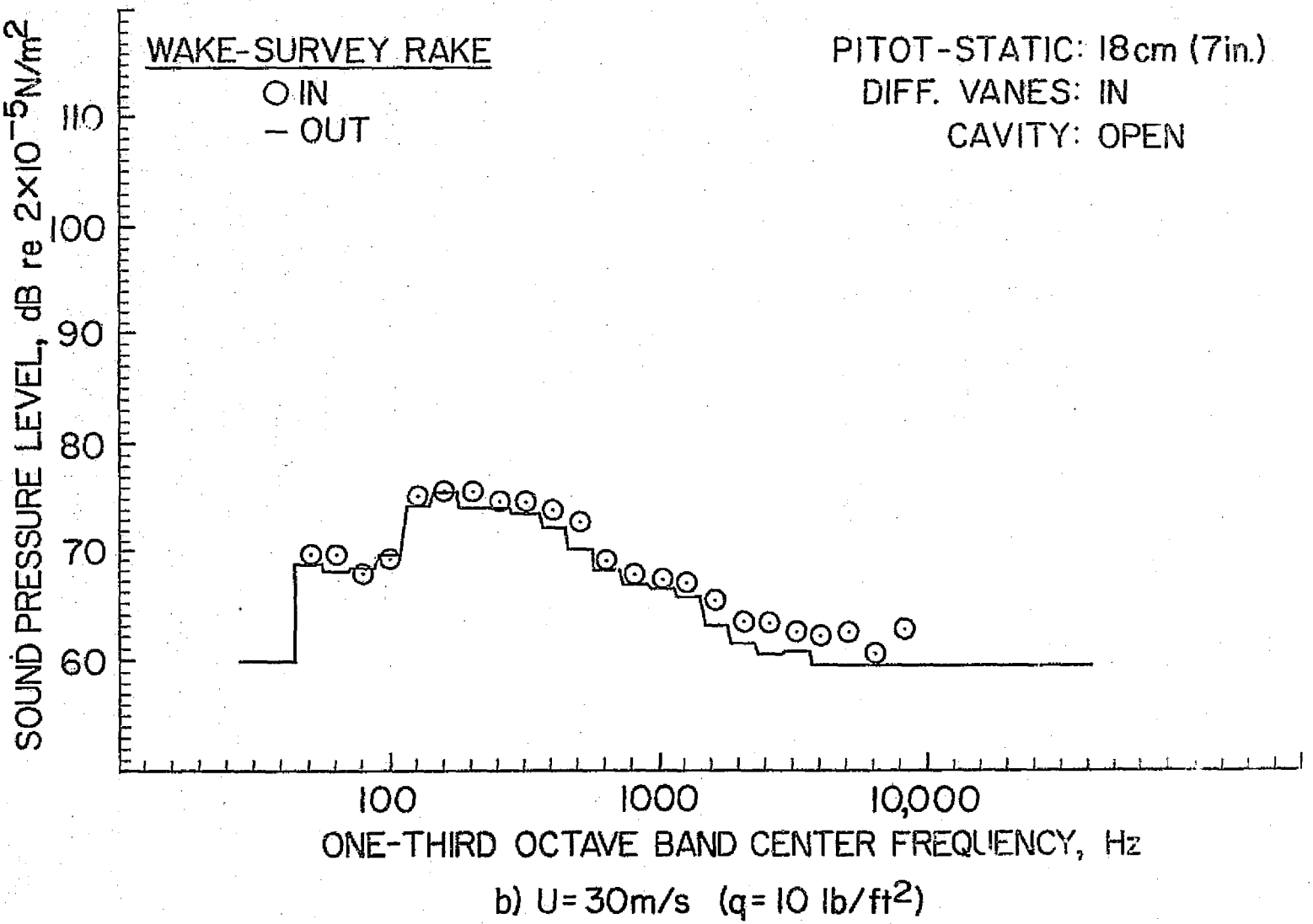

b) U = 30m/s (q = 10 lb/ft^2)

Figure 7.- Continued.

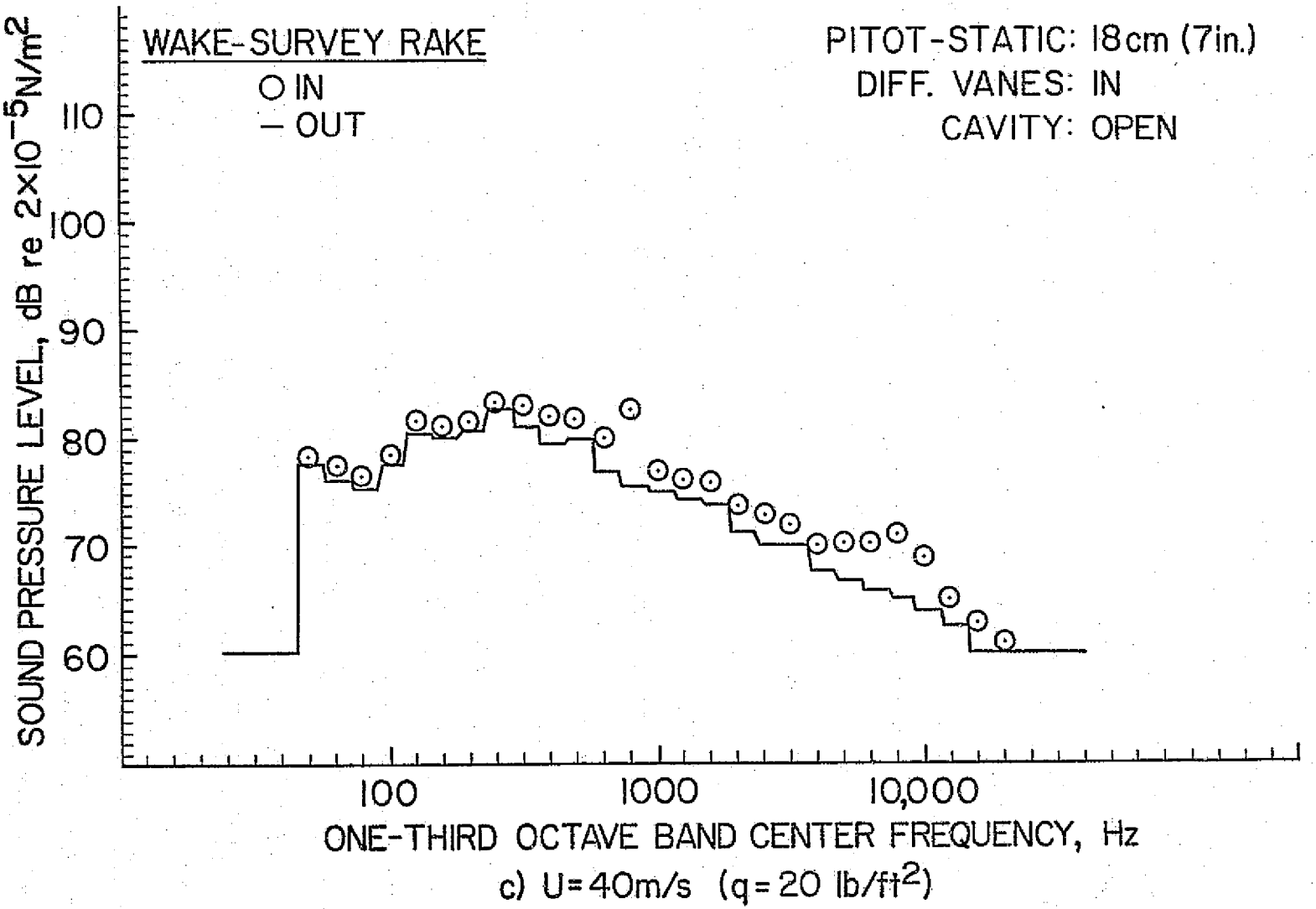

Figure 7.- Continued.

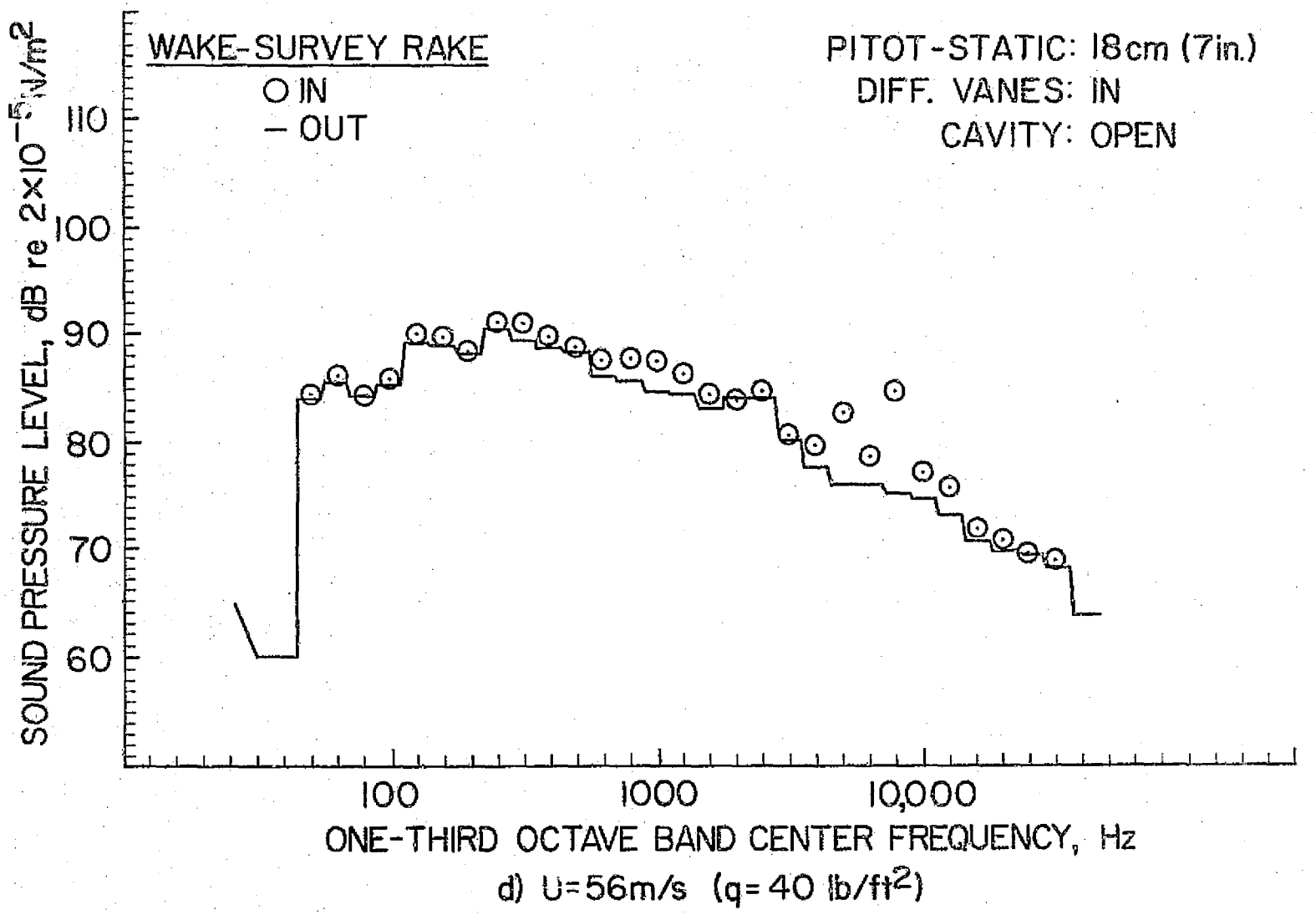

Figure 7.- Continued.

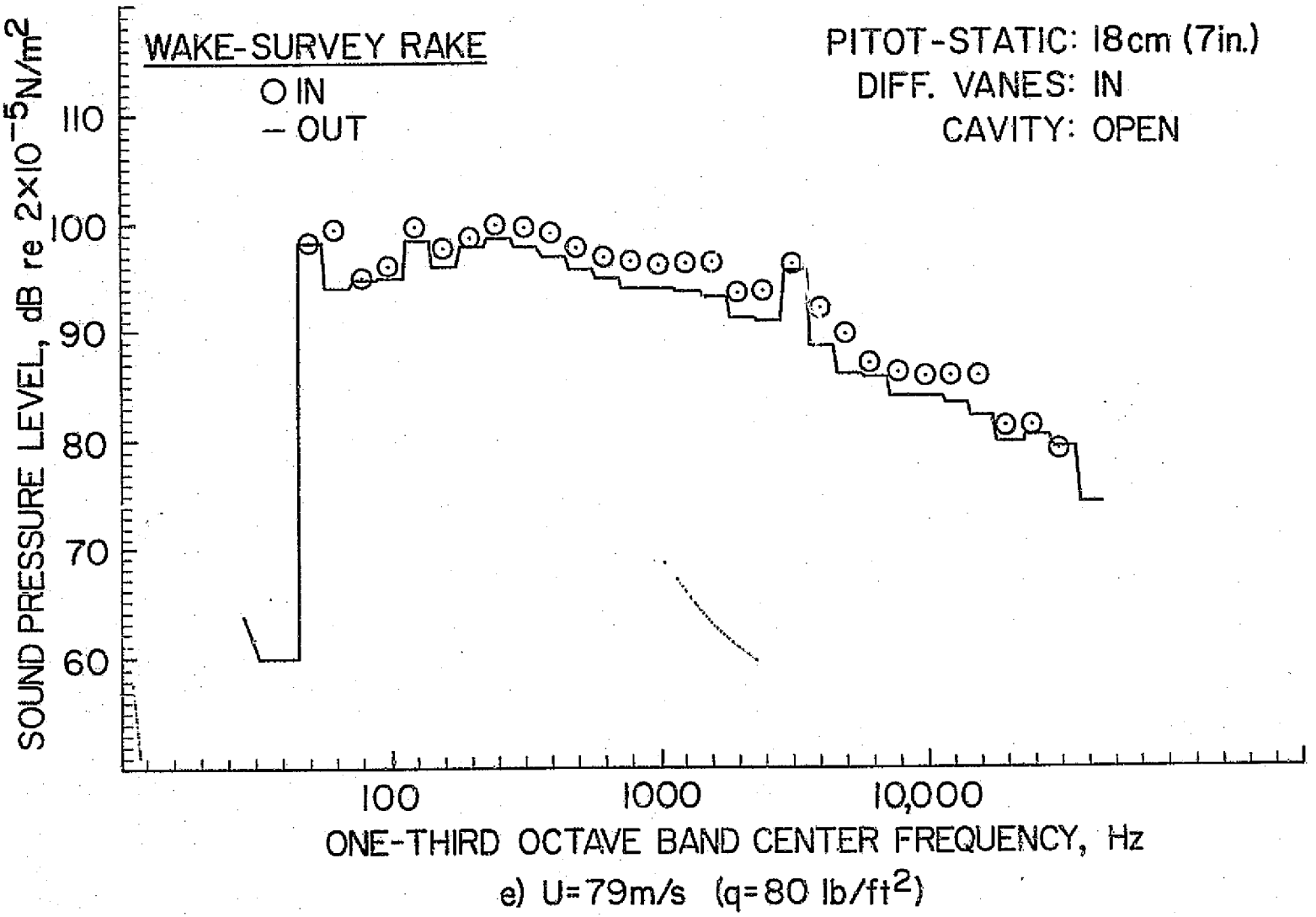

Figure 7.- Concluded.

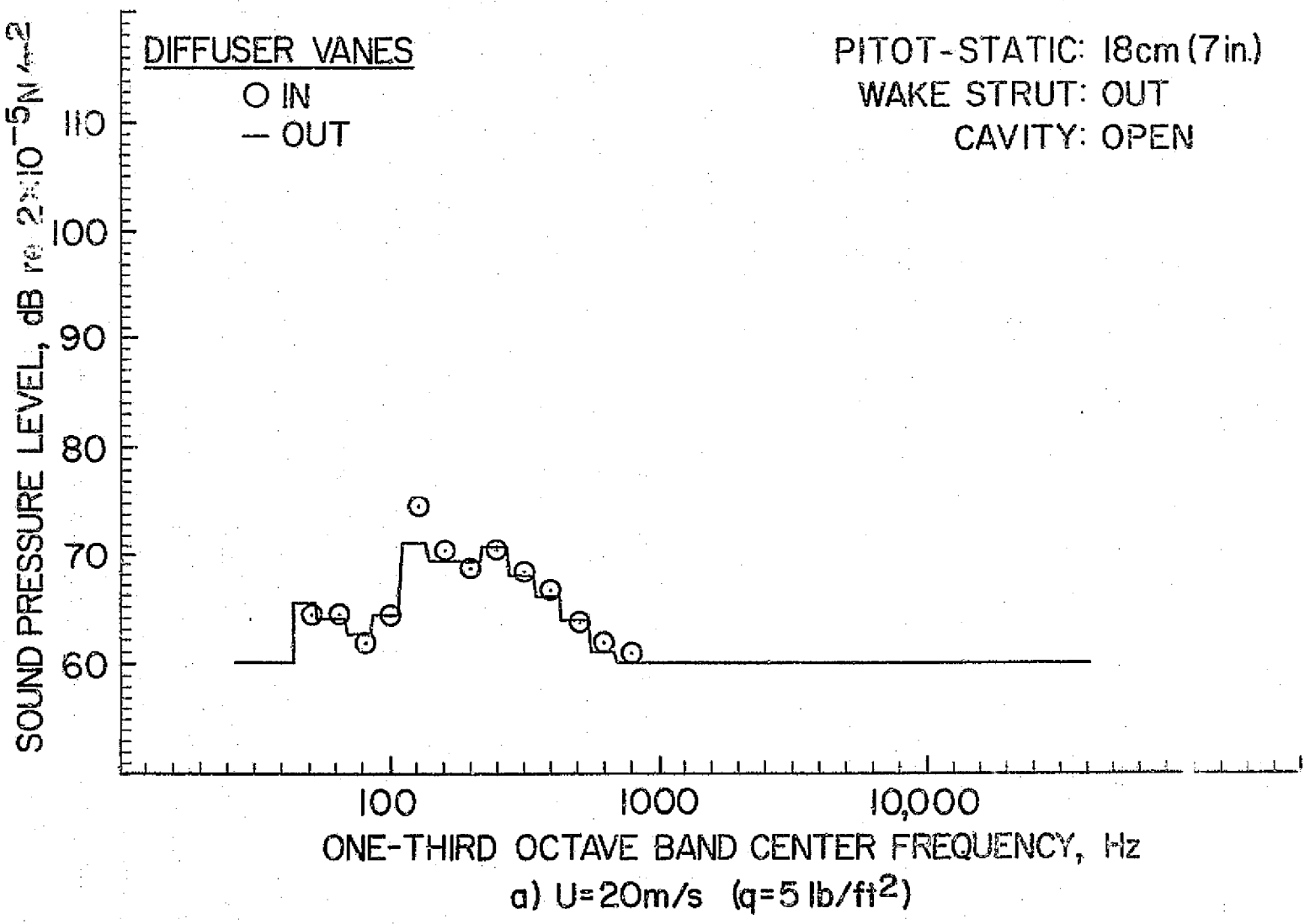

Figure 8.- Effect of diffuser entry vanes on test-section noise.

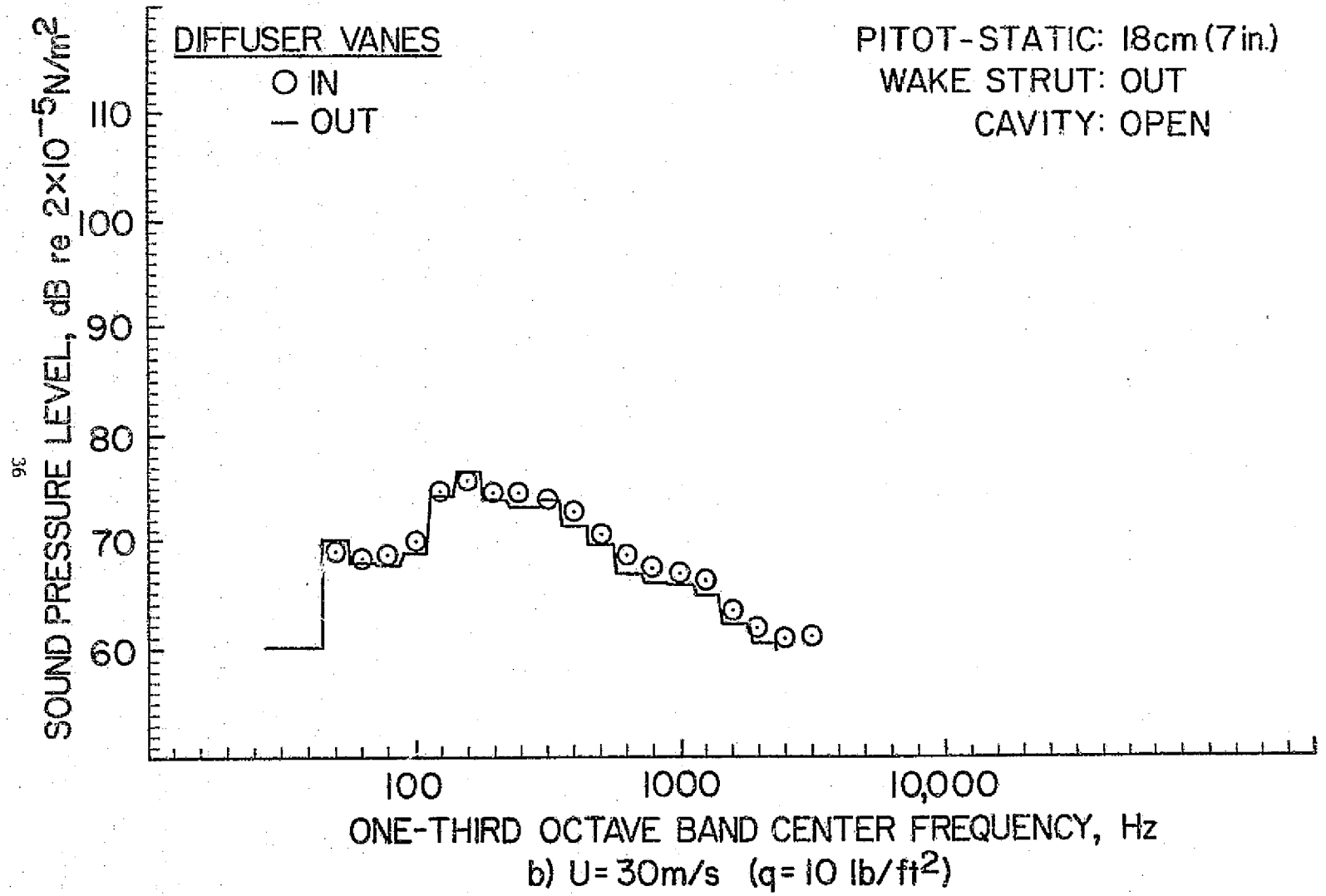

Figure 8.- Continued.

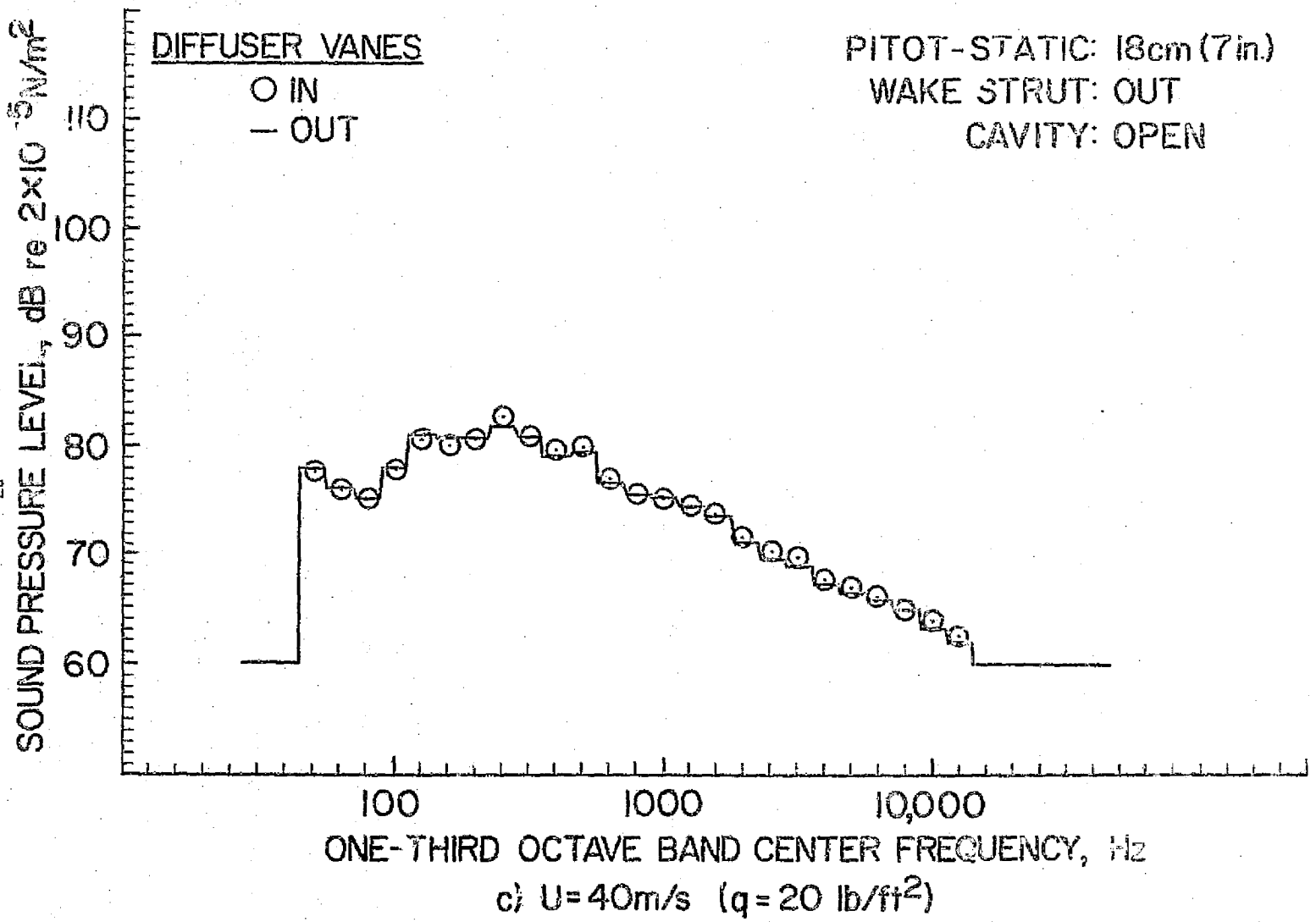

c) U=40m/s (q=20 lb/ft^2)

Figure 8.- Continued.

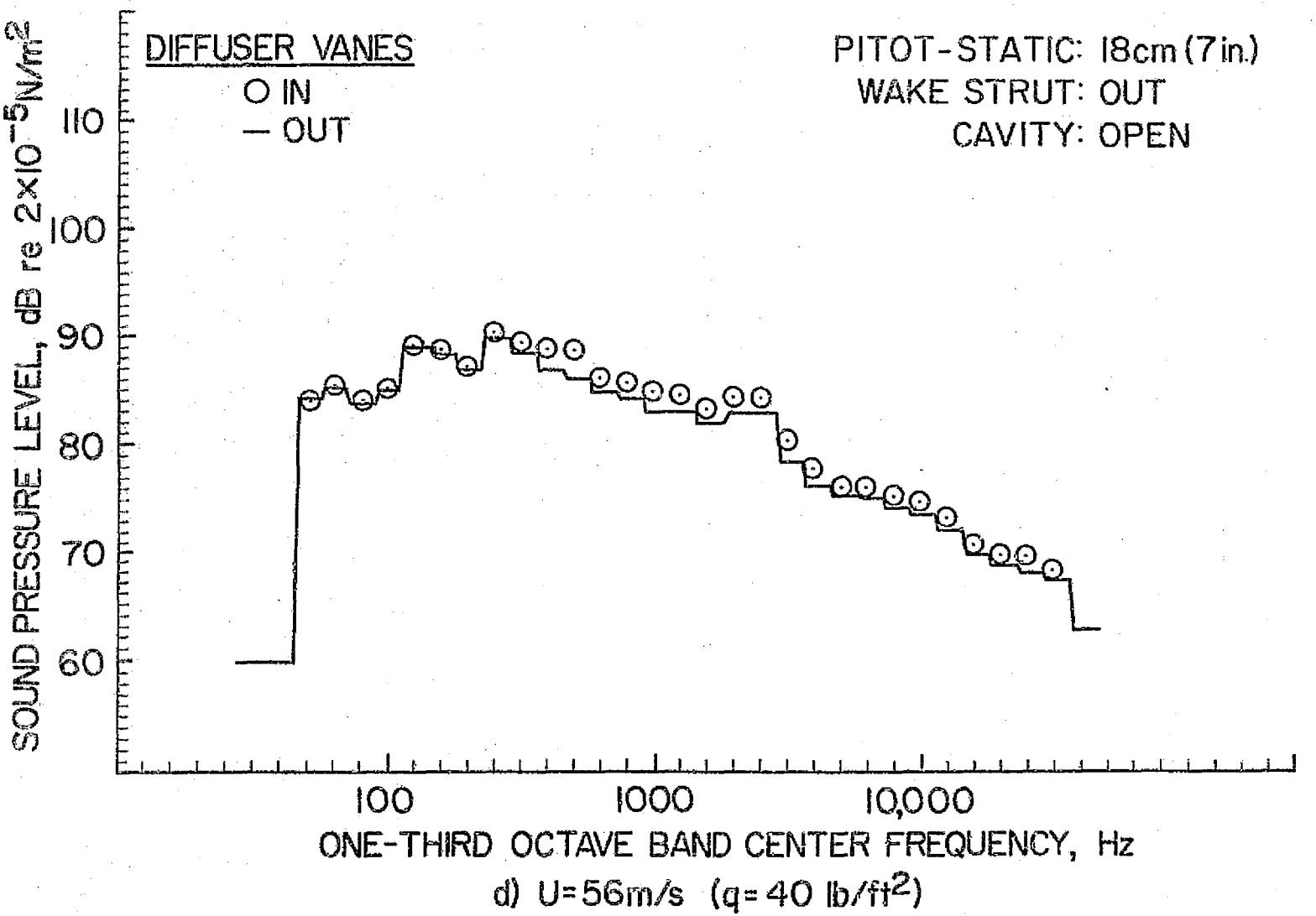

Figure 8.- Continued.

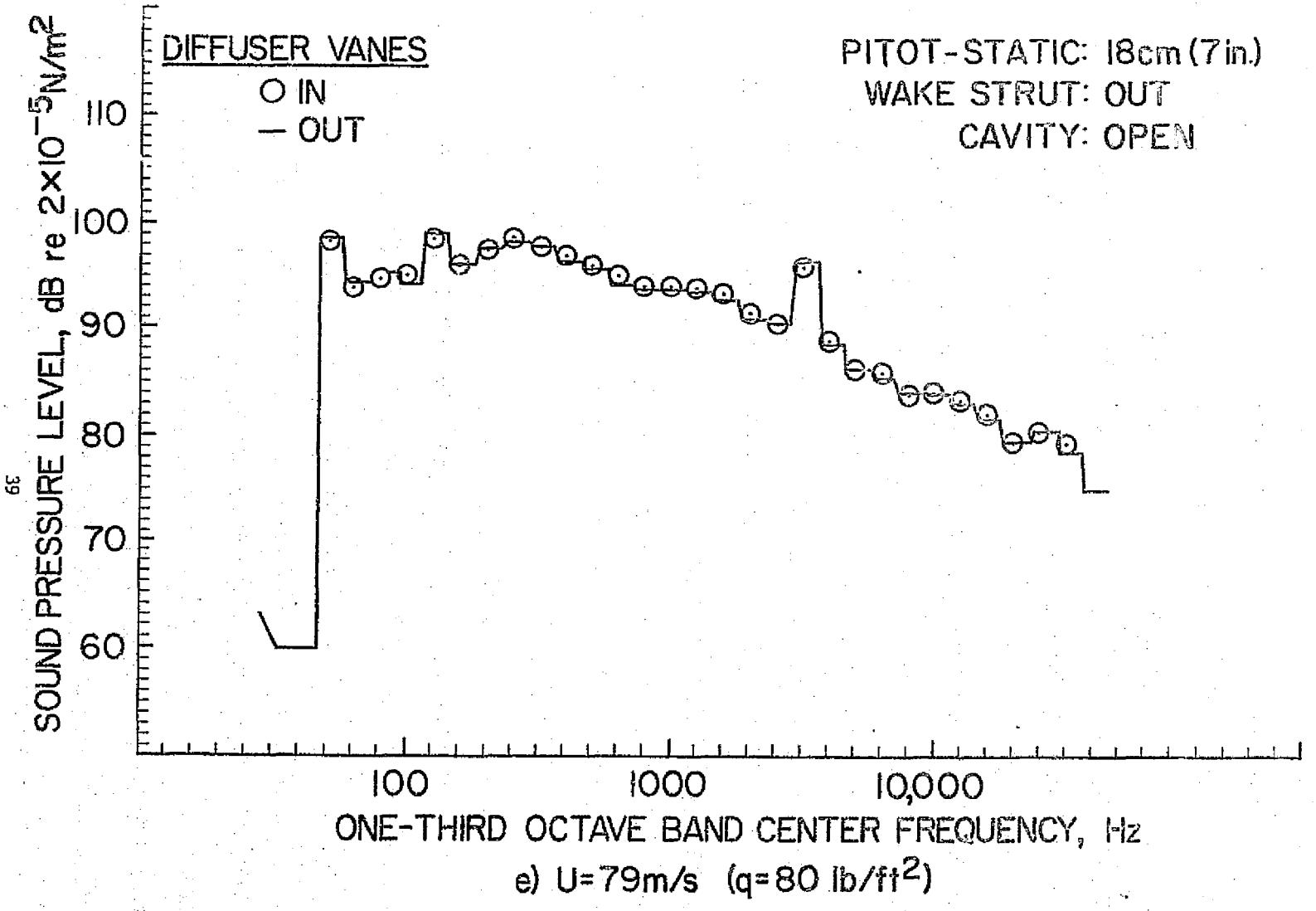

e) U=79m/s (q=80 lb/ft^2)

Figure 8.- Concluded.

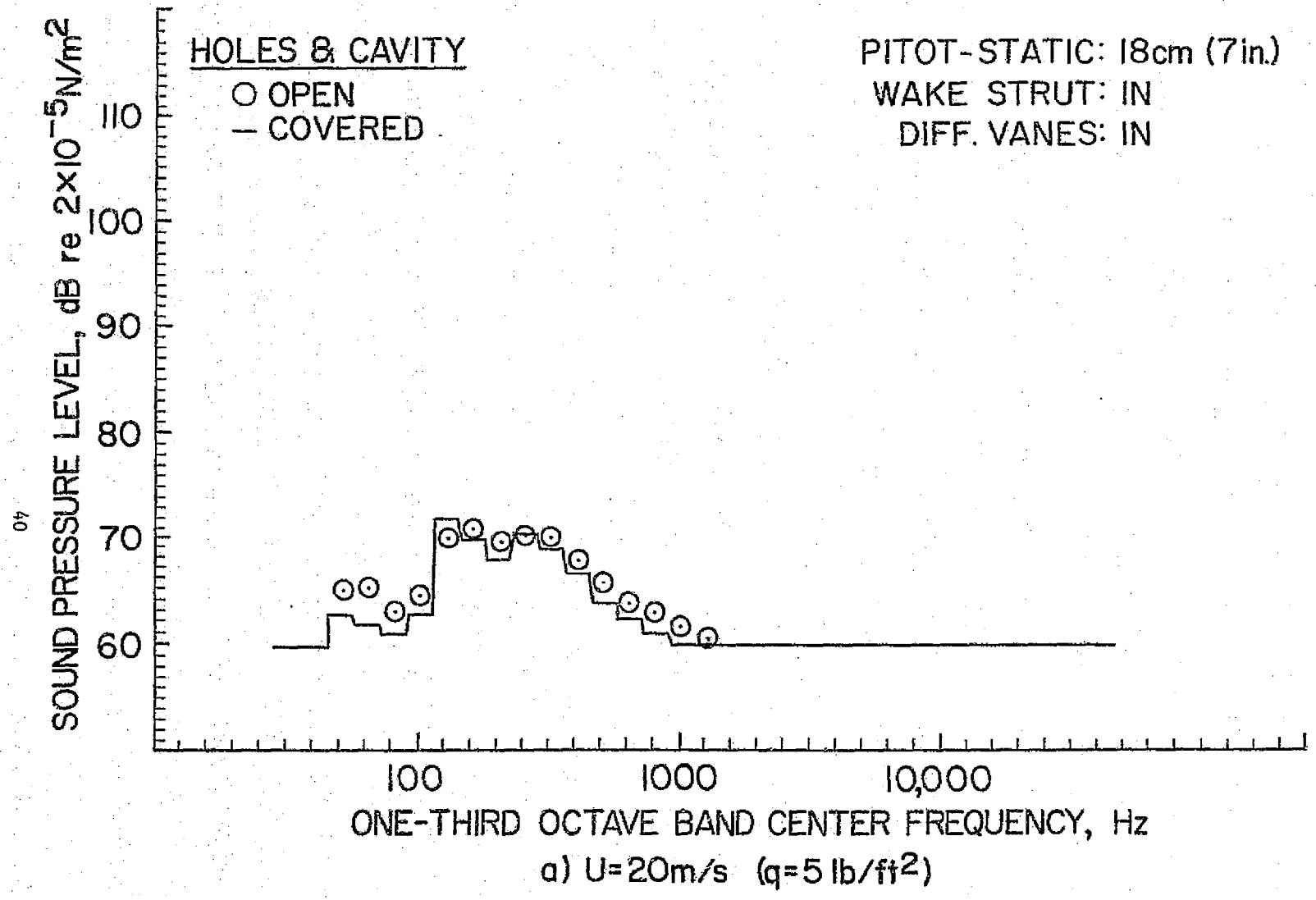

Figure 9.- Effect of wall holes and cavity on test-section noise.

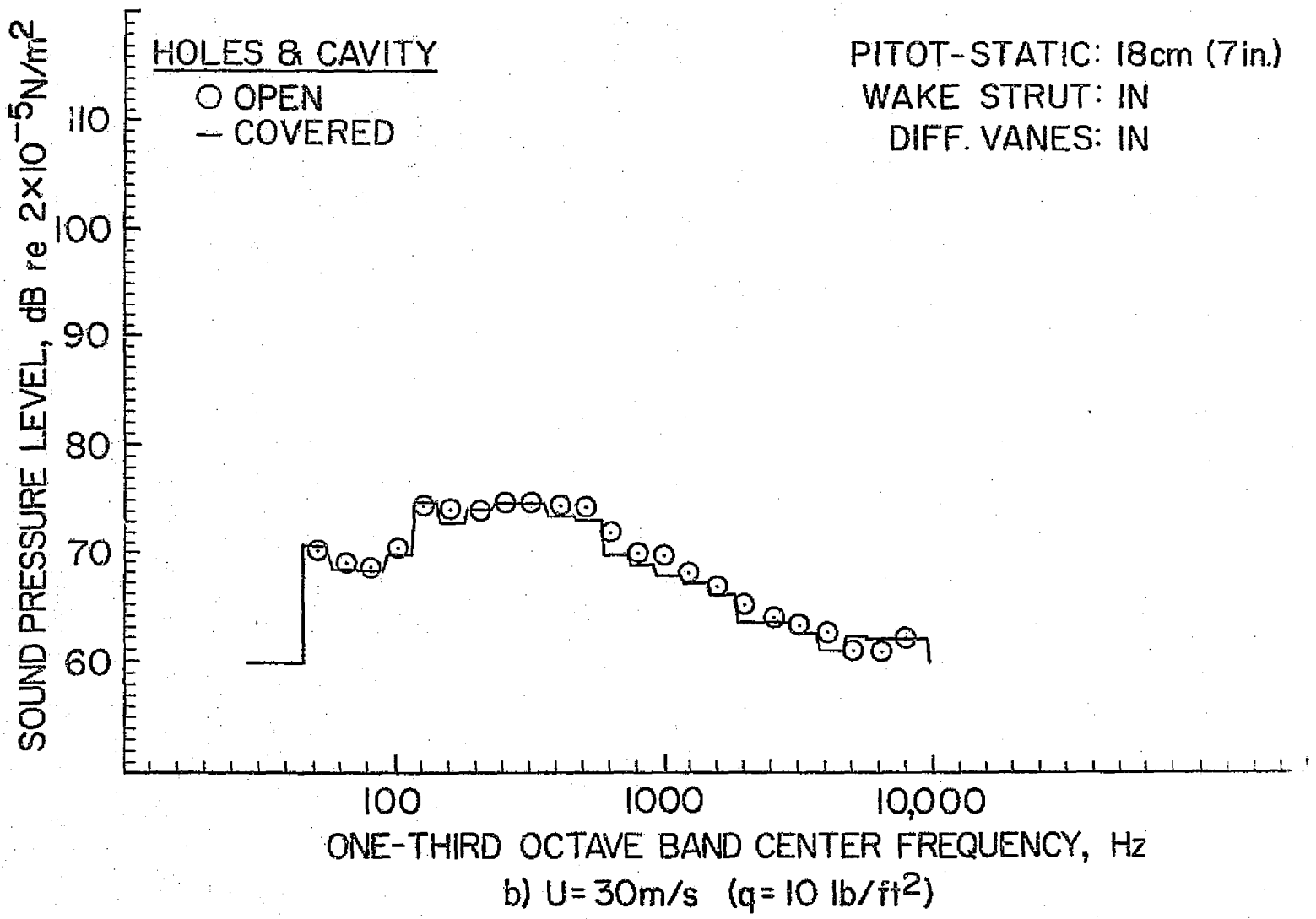

Figure 9.- Continued.

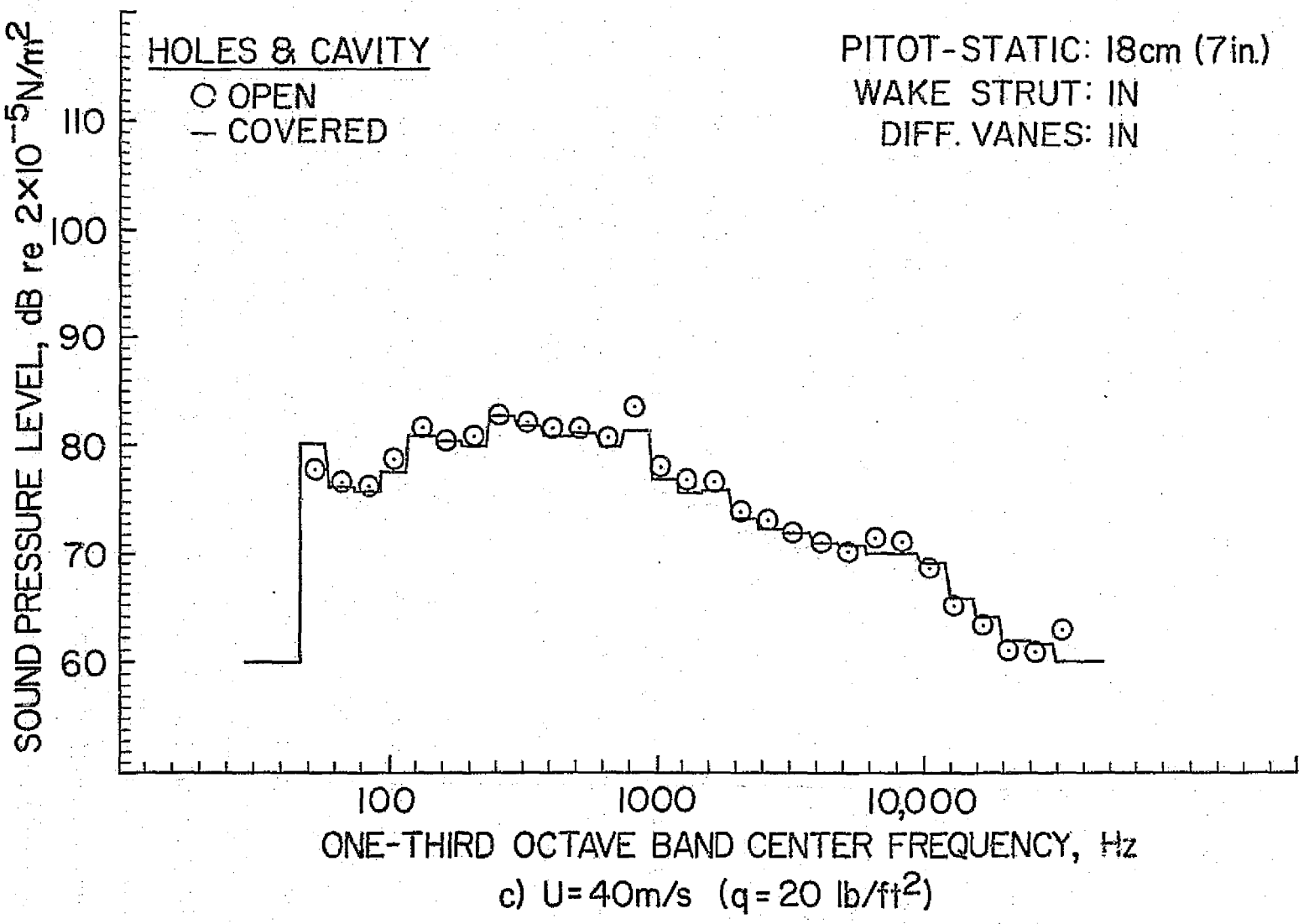

c) U = 40m/s (q = 20 lb/ft^2)

Figure 9.- Continued.

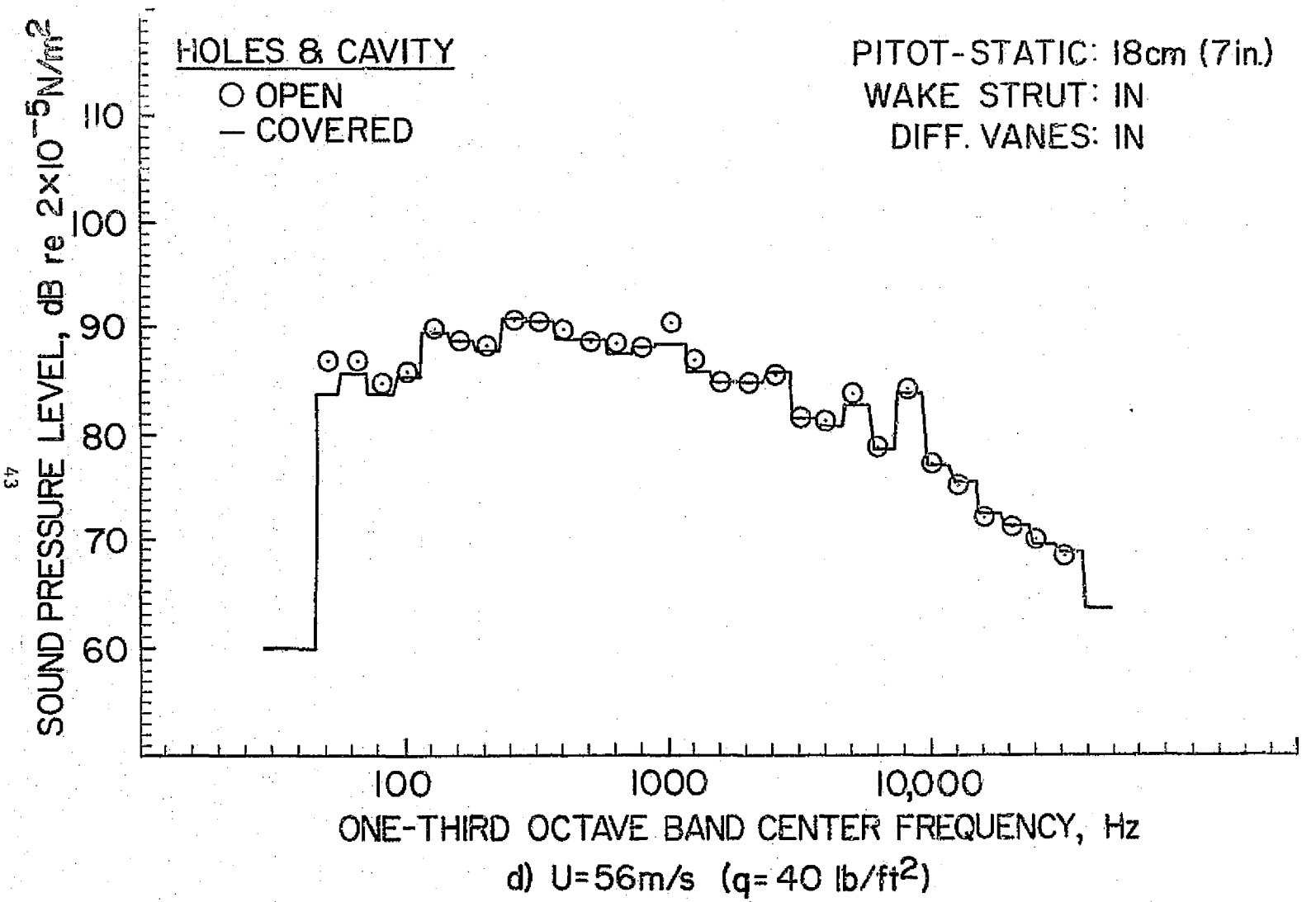

d) U=56m/s (q= 40 lb/ft^2)

Figure 9.- Continued.

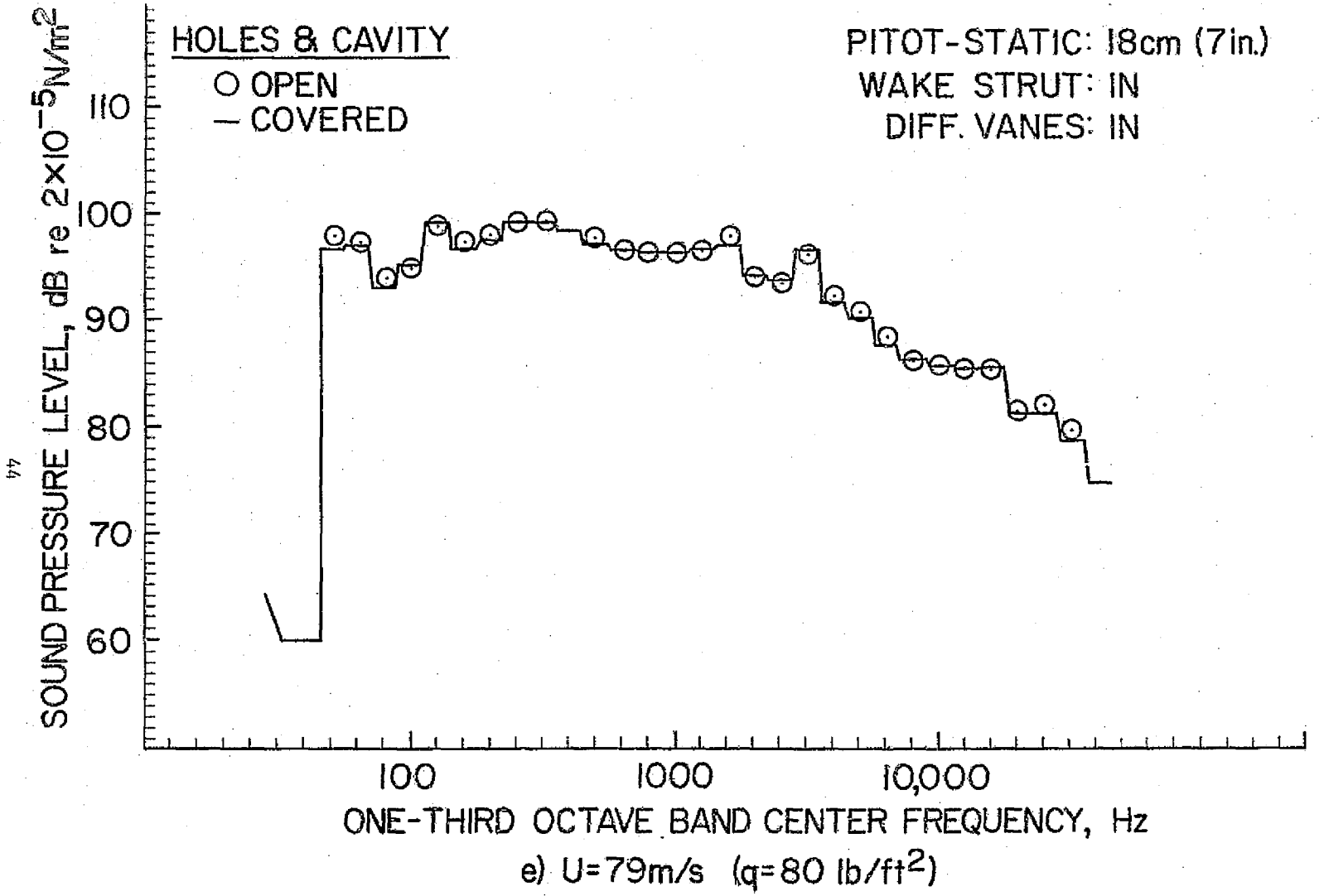

Figure 9.- Concluded.

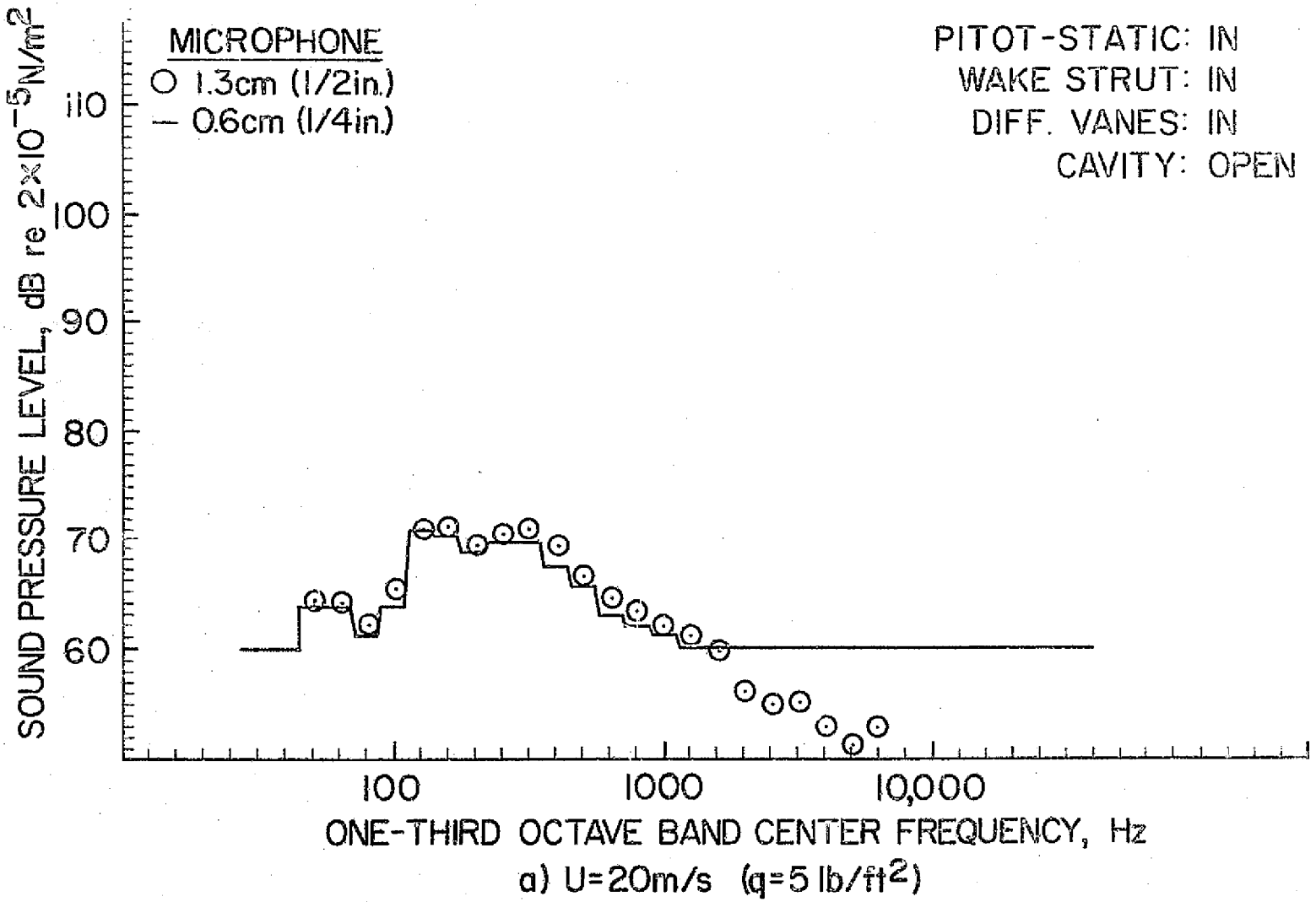

Figure 10.- Comparison of test-section noise levels measured with B&K 4133 (1/2 in.) and 4135 (1/4 in.) microphones.

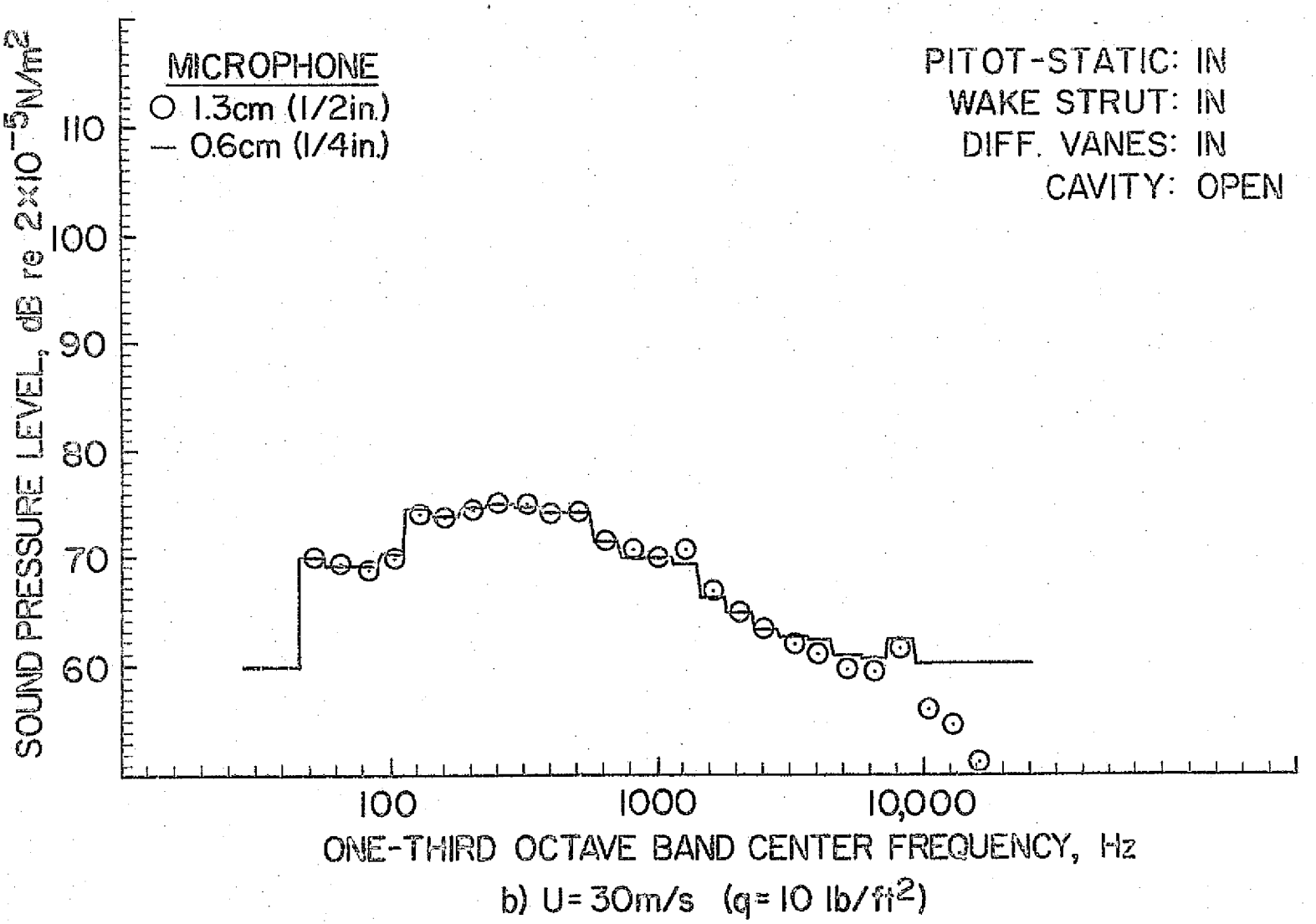

b) U = 30m/s (q = 10 lb/ft^2)

Figure 10.- Continued.

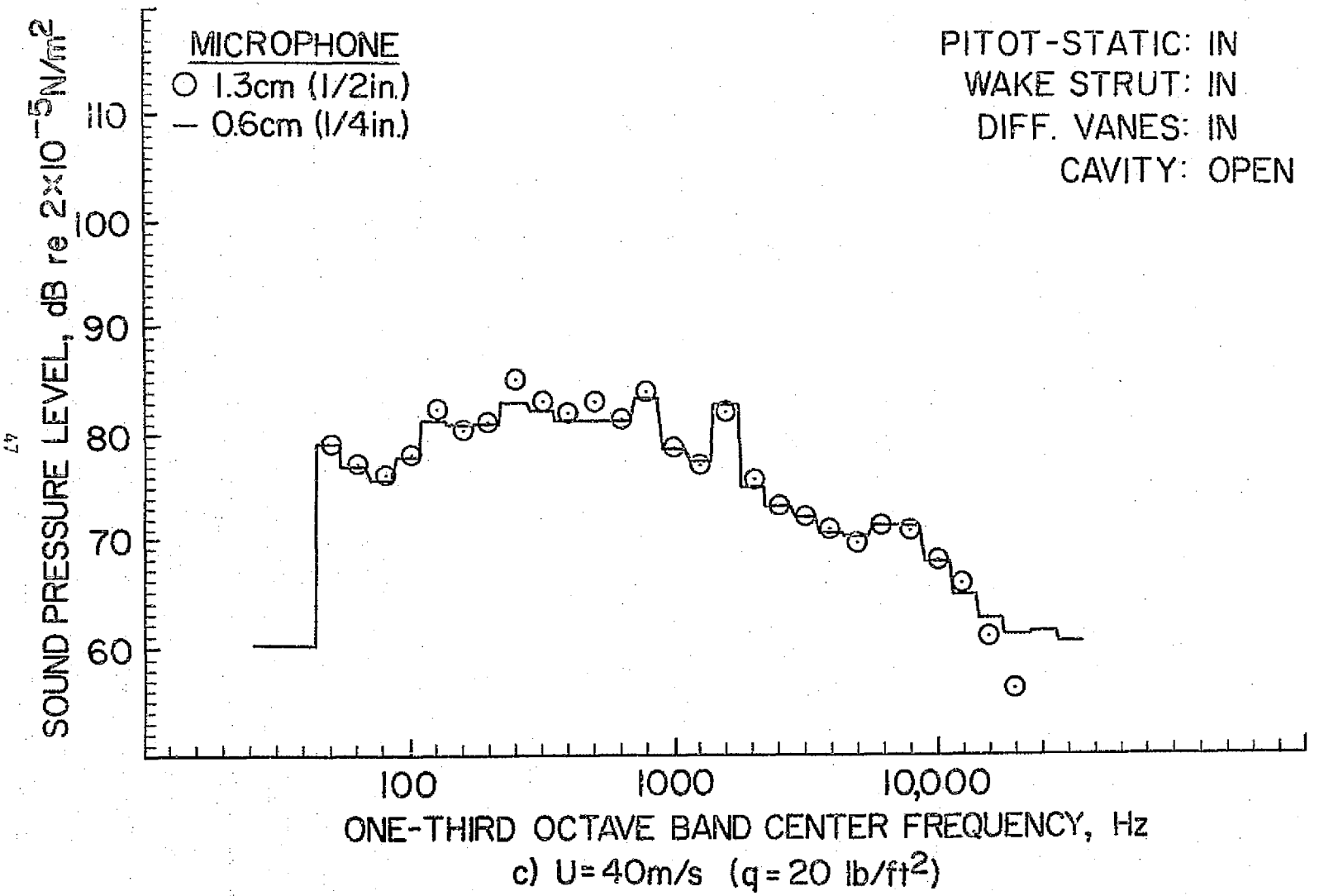

c) U = 40m/s (q = 20 lb/ft^2)

Figure 10.- Continued.

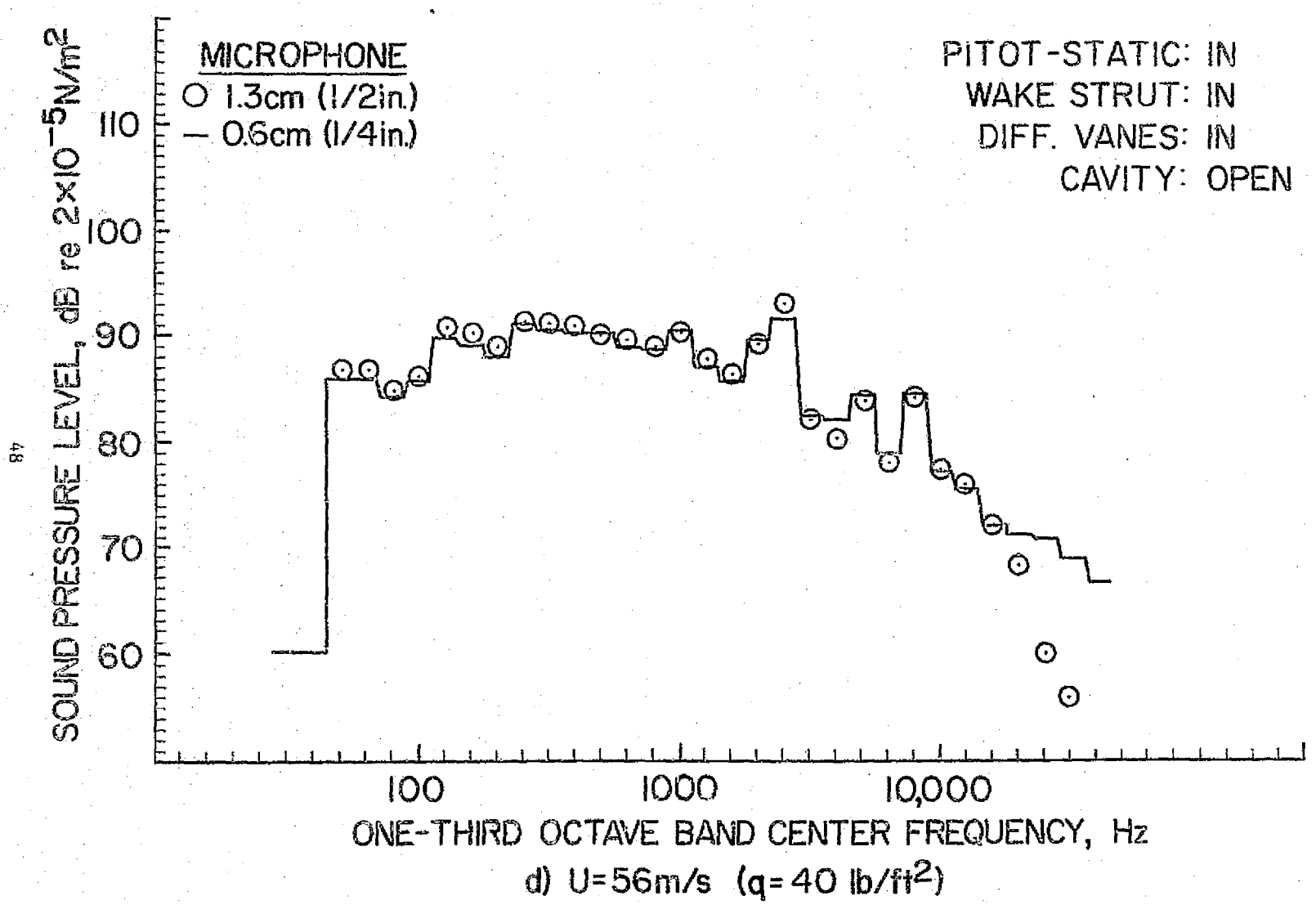

d) U=56m/s (q=40 lb/ft^2)

Figure 10.- Continued.

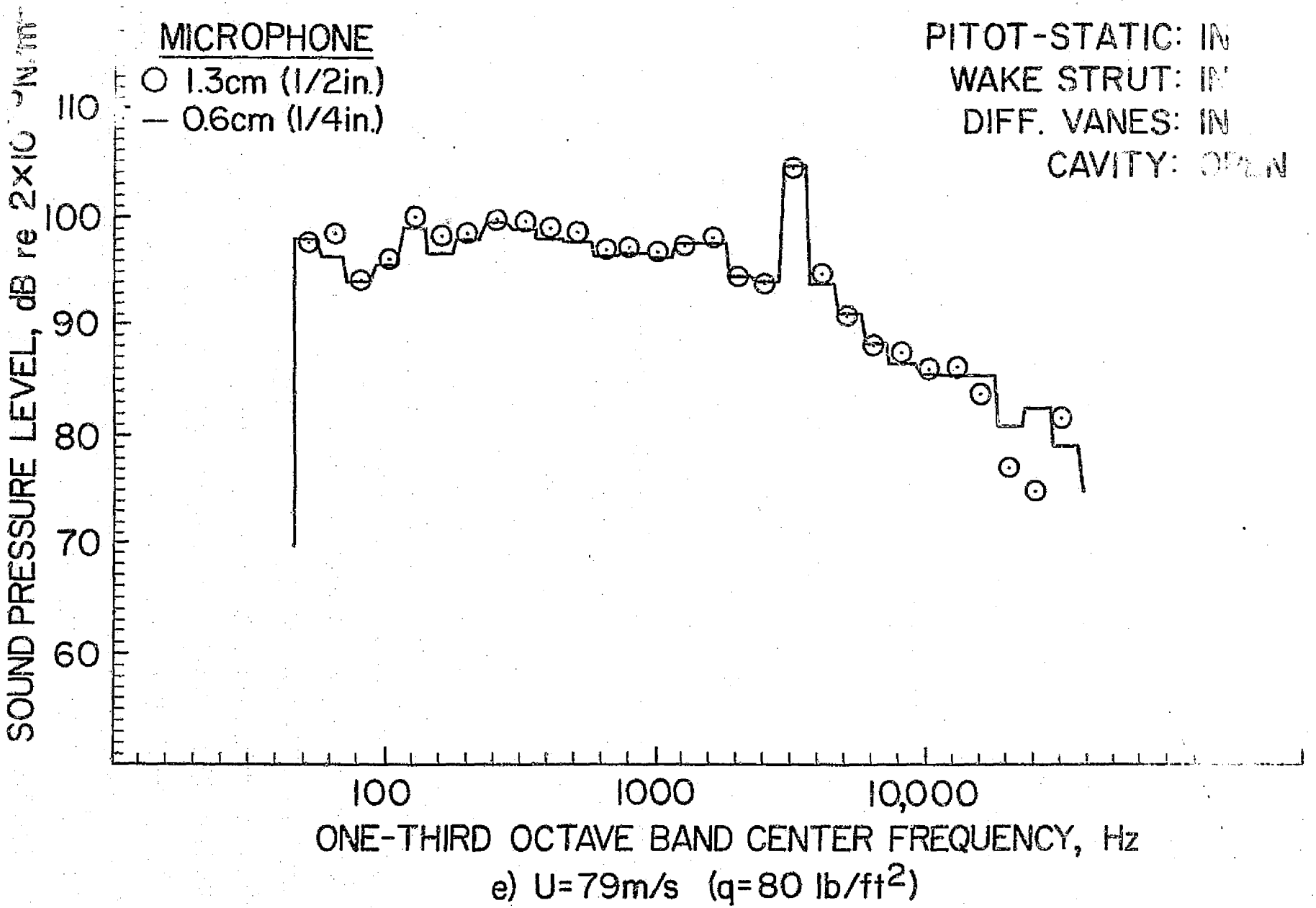

e) U=79m/s (q=80 lb/ft^2)

Figure 10.- Concluded.

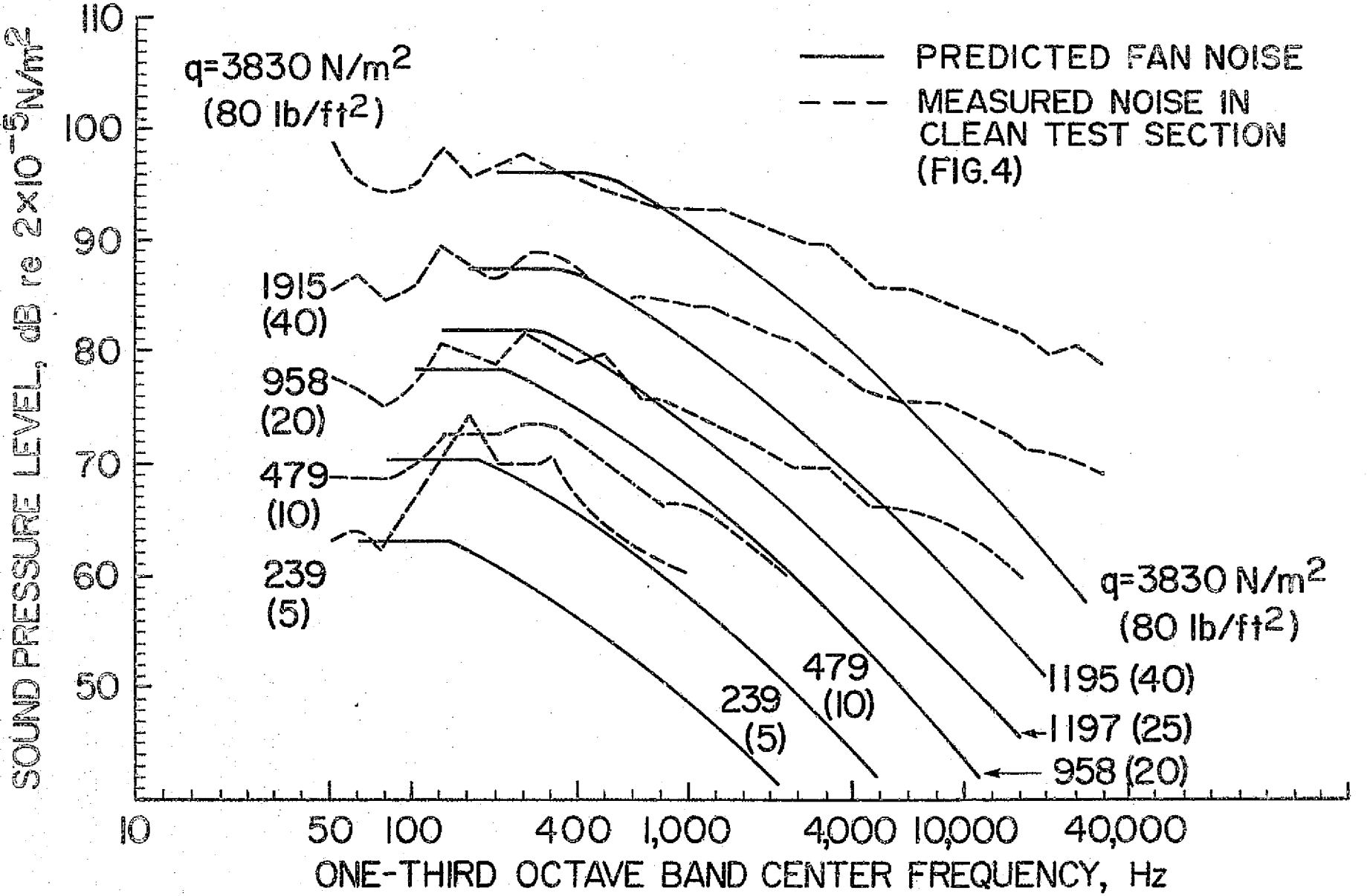

Figure 11.- Predicted fan noise in test section and measured noise in clean test section.

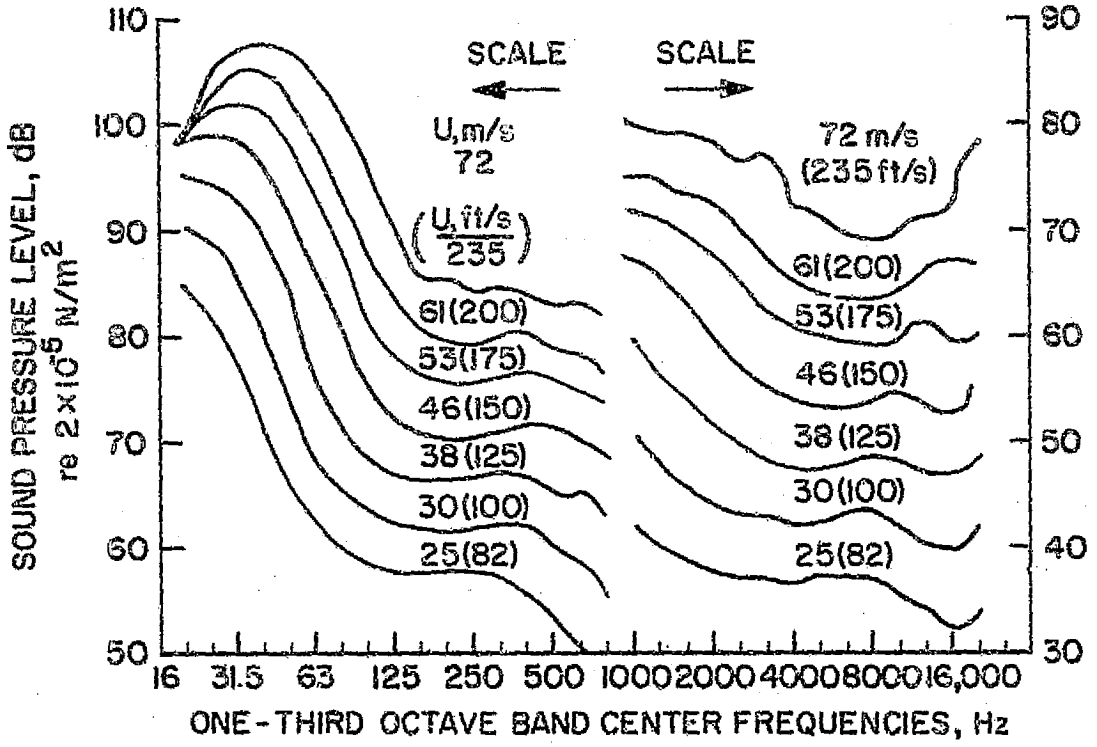

Figure 12.- Wind noise of B&K 4133 1.3 cm (1/2 in.) microphone and nose cone (ref. 4).

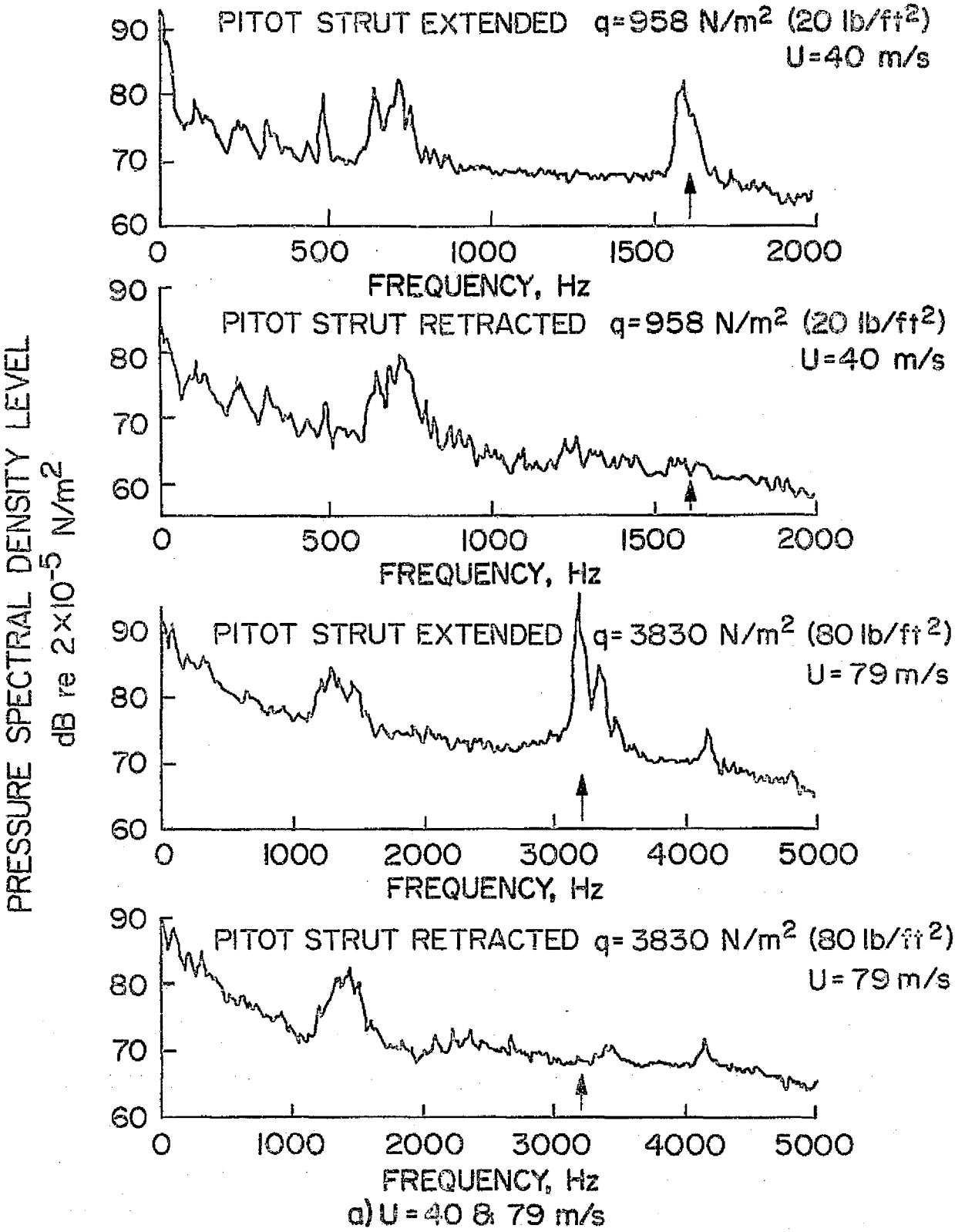

a) U = 40 & 79 m/s

Figure 13.- Narrowband spectra of noise levels in test section showing effect of retracting pitot strut (filter bandwidth 5 Hz (upper curves), 12.5 Hz (lower curves)); ref. 1.

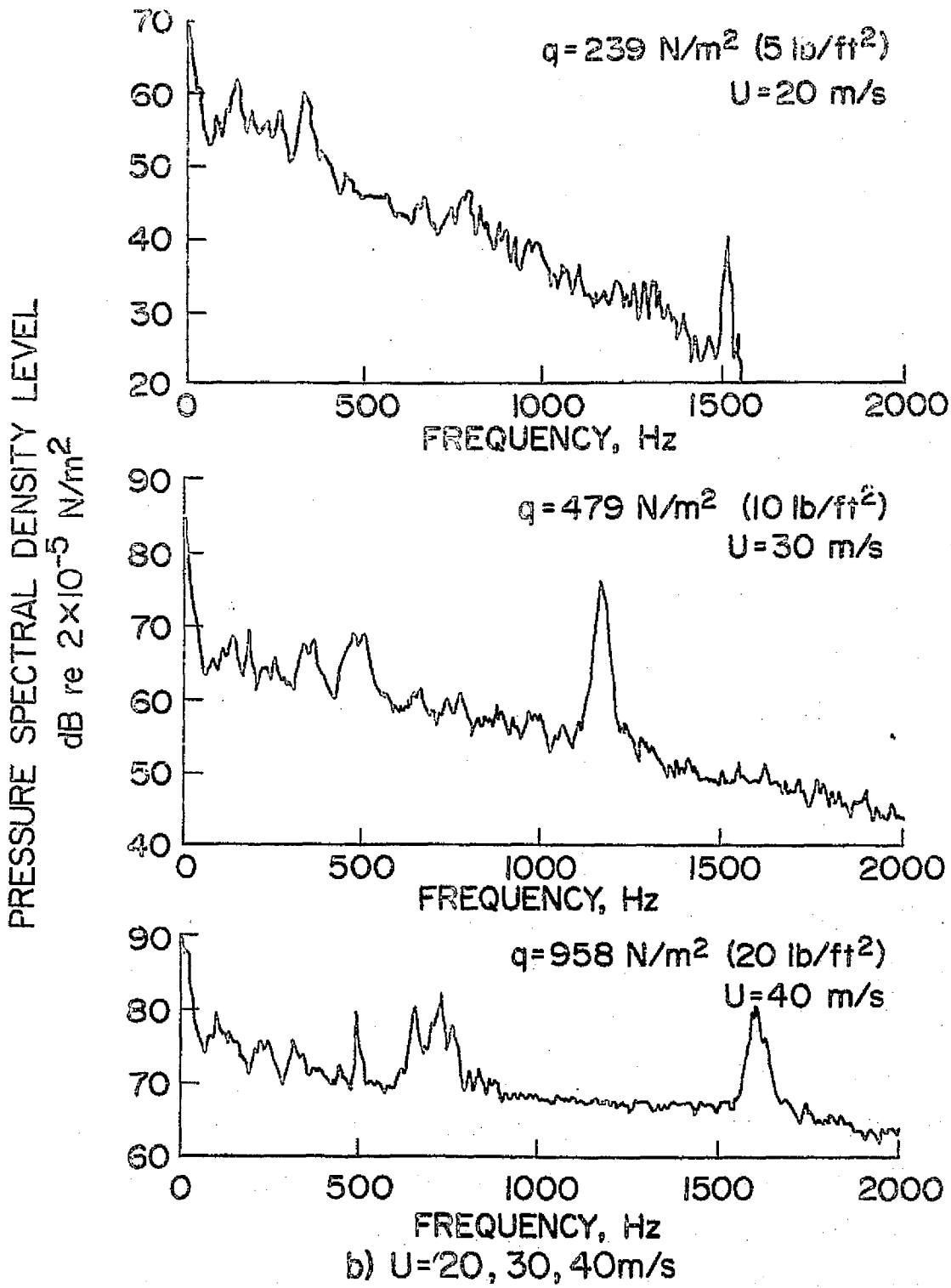

Figure 13.- Continued (5 Hz bandwidth).

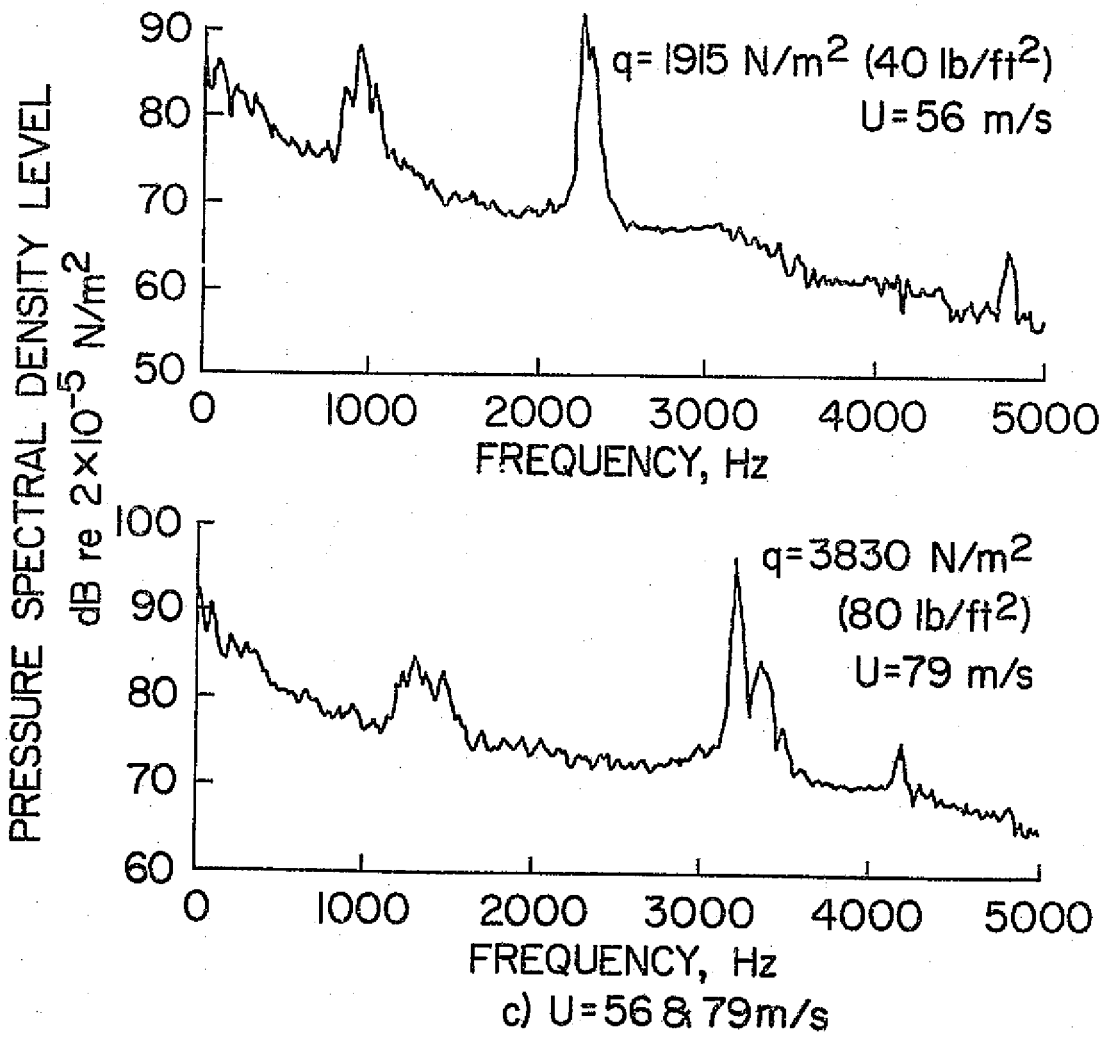

Figure 13.- Concluded (12.5 Hz bandwidth).

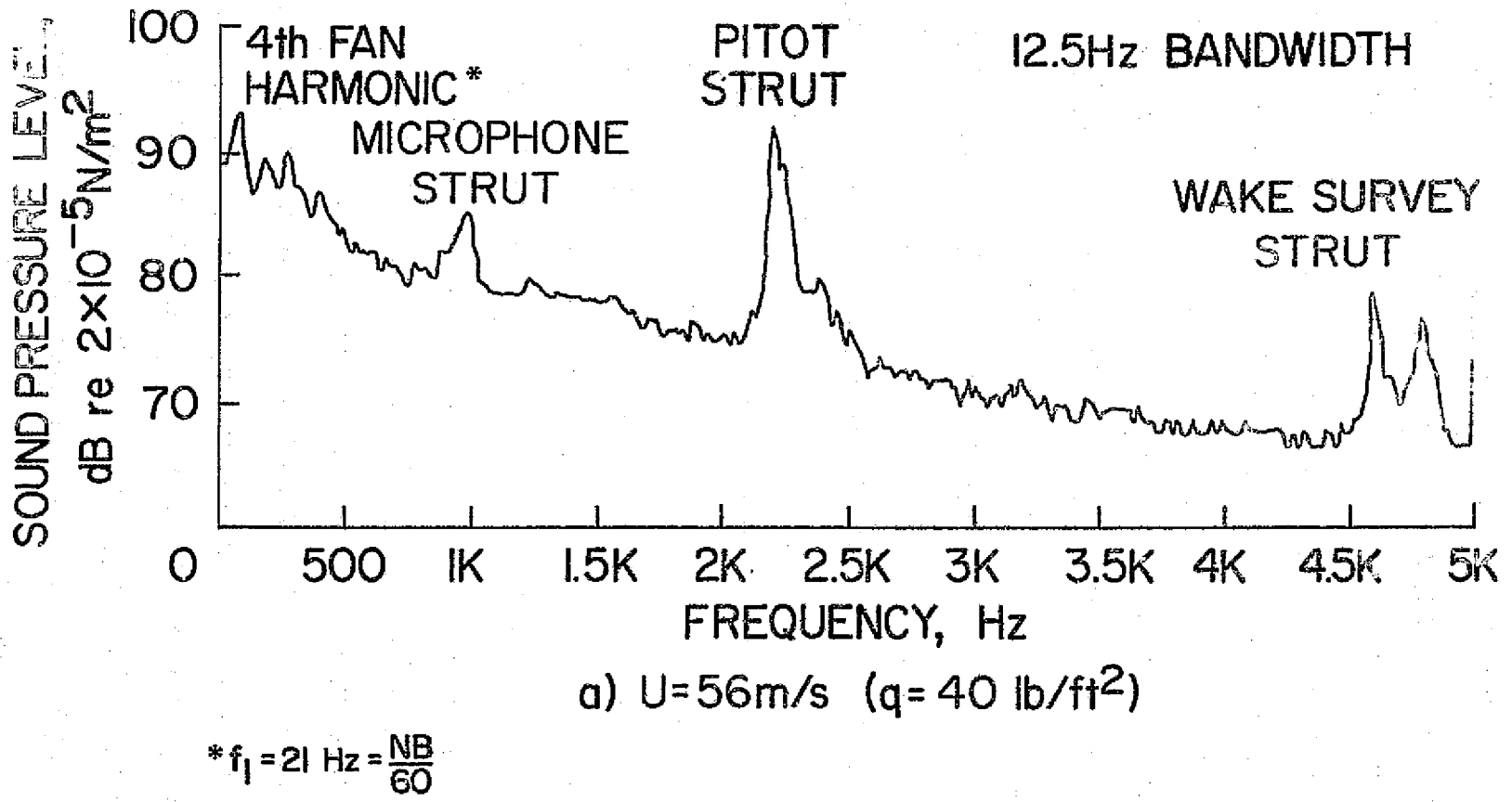

Figure 14.- Narrowband spectra of test-section noise, all struts in the flow. Constant-chord microphone strut.

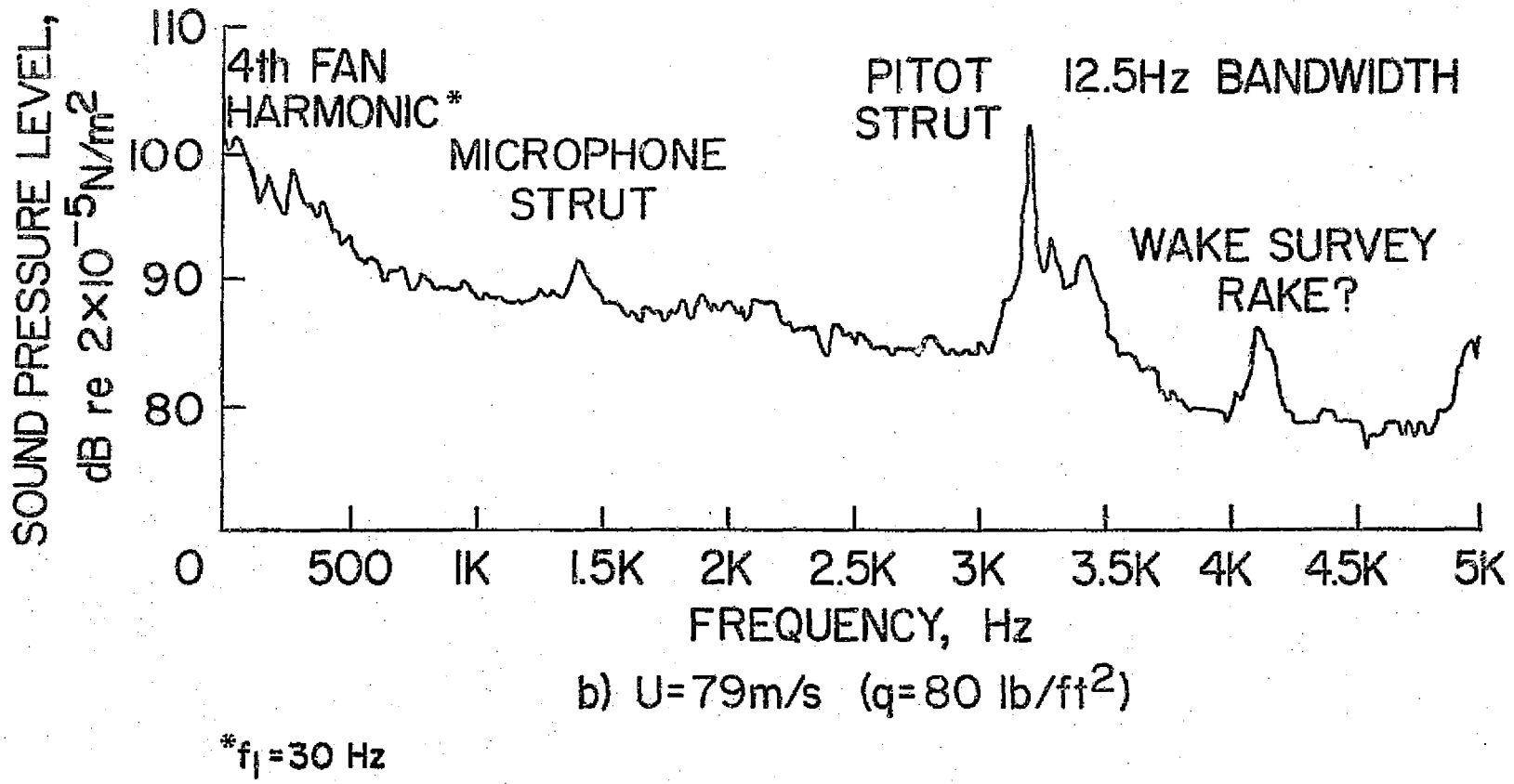

Figure 14.- Continued.

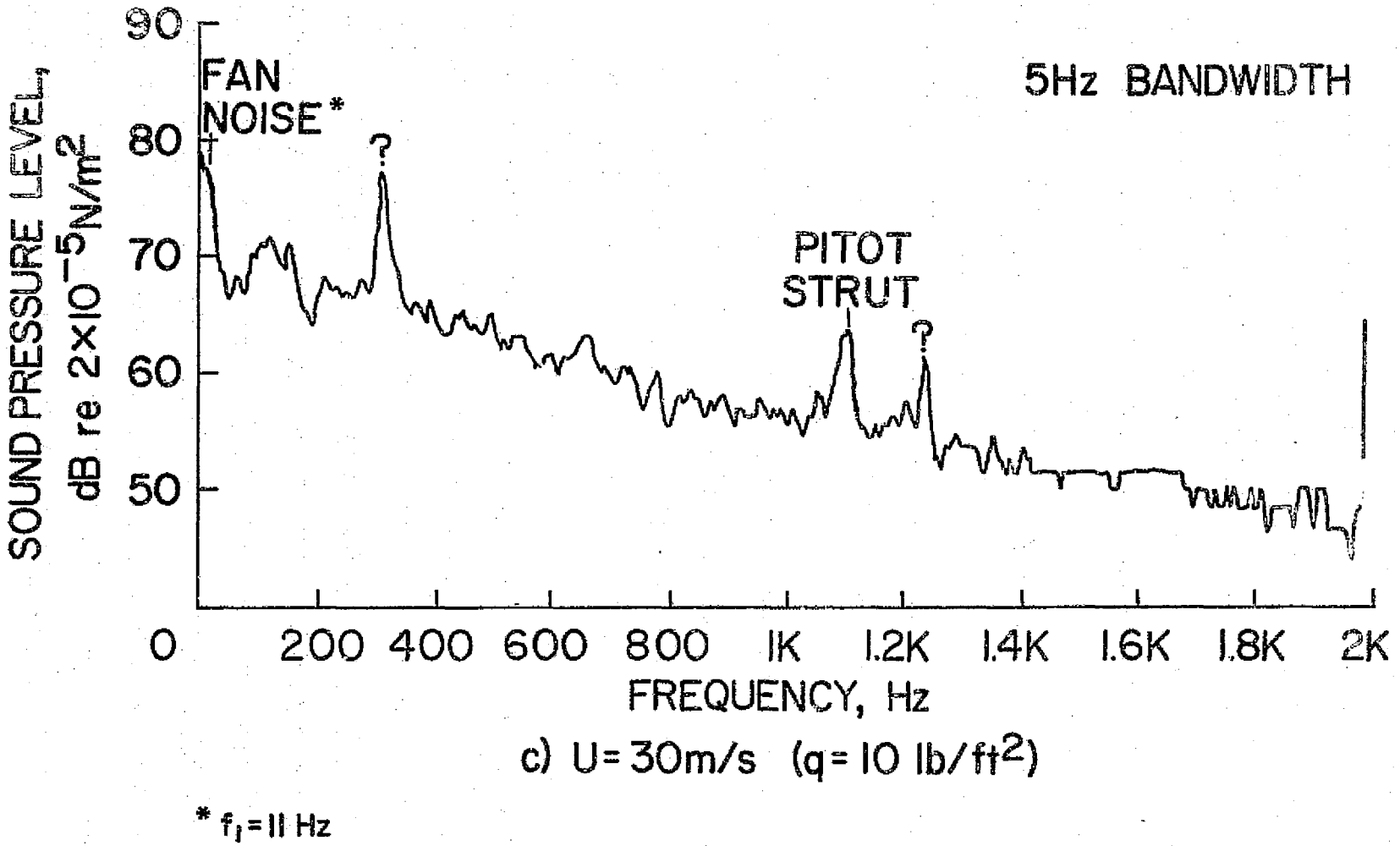

Figure 14.- Continued.

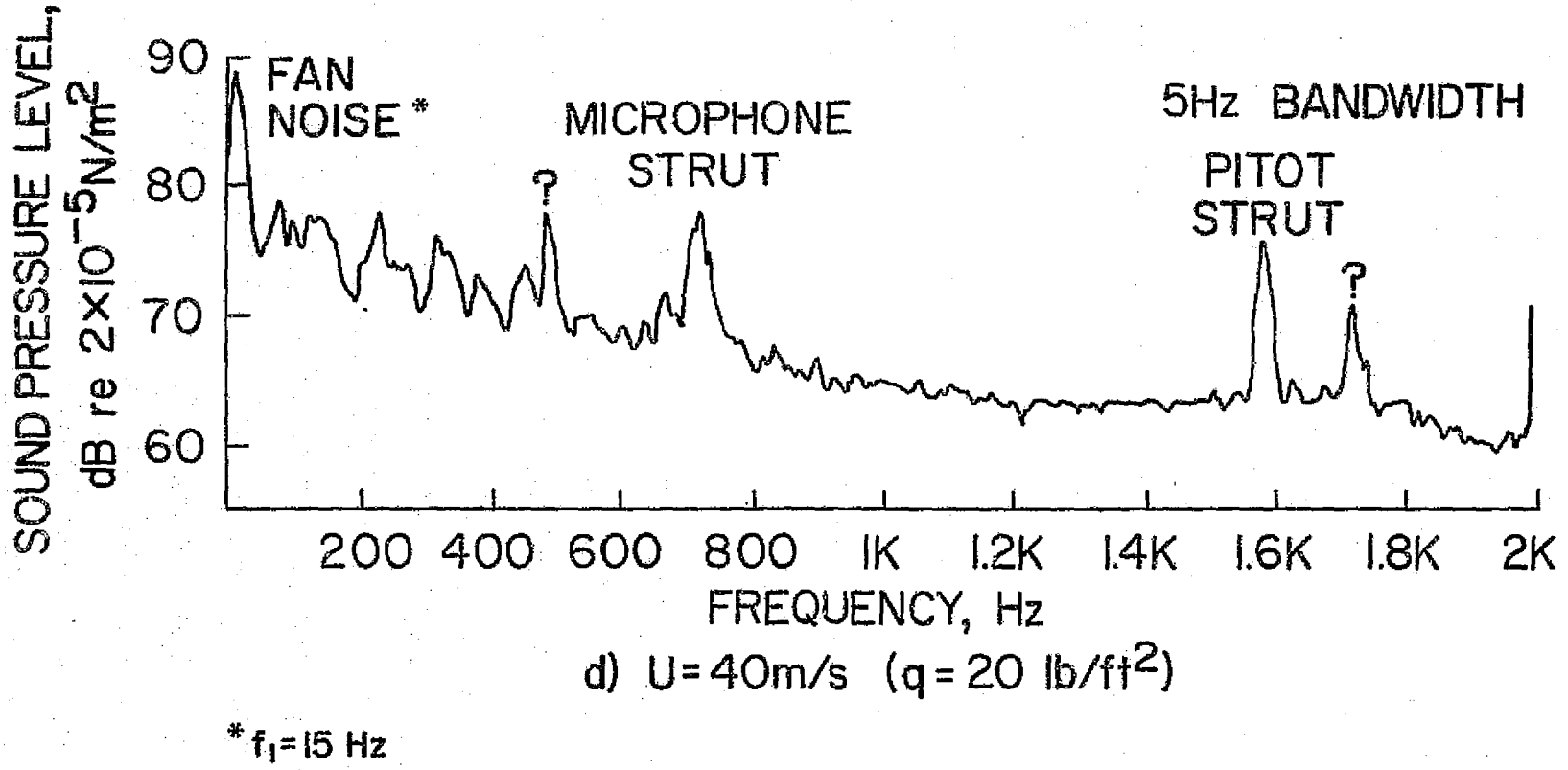

Figure 14.- Continued.

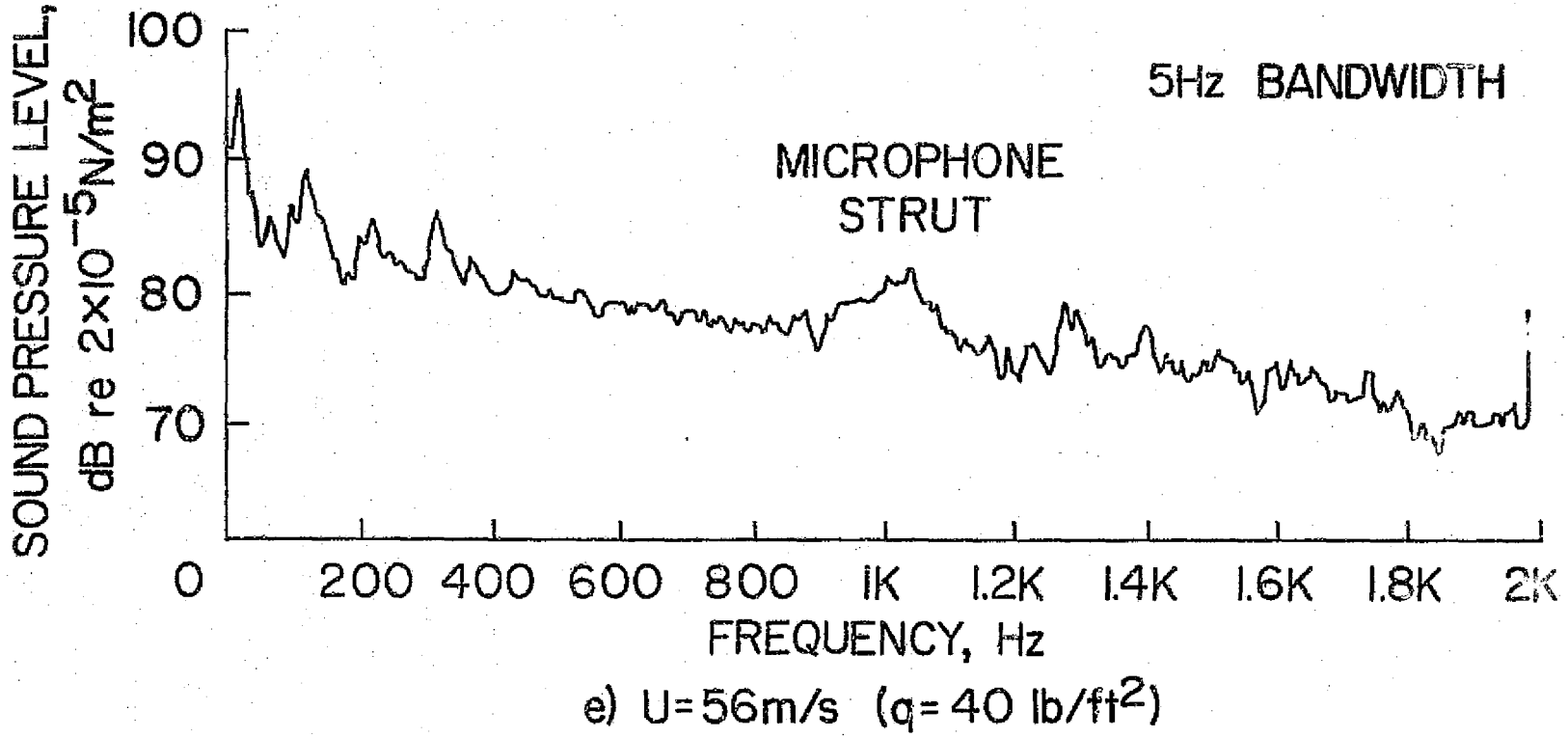

e) U=56m/s (q= 40 lb/ft^2)

Figure 14.- Continued.

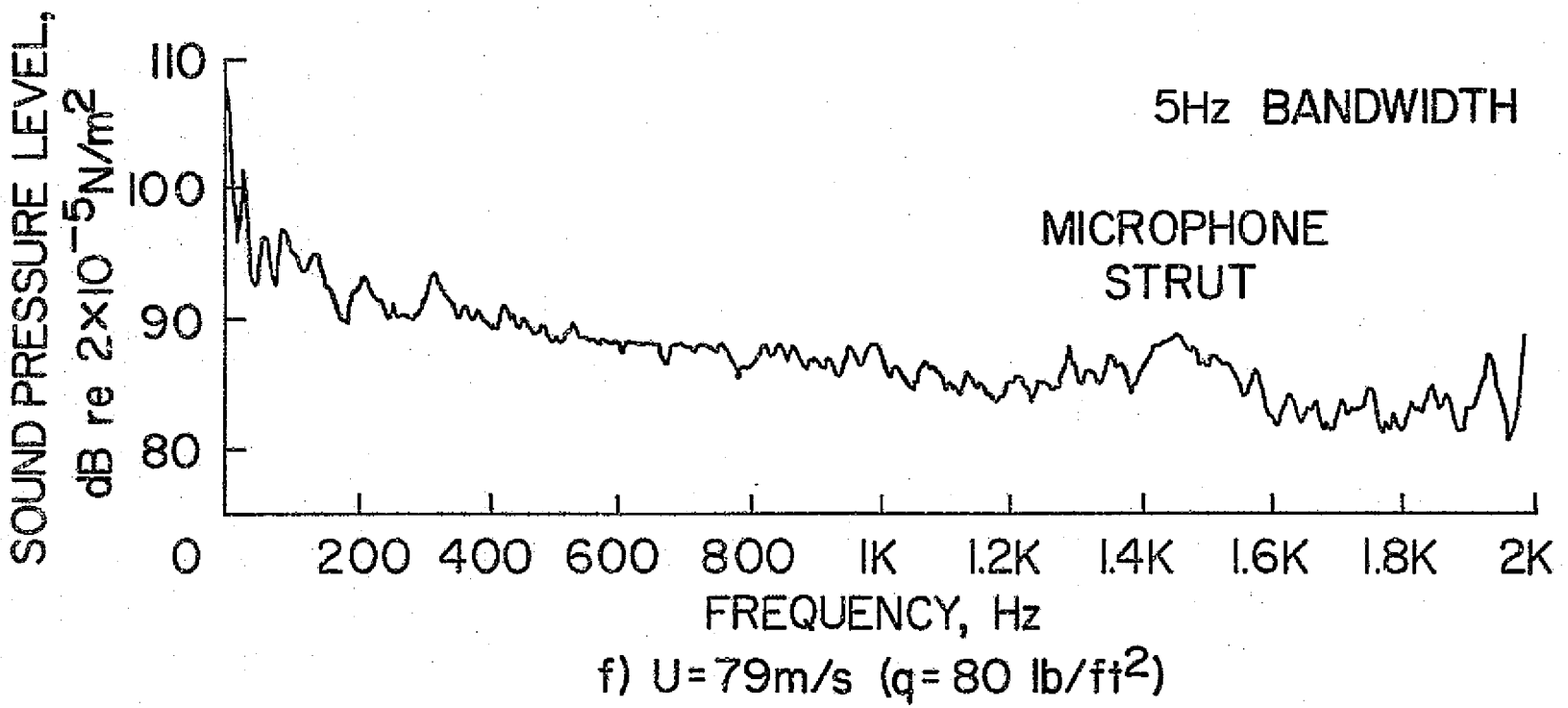

Figure 14.- Concluded.

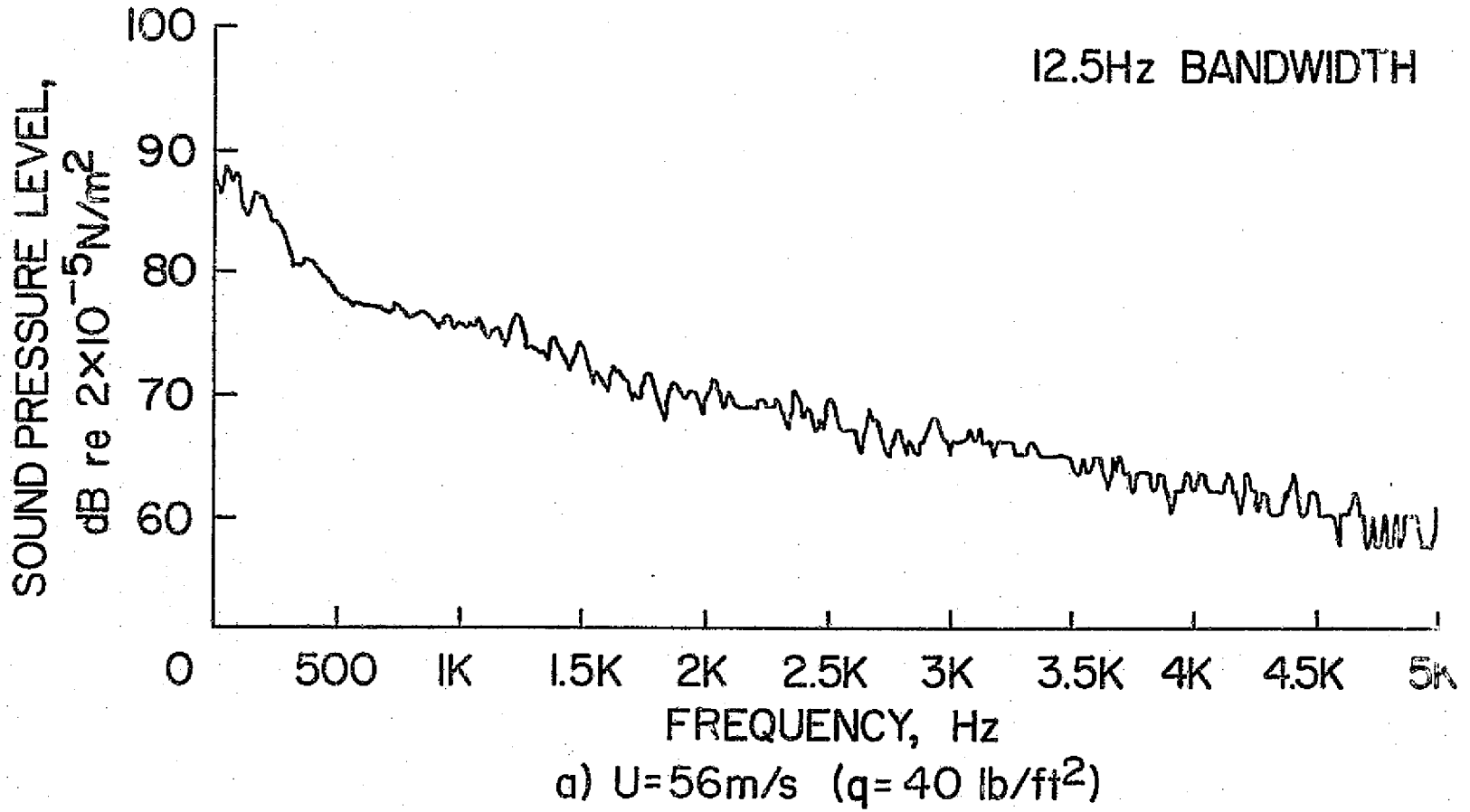

Figure 15.- Narrowband spectra of test-section noise, all struts out of flow except constant-chord microphone strut.

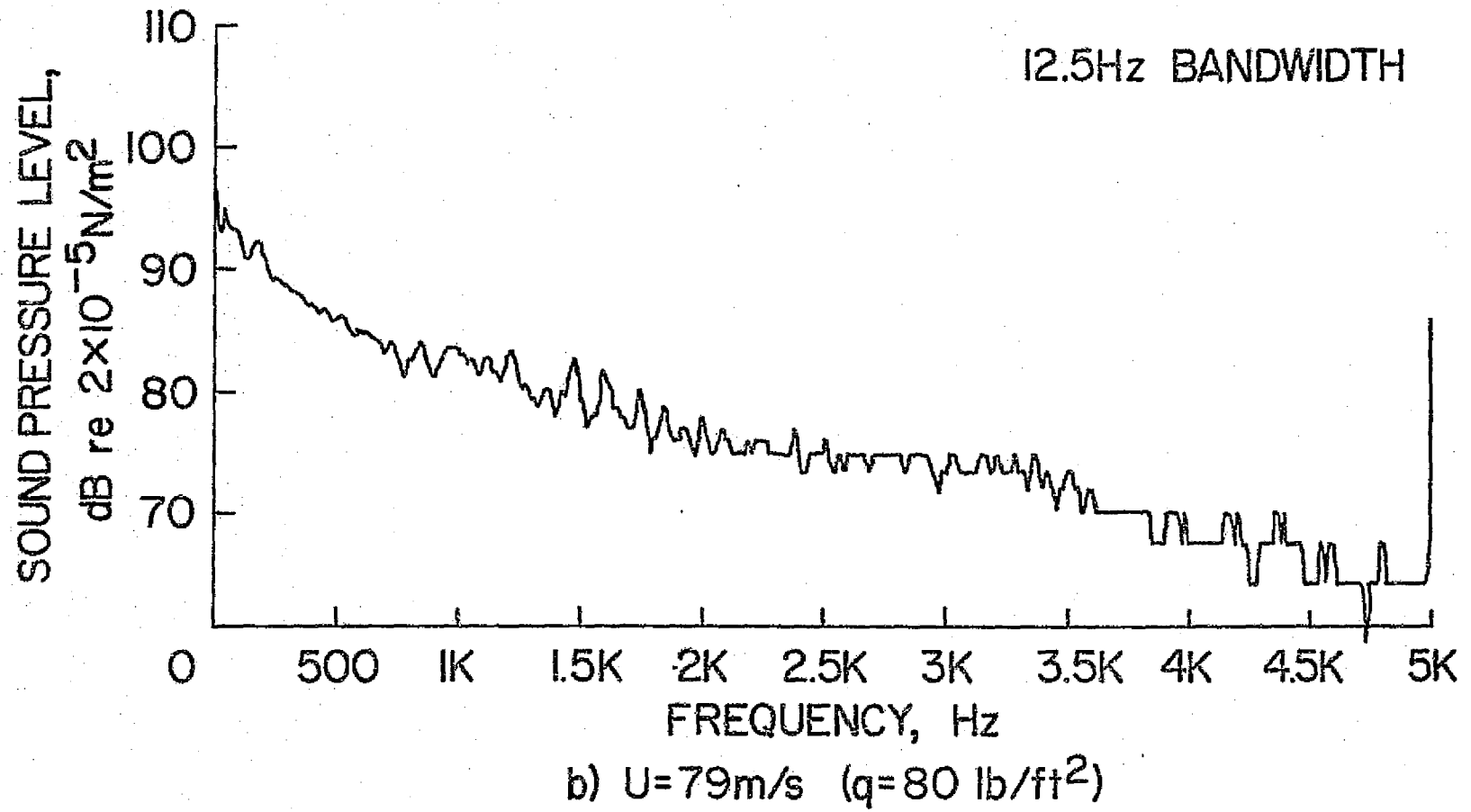

Figure 15.- Continued.

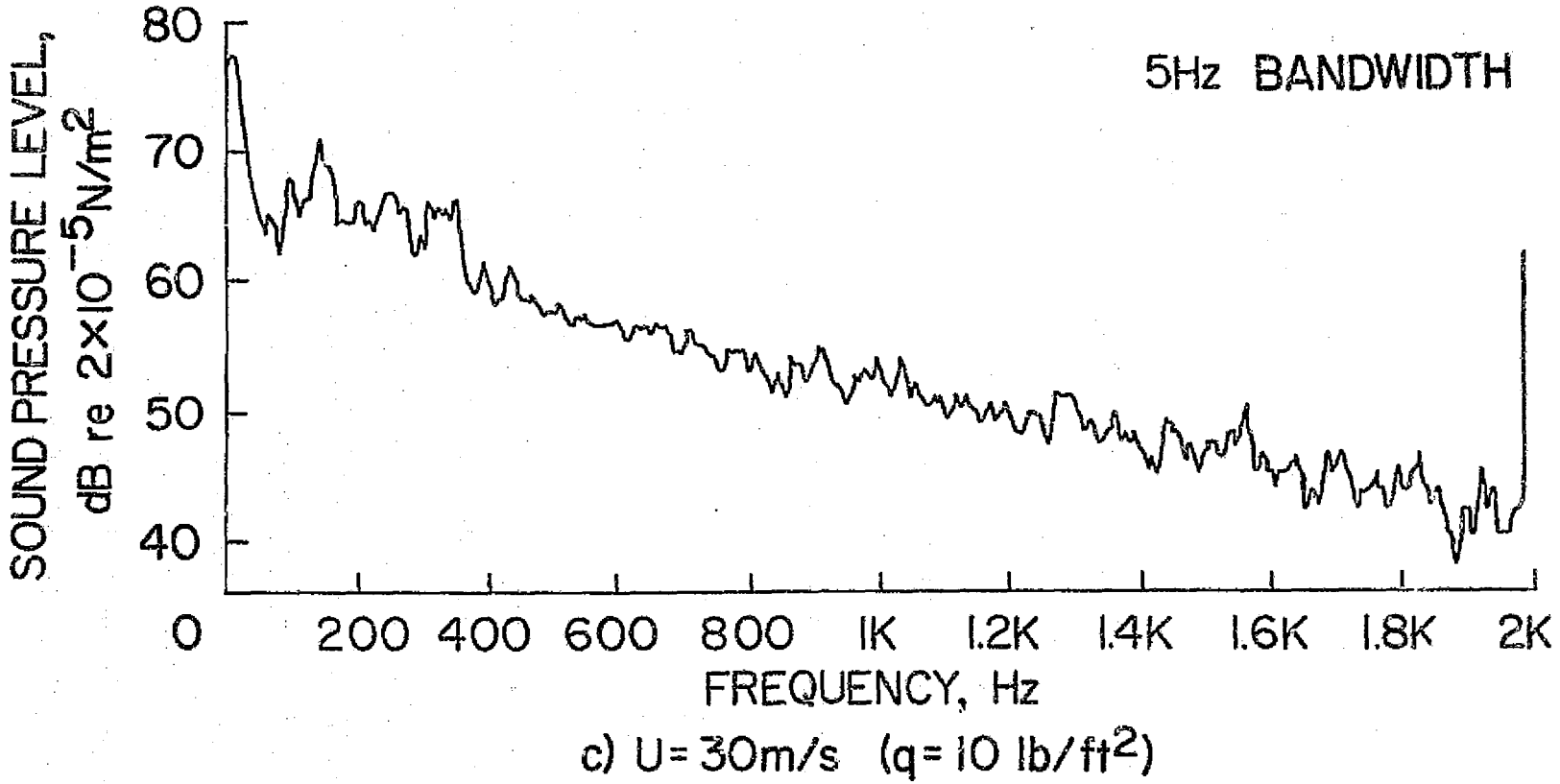

Figure 15.- Continued.

d) U=40m/s (q=20 lb/ft^2)

Figure 15.- Continued.

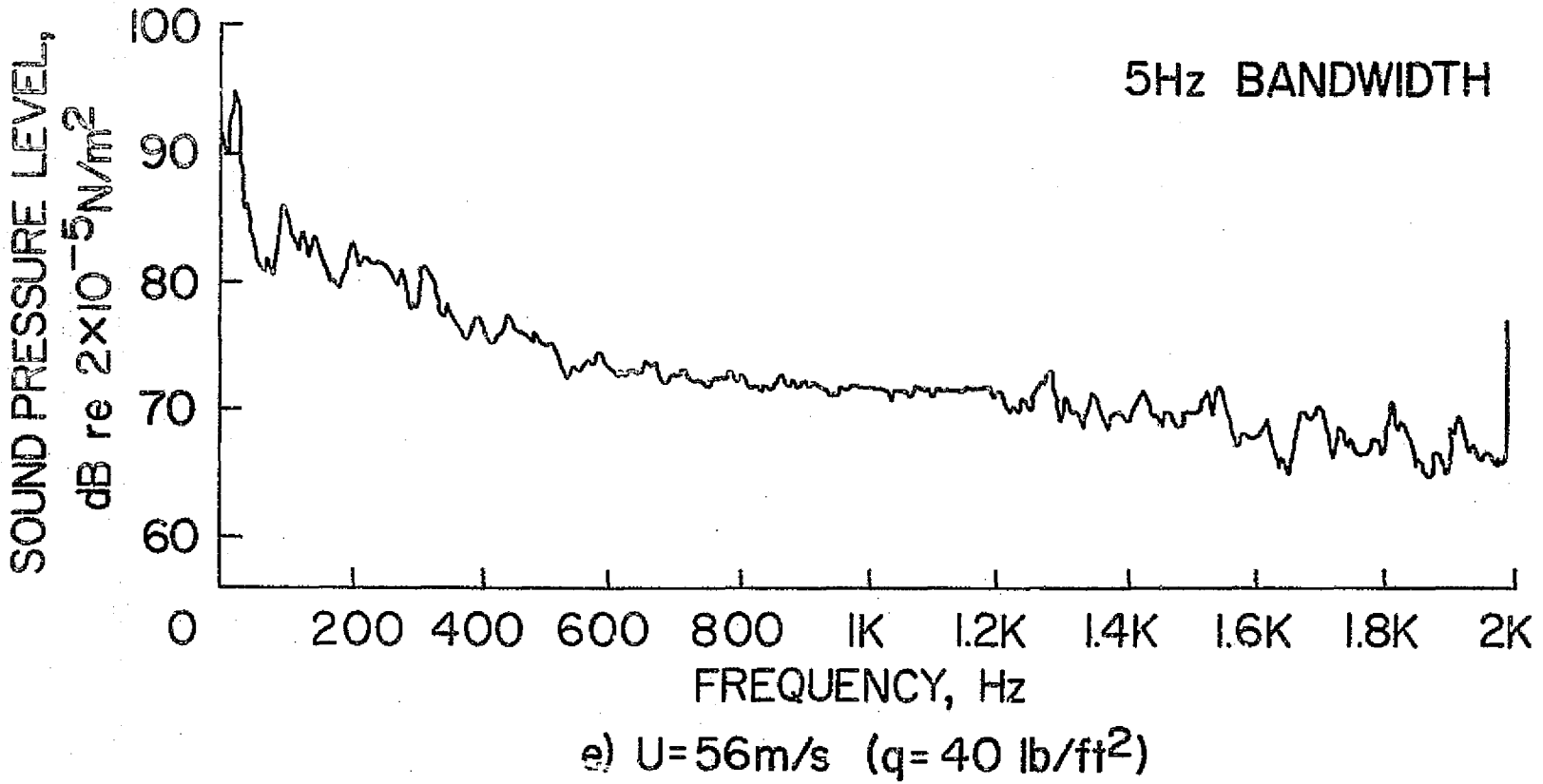

Figure 15.- Continued.

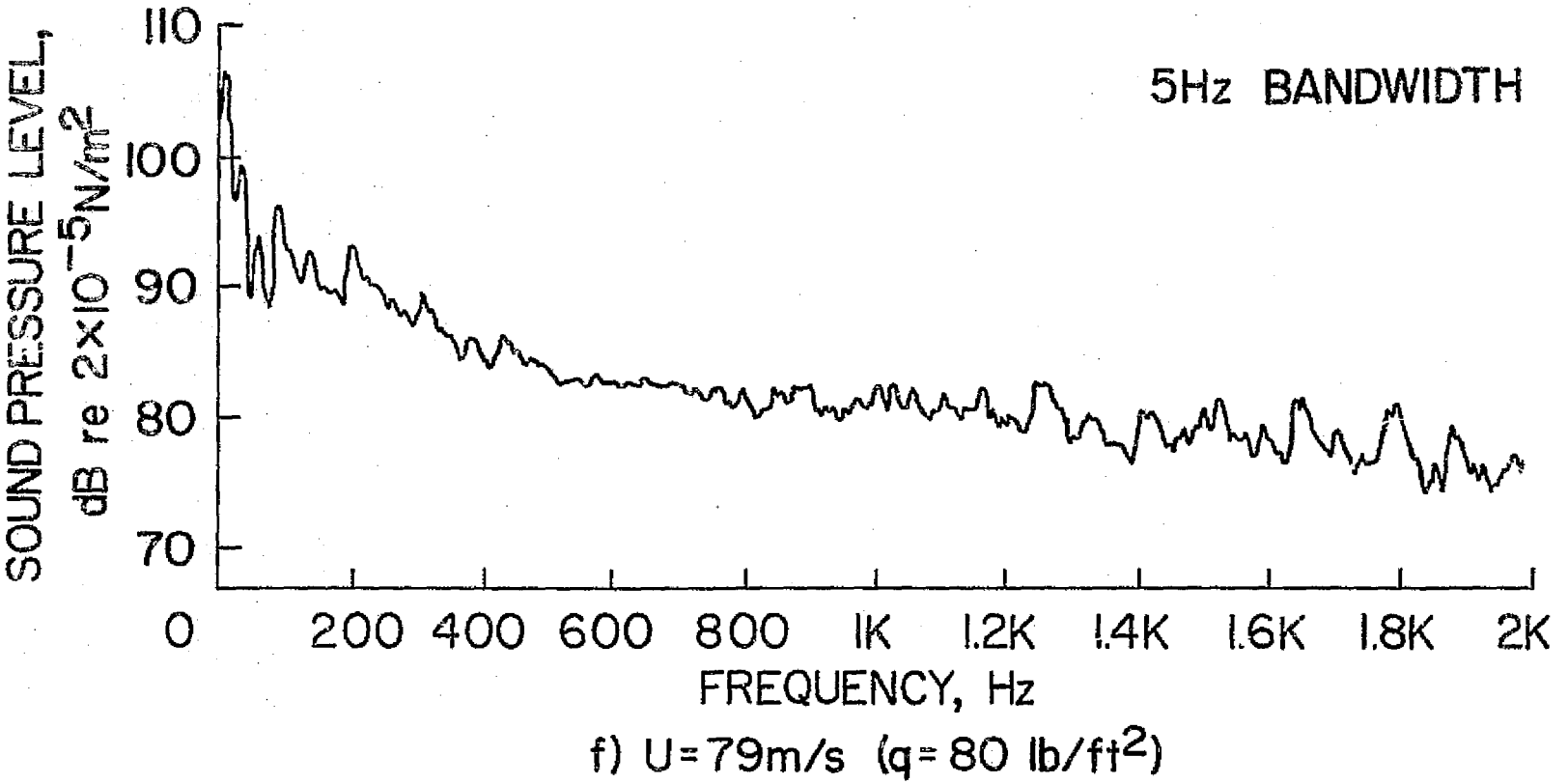

Figure 15.- Concluded.